Electronic Supplementary Information

Asymmetric synthesis of 3,4-annulated indoles through an organocatalytic cascade approach

Lorenzo Caruana, Mariafrancesca Fochi,* Mauro Comes Franchini, Silvia Ranieri, Andrea Mazzanti and Luca Bernardi*

Department of Industrial Chemistry "Toso Montanari"
School of Science
University of Bologna
V. Risorgimento, 4 I-40136 Bologna (Italy)
Tel.: +390512093653
Fax: +390512093654
E-mail: mariafrancesca.fochi@unibo.it; luca.bernardi2@unibo.it

Table of Contents

Optimisation of the reaction parameters in the reaction between indole derivatives **1** and crotonaldehyde **2b**……..**S2**

Determination of relative and absolute configuration of the adducts **3** and **6**, model for the observed stereoselectivity, structural determination of compound **5** and mechanistic hypothesis for its formation...……..……..**S4**

Experimental details…….……**S20**

Copies of the ^{1}H and ^{13}C NMR spectra and HPLC traces……...……**S31**

Optimisation of the reaction parameters in the reaction between indole derivatives 1 and crotonaldehyde 2b

Table S1. [a]

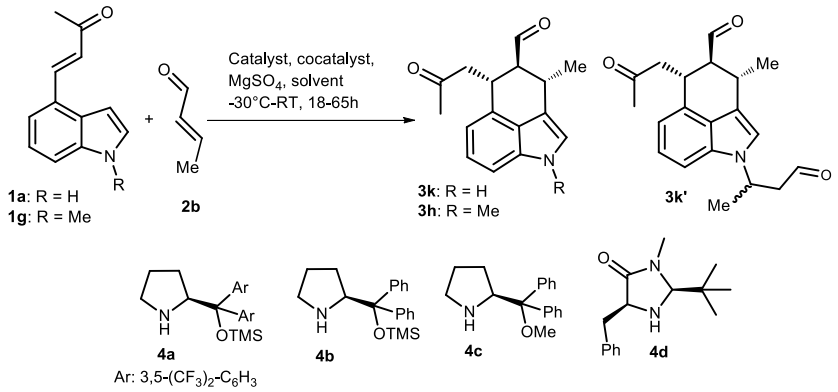

Entry	1	Solvent	Temp. (°C)	Time (h)	Cat. (20 mol%)	Cocat. (20 mol%)	Conv. [b] (%)	3k:3k' [b]	ee [c] (%)
1	**1a**	Dioxane	RT	18	**4b**	TFA	<5	\	\
2	**1a**	Dioxane	RT	18	**4a**	TFA	<5	\	\
3	**1a**	Dioxane	RT	18	**4c**	TFA	<5	\	\
4	**1a**	Dioxane	RT	65	**4a**	TFA	6	\	nd
5	**1a**	Dioxane	70	65	**4a**	TFA	8	\	nd
6	**1a**	Dioxane	RT	18	**4d**	TFA	96	80:20	48
7	**1a**	Acetonitrile	RT	18	**4d**	TFA	84	85:15	38
8	**1a**	MTBE	RT	18	**4d**	TFA	94	90:10	54
9	**1a**	Dioxane	RT	18	**4d**	PTSA	>95	<5:95	nd
10	**1a**	Dioxane	RT	18	**4d**	2-NO_2PhCO_2H	<5	\	nd
11	**1a**	Toluene	RT	18	**4d**	TFA	>95	<5:95	nd
12	**1a**	DCM/*i*-PrOH (8:2)	RT	18	**4d**	TFA	>95	40:60	76
13[d]	**1a**	DCM/*i*-PrOH (8:2)	RT	18	**4d**	TFA	76	43:57	80
14	**1g**	DCM/*i*-PrOH (8:2)	RT	18	**4d**	TFA	>95	\	78
15	**1g**	DCM/*i*-PrOH (8:2)	-30	65	**4d**	TFA	94	\	86
16	**1g**	DCM/*i*-PrOH (8:2)	-60	65	**4d**	TFA	80	\	79

[a] Conditions: indole derivative **1a** or **1g** (0.10 mmol), catalyst **4**, cocatalyst, crotonaldehyde **2b** (0.25 mmol), 50 mg $MgSO_4$, solvent (0.20 mL). In the case of entries 7 and 8 the diastereomeric ratio was evaluated to be 83:17 and 75:25 respectively; in all the other cases, a single diastereoisomer was observed by ^{1}H NMR spectroscopy in the crude mixture. [b] **3k**:**3k'** ratio and conversion were determined by ^{1}H NMR spectroscopy on the crude mixture. [c] Determined by chiral stationary phase HPLC and referred to **3k** or **3h**. [d] In this case 0.10 mmol of **2b** were used.

We first tried to extend the optimised reaction conditions between **1a** and acrolein **2a** to crotonaldehyde **2b**, but every attempt failed. Under conditions optimised for the reaction with acrolein **2a**, all the diarylprolinol derived catalysts **4a-c** were unable to promote the reaction between **1a** and **2b** (Table S1, entries 1-3). The extension of the reaction time to 65 h as well as the increasing of the temperature to 70 °C, did not produce any valuable effect (Table S1, entries 4-5).

Therefore we tested the MacMillan's second generation type catalyst **4d** using various polar and aprotic solvents (Table S1, entries 6-8), TFA as cocatalyst, at RT; the conversion increased dramatically, but besides the tricyclic target product **3k**, the related *N*-alkylated compound **3k'** was formed in not negligible amount and moreover, the enantiomeric excesses were unsatisfactory. No improvement was observed by replacing the cocatalyst: PTSA gave the *N*-alkylated **3k'** as the predominantly product, while 2-nitro benzoic acid did not promote the reaction at all (Table S1, entries 9-10). By using DCM/*i*-PrOH mixture as solvent, as originally employed for the reaction between simple indoles and enals catalysed by **4d**,[1] the enantioselectivity was improved to encouraging values, although the ratio between **3k** and **3k'** remained poor (Table S1, entry 12). We were unable to discriminate beetwen **3k** and **3k'**, even by decreasing the amount of **2b** (Table S1, entry 13). Thus, we switched to the *N*-Me indole derivative **1g** as substrate. At RT, the reaction proceeded to complete conversion furnishing **3h** as the only product with moderate enantioselectivity (Table S1, entry 14) which was improved by decreasing the temperature to -30 °C (Table S1, entry 15). A further decrease in the temperature did not increase the enantioselectivity (Table S1, entry 16).

[1] J. F. Austin and D. W. C. MacMillan, *J. Am. Chem. Soc.*, 2002, **124**, 1172.

Determination of relative and absolute configuration of the adducts 3 and 6, model for the observed stereoselectivity, structural determination of compound 5 and mechanistic hypothesis for its formation

Compound 3a

All the attempts to obtain good crystals of the prepared compounds were not successful. Moreover, with the exception of **3c**, a suitable heavy atom (Z> Si using standard Mo-Kα radiation[2]) was not available for the assignment of the absolute configuration by the anomalous dispersion X-ray method.[3] For this reason the relative and absolute configuration was determined by a combination of conformational analysis and theoretical simulations of chiro-optical spectra. Compound **3a** was selected as representative compound.

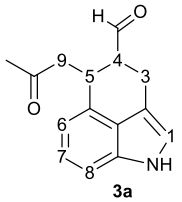

3a

Relative configuration

The relative stereochemistry of the two stereogenic centres at C-4 and C-5 was determined by means of NMR spectroscopy. Full assignment of the ^{1}H and ^{13}C spectra was preliminarily achieved by bi-dimensional experiments (gHSQC and gHMBC, taken in $CDCl_3$ solutions). The two diastereotopic hydrogens belonging to C-3 were found at 3.00 and 3.38 ppm whereas the two diastereotopic hydrogens belonging to C-9 were found at 2.77 and 2.85 ppm (by HMBC correlation with the C=O). The latter showed an additional coupling with the signal at 4.14 ppm (H-5).The signal of the NH (7.98 ppm) was assigned by the lack of correlation in the ^{13}C-^{1}H HSQC spectrum. DPFGSE-NOE experiments[4] were acquired in order to assign the relative stereochemistry at C-4 and C-5. This centres are bearing respectively the CHO and the CH_2COCH_3 substitution, that can assume a *cis* or *trans* relative disposition. On saturation of the aldehyde hydrogen (9.54 ppm, trace b in Scheme S1), NOE enhancement was observed for H-5 and for one of the diastereotopic protons at C-3 at 3.38 ppm ($H\text{-}3_a$). No enhancement was observed for the other proton $H\text{-}3_b$,and on the two hydrogens belonging to C-9. The observed NOEs suggested that the aldehyde and the CH_2COCH_3 substituents lie on opposite sides of the hexa-atomic cycle. On saturation of both the diastereotopic C-9 hydrogens (trace a), large NOEs were observed at 4.14 ppm (H-5), 2.92 ppm (H-4) and 3.0 ppm

[2] R. W. W. Hooft, L. H. Stravera and A. L. Spek, *J. Appl. Cryst.*, 2008,**41**, 96
[3] J. M. Bijvoet, A. F. Peerdeman and A. J. Van Bommel, *Nature*, 1951, **168**, 271.
[4]K. Stott, J. Stonehouse, J. Keeler, T-L. Hwang and A. J. Shaka, *J .Am. Chem. Soc.*, 1995, **117**, 4199.

($H\text{-}3_b$). While the first two NOEs have to be visible independently from the relative configuration of the two stereogenic centres, the latter confirmed that the CH_2COCH_3 moiety is on the opposite side of the cycle with respect to the CHO group. On saturation of H-5 (trace c), NOEs were observed on the aldehyde, on the two hydrogens at C-9, but no enhancement was observed on the two hydrogens at C-3. This confirms that H-5 is a pseudo-equatorial position. Finally, on saturation of the COMe signal (not shown in figure), NOE were observed only on $H\text{-}9_a$ and $H\text{-}9_b$, suggesting that the COMe moiety adopts a conformation that places the methyl far from the cycle. NMR analysis thus suggests the *trans* relationship of the two stereogenic centres (thus 4*R**,5*S** relative configuration).

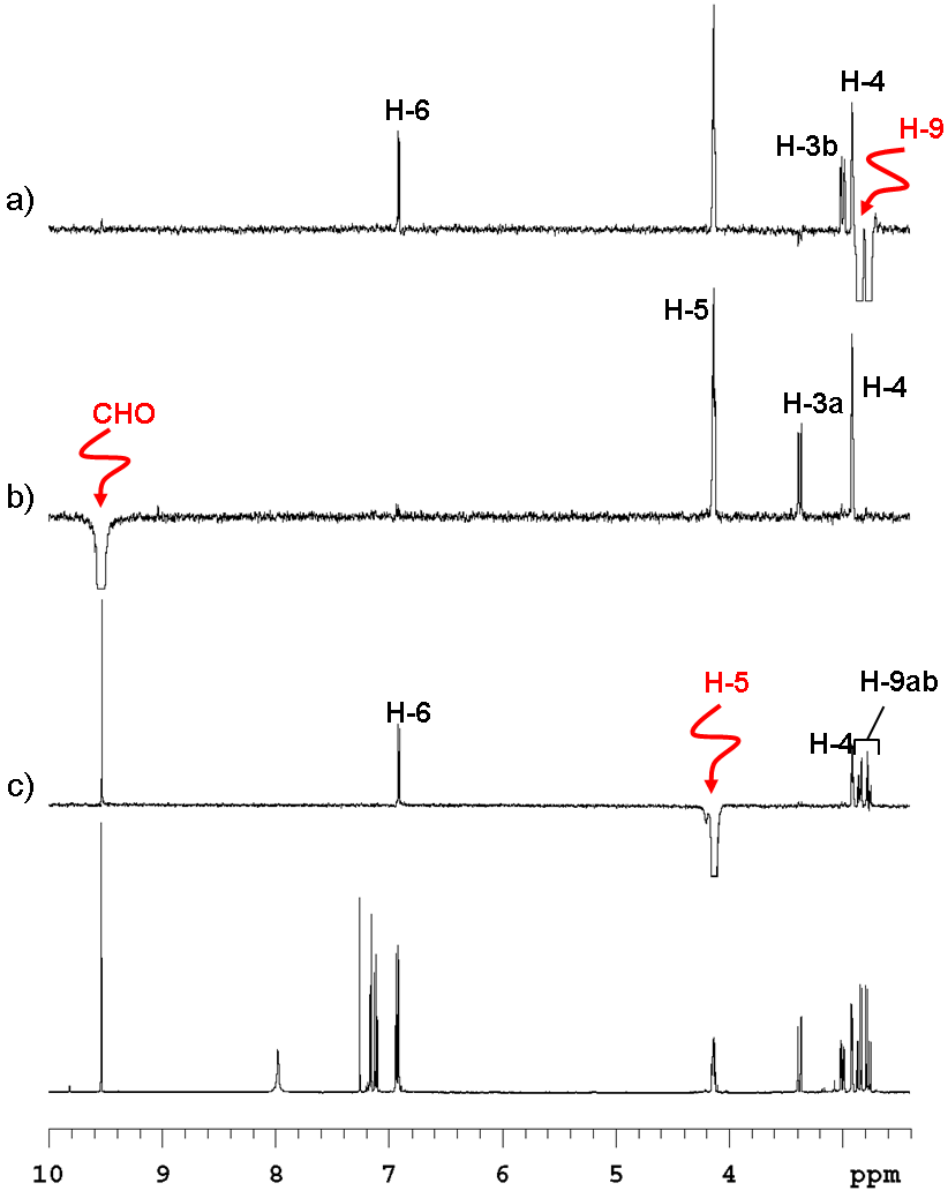

Scheme S1: DPFGSE-NOE spectra of **3a** (600 MHz in $CDCl_3$). Bottom: ^{1}H-NMR control spectrum; trace a) saturation of H-9; trace b) saturation of CHO; trace c) saturation of H-5.

Conformational analysis

Although the rigidity of the heterocyclic core of compound **3a** helps in the reduction of the number of conformations to be considered,[5] the conformational degrees of freedom due to the rotation of the aldehyde and CH_2COCH_3 moieties represent a challenging issue for the conformational analysis step.

As the first stage, we performed a conformational search on compound **3a**, with the 4R*,5S* relative configuration. The whole conformational space was explored by means of Monte Carlo searching together with the MMFF94 molecular mechanics force field as implemented in Titan 1.0.5 (Wavefunction inc.).

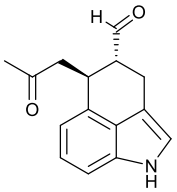

All the conformations found by MM search within a 10 kcal/mol window were then optimized using DFT at the B3LYP/6-31G(d) level using the Gaussian 09 suite of programs.[6] The harmonic vibrational frequencies of each optimized conformation were calculated at the same level to confirm their stability (no imaginary frequencies were observed) and to evaluate the free energy of each conformation. After DFT minimization, five conformations were found to be enclosed in a 2 kcal/mol window, as reported in Scheme S2 and Table S2. All of them exhibit the same shape of the six-membered ring, that corresponds to a pseudo boat conformation where both the aldehyde and the CH_2COCH_3 moiety occupies a pseudo-axial position. Conformation **b** differs from **a** because of the different disposition of the ketone chain, and they both have the CH of the aldehyde pointing towards the H-5. Conformation **c** instead has a different orientation of the aldehyde moiety, so the CH of the aldehyde is pointing toward H-3a. The relative internal and free energies suggest that all these conformations should be populated (Scheme S2).

[5] P. L. Polavarapu, E. A. Donahue, G. Shanmugam, G. Scalmani, E. K. Hawkins, C. Rizzo, I. Ibnusaud, G. Thomas, D. Habeland and D. Sebastian, *J. Phys. Chem. A,* 2011, **115**, 5665.

[6] Program Gaussian 09, rev A.02M. J. Frisch, G. W. Trucks, H. B. Schlegel, G. E. Scuseria, M. A. Robb, J. R. Cheeseman, G. Scalmani, V. Barone, B. Mennucci, G. A. Petersson, H. Nakatsuji, M. Caricato, X. Li, H. P. Hratchian, A. F. Izmaylov, J. Bloino, G. Zheng, J. L. Sonnenberg, M. Hada, M. Ehara, K. Toyota, R. Fukuda, J. Hasegawa, M. Ishida, T. Nakajima, Y. Honda, O. Kitao, H. Nakai, T. Vreven, J. A. Montgomery, Jr., J. E. Peralta, F. Ogliaro, M. Bearpark, J. J. Heyd, E. Brothers, K. N. Kudin, V. N. Staroverov, R. Kobayashi, J. Normand, K. Raghavachari, A. Rendell, J. C. Burant, S. S. Iyengar, J. Tomasi, M. Cossi, N. Rega, J. M. Millam, M. Klene, J. E. Knox, J. B. Cross, V. Bakken, C. Adamo, J. Jaramillo, R. Gomperts, R. E. Stratmann, O. Yazyev, A. J. Austin, R. Cammi, C. Pomelli, J. W. Ochterski, R. L. Martin, K. Morokuma, V. G. Zakrzewski, G. A. Voth, P. Salvador, J. J. Dannenberg, S. Dapprich, A. D. Daniels, Ö. Farkas, J. B. Foresman, J. V. Ortiz, J. Cioslowski, and D. J. Fox, Gaussian, Inc., Wallingford CT, 2009.

Table S2. Relative energies of the four conformations of **3a** evaluated using ZPE-corrected free energies and different optimization levels: B3LYP/6-31G(d) and M06-2X/6-31+G(d,p). Populations are calculated using Boltzmann distribution at 298°K.

Conformation	G° (B3LYP)	G° (M06-2X)	Pop. (B3LYP)	Pop. (M06-2X)
a	0.0	0.0	48	53
b	0.80	0.46	12	25
c	0.20	0.79	34	14
d	1.29	1.10	6	8

Albeit with different intensity, NMR spectra showed large NOE effects on H-5 and H-3a when the CHO signal was saturated, thus confirming that both conformations are populated in solution. The stronger NOE enhancement observed for H-5 confirms the conformational preference suggested by DFT calculations. The CHO-H_5 and CHO-H_{3a} calculated distances in the two conformations **a** and **c** are 2.30 and 2.33 Å respectively. Being the expected NOE almost equivalent, the observed difference can provide a good estimate of the experimental ratio of the conformations. The experimental NOE ratio was 63:37, corresponding to a free energy difference of 0.31 kcal/mol.

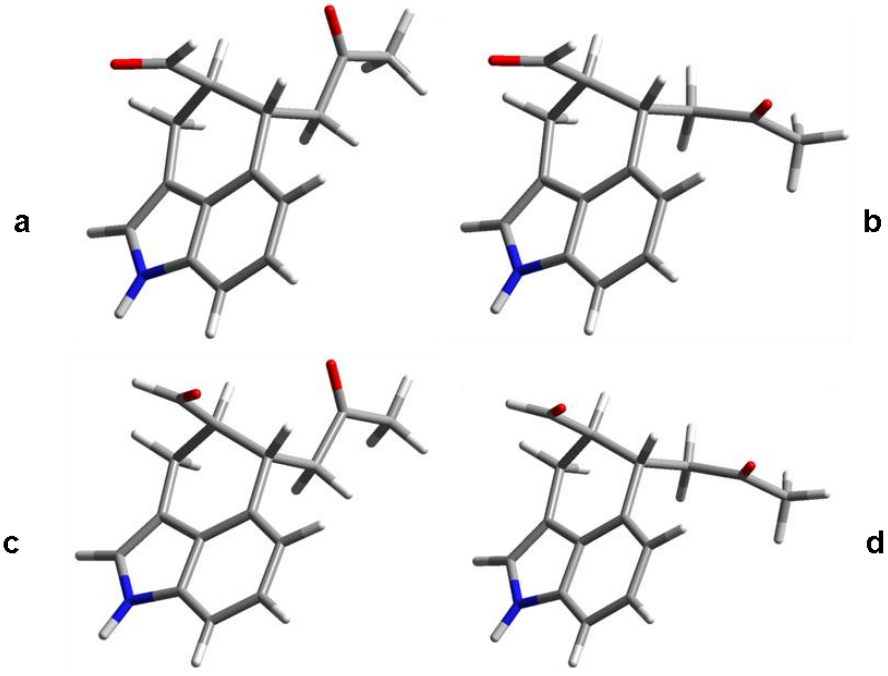

Scheme S2. 3D view of the four conformations of the model compound **3a**

Having in hand the relative configuration and suitable experimental data supporting the preferred conformations, the assignment of the absolute configuration was tackled by chiro-optical methods.

The determination of the absolute configuration (AC) of chiral molecules using chiroptical techniques like optical rotation (OR), electronic circular dichroism (ECD), and vibrational circular

dichroism (VCD) has gained feasibility and reliability because of the development of methods for the prediction of these properties based on density functional theory (DFT) and on its Time-Dependent formalism (TD-DFT).[7] In the present case the theoretical calculation of the electronic circular dichroism spectra (ECD) was selected for the absolute configuration assignment.

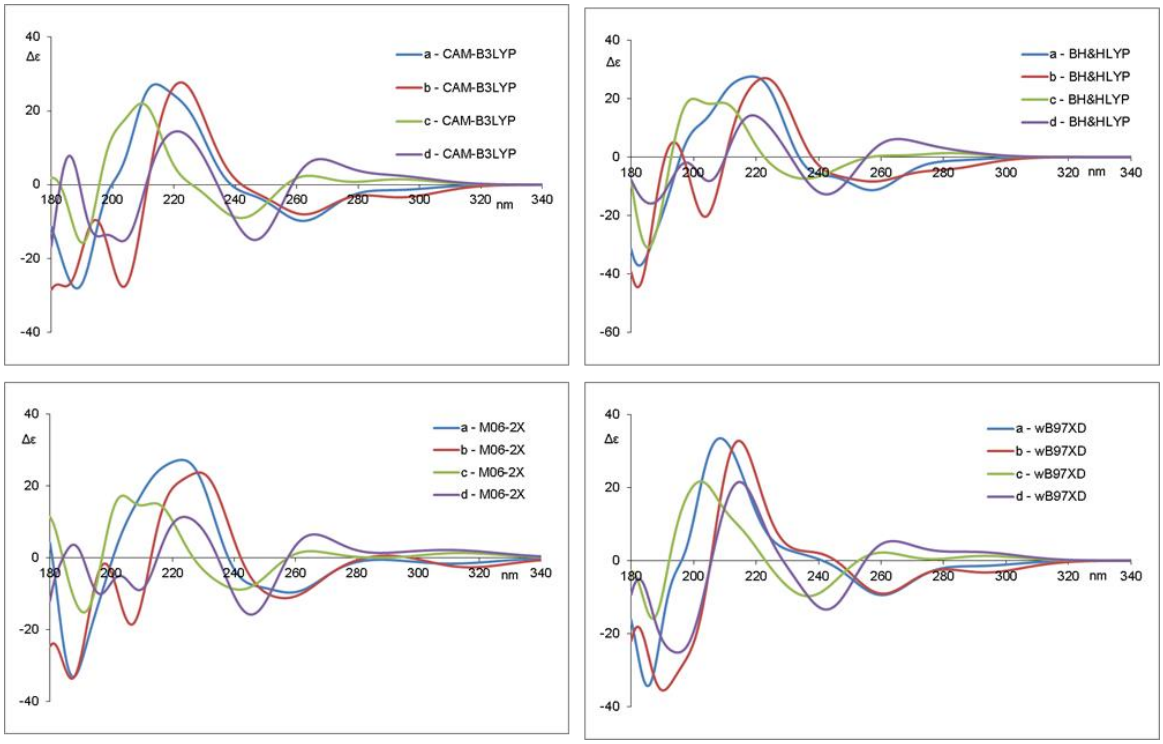

Scheme S3.TD-DFT simulated spectra calculated for the four conformations of **3a** using four different functionals (CAM-B3LYP, BH&HLYP, M06-2X, ωB97-XD) and the same 6-311++G(2d,p) basis set. For each conformation the first 50 excited states were calculated, and the spectrum was obtained using a 0.40 eV line width at half height. All the simulations are for the 4*R*, 5*S* absolute configuration

The electronic excitation energies and rotational strengths have been calculated for the isolated molecule in the gas phase for the four conformation of **3a** using TD-DFT with four different methods (functionals), to ascertain if different computational approaches provide different shapes of the simulated spectra (see Scheme S3).[8] Simulations were performed with the hybrid functionals BH&HLYP[9] and M06-2X,[10] ωB97XD that includes empirical dispersion,[11] and CAM-B3LYP that includes long range correction using the Coulomb Attenuating Method.[12] The calculations employed the 6-311++G(2d,p) basis set that proved to be sufficiently accurate at a reasonable

[7]For reviews see: (*a*) G. Bringmann, T. Bruhn, K. Maksimenka, and Y. Hemberger, *Eur. J. Org. Chem*. 2009, 2717; (*b*) T. D. Crawford, M.C. Tam, and M.L. Abrams, *J. Chem. Phys. A*, 2007, **111**,12057. G. Pescitelli, L. Di Bari and N. Berova, *Chem.Soc.Rev.* 2011, **40**, 4603. For a review on conformational analysis for the AC determination see: A. Mazzanti, and D. Casarini, D. WIREs, *Comput. Mol. Sci.* 2012, **2**, 613.
[8]C. E. Check and T. M. Gilbert. *J. Org. Chem.*, 2005, **70**, 9828.
[9] In Gaussian 09 the BH&HLYP functional has the form: $0.5*E_X^{HF} + 0.5*E_X^{LSDA} + 0.5*\Delta E_X^{Becke88} + E_C^{LYP}$
[10]Y. Zhao and D. G. Truhlar, *Theor. Chem. Acc*., 2008, **120**, 215.
[11] J-D. Chai and M. Head-Gordon, *Phys. Chem. Chem. Phys.*, 2008, **10**, 6615.
[12] T. Yanai, D. Tewand and N. Handy, *Chem. Phys. Lett.*, 2004, **393**, 51.

computational cost.[13] Rotational strengths were calculated in both length and velocity representation, the resulting values being very similar (RMS differences < 5%). For this reason the errors due to basis set incompleteness should be very small, or negligible.[14] Although the spectra simulated within the same functional for the four conformation are quite different, they are nevertheless consistent with the simulation of the positive Cotton effect at about 220 nm, and with the negative part in the 240-260 nm region. The almost coincidence of the simulates spectra for the same conformation on varying the functional represent a good proof of the simulation consistency.

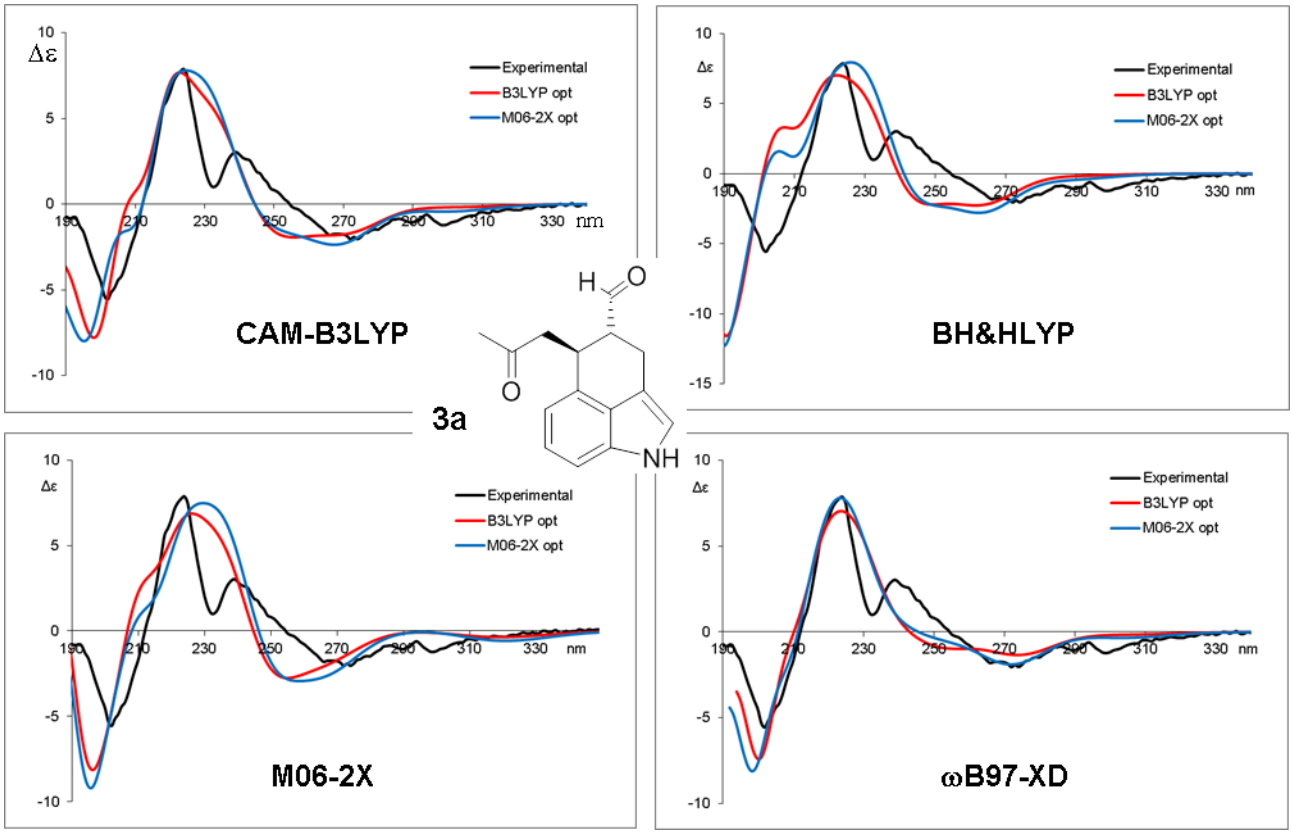

Scheme S4: Simulations of the experimental ECD spectrum of **3a** (black traces). For each section, the black line correspond to the experimental spectrum (acetonitrile solution, $1.5 \cdot 10^{-4}$M, 0.2 cm path length Δε in Mol L^{-1} cm^{-1}). The red lines correspond to the simulations obtained using the populations derived from B3LYP/6-31G(d) optimization. The blue lines correspond to the simulations obtained using the populations derived from M06-2X/6-31+G(d,p) optimization. The simulated spectra were vertically scaled and red-shifted by 7-14 nm to get the best match with the experimental spectrum. All the simulations are for the 4*R*, 5*S* absolute configuration.

The population-weighted spectra to be compared with the experimental spectrum were obtained using the percentages of Table S2. As shown in Scheme S4, the simulated spectra match well the Cotton effects at 224 nm and 270 nm when the 4*R*, 5*S* absolute configuration is assumed in

[13](*a*) G. Cera, M. Chiarucci, A. Mazzanti, M. Mancinelli and M. Bandini, *Org. Lett.*, 2012, **14**, 1350; (*b*) F. Pesciaioli, P. Righi, A. Mazzanti, G. Bartoli and G. Bencivenni, *Chem. Eur. J.*, 2011, **17**, 2482; (*c*) S. Duce, F. Pesciaioli, L. Gramigna, L. Bernardi, A. Mazzanti, A. Ricci, G. Bartoli and G. Bencivenni, *Adv. Synt. Catal.*, 2011, **353**, 860; (*d*) L. Bernardi, M. Comes-Franchini, M. Fochi, V. Leo, A. Mazzanti and A. Ricci, *Adv. Synt. Catal.*, 2010, **352**, 3399.
[14]P. J. Stephens, D. M. McCann, F. J. Devlin, J. R. Cheesemanand M. J. Frisch, *J. Am. Chem. Soc.*, 2004, **126**, 7514

the calculations. The best simulation was obtained by the ωB97-XD functional, but all the simulated spectra show a good agreement with the experimental one. It has to be noted that the simulated spectra derived from the conformational geometries and energies obtained with B3LYP/6-31G(d) optimization have the same level of accuracy with respect to those obtained with the more recent and computationally heavier M06-2X/6-31+G(d,p) optimization level. This seems to confirm the good performance of B3LYP in the conformational analysis of organic molecules.

A plausible catalytic cycle for the cascade reaction is reported in Scheme S5. The cascade reaction is initiated by activation of acrolein **2a** with the chiral amine catalyst **4b** through the formation of an iminium ion, to which the indole derivatives **1** add by performing a Friedel-Crafts alkylation. The resulting enamine subsequently undergoes an intramolecular Michael addition furnishing the tricyclic products **3** and releasing the catalyst for the next catalytic cycle.

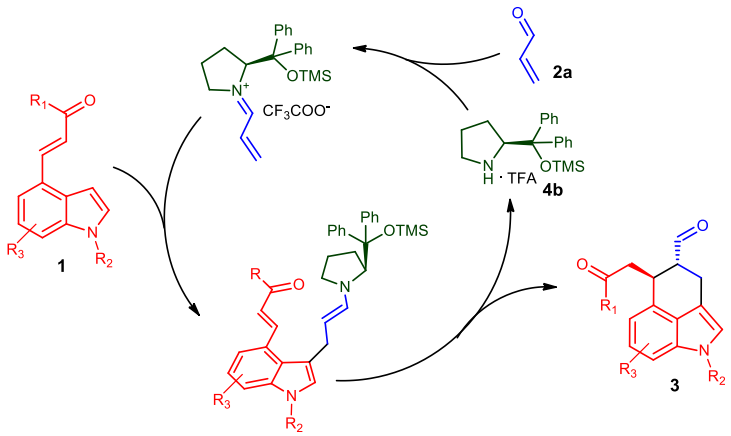

Scheme S5. Proposed catalytic cycle for the cascade reaction between **1** and **2a**

To account for the observed (4*R*,5*S*) absolute configuration, we refer to a transition state model in which the enantiocontrol is provided by the bulky group on the catalyst (Scheme S6). The chirality is generated in the Michael addition step, which is triggered by the Friedel-Crafts addition. In this Michael addition step it can be assumed that the electrophile will approach the enamine intermediate from the least hindered face. In the transition state the large aryl and silyloxy substituents of the catalyst keep the enamine in the conformation shown and shield the *Re*-face of the enamine. As a consequence the unhindered *Si*-face of the enamine attacks the electron-poor olefin. This assumption is in line with the generally accepted models describing α-functionalization of aldehydes mediated by diarylprolinol silyl ethers enamine-catalysis.[15]

[15] (*a*) J. Franzen, M. Marigo, D. Fielenbach, T. C. Wabnitz, A. Kjaersgaard and K. A. Jørgensen, *J. Am. Chem. Soc.*, 2005, **127**, 18296; (*b*) Y. Hayashi, H. Gotoh, T. Hayashi and M. Shoji, *Angew. Chem Int. Ed.*, 2005, **44**, 794; (*c*) K. L. Jensen, P. T. Franke, L. T. Nielsen, K. Daasbjerg and K. A. Jørgensen, *Angew. Chem. Int. Ed.*, 2010, **49**, 129; (*d*) K. L. Jensen, G. Dickmeiss, H. Jiang, Ł. Albrecht and K. A. Jørgensen, *Acc. Chem. Res.*, 2012, **45**, 248.

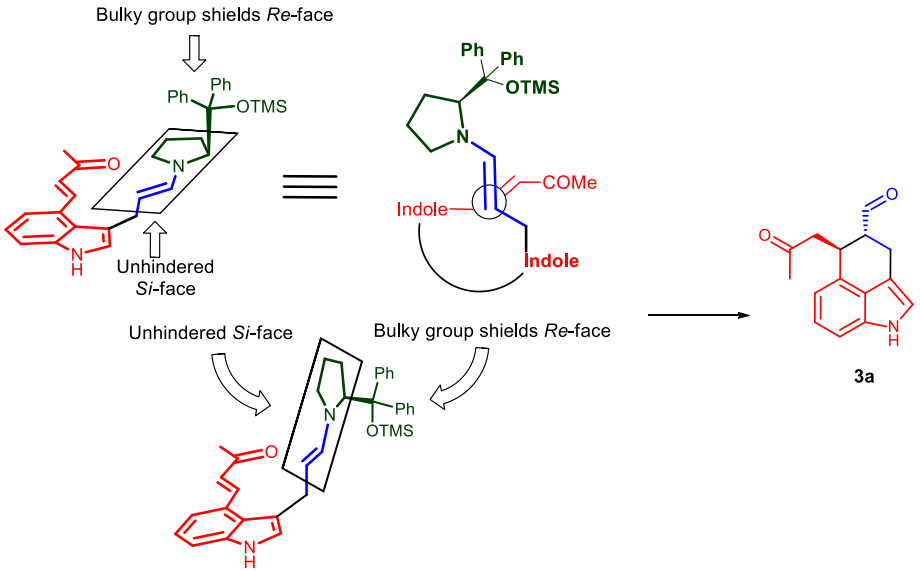

Scheme S6. Model accounting for the observed enantioselectivity in the enamine-mediated enantioselectivity determining step.

We have observed only the *trans*-configured tricyclic products in all cases, which can be due either or both to a high diastereoselectivity in the Michael reaction, as shown in the model depicted in Scheme S6, or to the greater thermodynamic stability of the *trans*-adduct compared to the *cis* (i.e. product epimerization leads to the more stable *trans*-isomer after the Michael addition reaction has taken place).

Compound 3h

Compound **3h** was selected as representative compound for the compounds **3** having three contiguous stereocentres The relative configuration of compound **3h**, was determined by NMR spectroscopy, as detailed below.

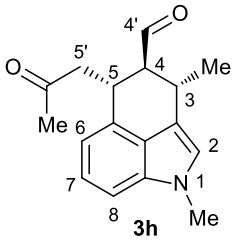

3h

^{1}H NMR ($CDCl_3$, 400 MHz) δ = 9.66 (d, J = 4.6 Hz, 1H), 7.19-7.11 (m, 2H), 6.80 (d, J = 1.6 Hz, 1H), 6.76 (d, J = 6.8 Hz, 1H), 4.10 (dt, J = 5.7.; 9.1 Hz 1H), 3.77 (s, 3H), 3.57-3.49 (m, 1H), 3.09 (dd, J = 18.3; 5.9 Hz, 1H), 2.86 (dd, J = 18.3; 5.9 Hz, 1H), 2.36 (td, J = 4.6; 9.1 Hz 1H), 2.24 (s, 3H), 1.36 (d, J = 6.9 Hz, 3H).

Full assignment of the signals in the ^{1}H spectrum was preliminarily achieved by a bi-dimensional gCOSY experiment. This gCOSY spectrum showed a coupling between the aldehyde hydrogen at 9.66 ppm and the hydrogen at 2.36 ppm, allowing us to assign this signal as H-4. Moreover, this hydrogen at 2.36 ppm showed additional couplings with the signals at 4.10 and 3.52 ppm. Since the signal at 3.52 ppm was coupled with the signal of the methyl group belonging to C-3 (1.36 ppm, doublet) and the signal at 4.10 ppm coupled with the two diasterotopic protons of C-5' (3.09 and 2.86 ppm, two dd), we assigned the signal at 3.52 ppm to H-3 and the signal at 4.10 ppm to H-5.

The signal of the proton at C-4 (2.36 ppm) appears as a triplet of doublets and exhibits two coupling constants of 9.1 Hz and one of 4.6 Hz. This implies that H-4 couples with two hydrogens with a large coupling constant and with one hydrogen with a smaller coupling constant. Moreover the aldehyde proton appears as a doublet with one coupling constant of 4.6 Hz, that is the coupling constant with H-4. This is consistent with a coupling of H-4 with two large *trans*-diaxial coupling with H-3 and H-5, with a dihedral angle close to 180 °. This indicates that H-3, H-4 and H-5 are in axial position of the pseudo-chair six-membered ring, while the 2-oxopropyl, the aldehyde and the methyl moieties occupy the equatorial positions (see Scheme S7). This assignment was confirmed by the signal of H-5, which appears as double triplet and exhibits two couplings of 5.7 Hz with the diastereotopic hydrogens at C-6' and the same coupling of 9.1 Hz with H-4.

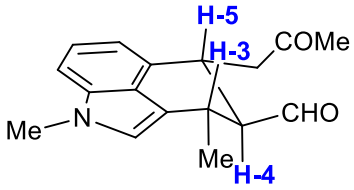

Scheme S7: All-*trans* configuration of compound **3h**, with the pseudo-axial relationships justifying the observed large coupling constants between H-4, H-3 and H-5.

Mono-dimensional DPFGSE-NOE experiments[4] were acquired in order to confirm the relative stereochemistry at C-3, C-4 and C-5. Significant NOE enhancements were observed as follows (Scheme S8). On saturation of H-3, a NOE enhancement was observed for the aldehyde proton, and for H-5. On saturation of H-4, NOE enhancement was observed for the hydrogens belonging to the methyl group at C-3. On saturation of H-5, NOE enhancement was observed for H-3 and for the aldehyde proton. All these experimental evidences confirm the axial relationships between H-3, H-4 and H-5, already deduced from the analysis of the *J*-couplings of the ^{1}H NMR spectrum, thus confirming the *trans* relative configuration of the three contiguous asymmetric centres.

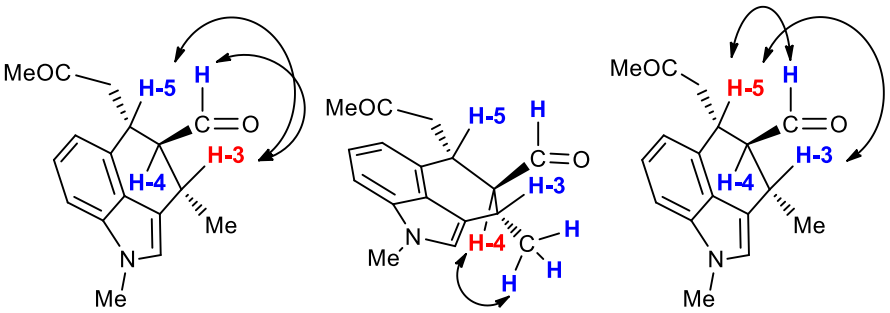

Scheme S8. Significant NOE enhancements on saturation of the protons indicated in red.

For what concerns the explanation of the absolute configuration of **3h**, in the reaction between indole derivative **1g** and β-substituted enals we can hypothesize a similar catalytic cycle to that outlined in Scheme S5, in which diarylprolinol catalyst **4b** is replaced by catalyst **4d**. Contrary to the reaction between **1** and acrolein **2a**, in this reaction the chirality is generated in the first Friedel-Crafts step; therefore, in agreement with the report describing the enantioselective alkylation of indoles with enals catalysed by **4d**,[1] it can be assumed that the indole derivative **1g** attacks the iminium ion at its unshielded *Re*-face (Scheme S9), delivering after enamine mediated Michael addition the products **3h** featuring the relative and absolute configuration shown below.

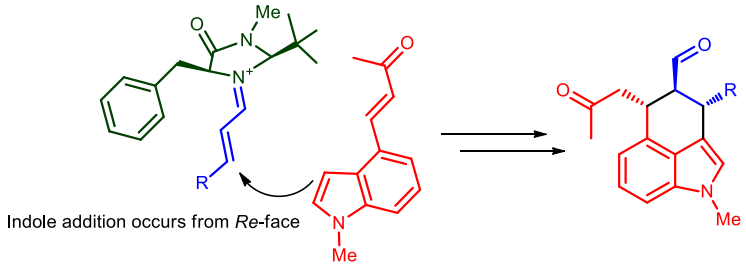

Scheme S9. Model for the enantioselectivity in the iminium ion-mediated enantioselectivity determining step.

Compounds 6

Due to the epimerization process observed in the Robinson annulation of **3a** to compounds *cis*-**6** and *trans*-**6**, the determination of their relative and absolute configuration was desirable. During the reaction, only the stereogenic centre in position 4 of **3a** could be epimerized. Being more conformationally constrained by the tetracyclic scaffold, compounds *cis*-**6** and *trans*-**6** are very rigid. This helps in the conformational analysis to reduce the populated conformations.

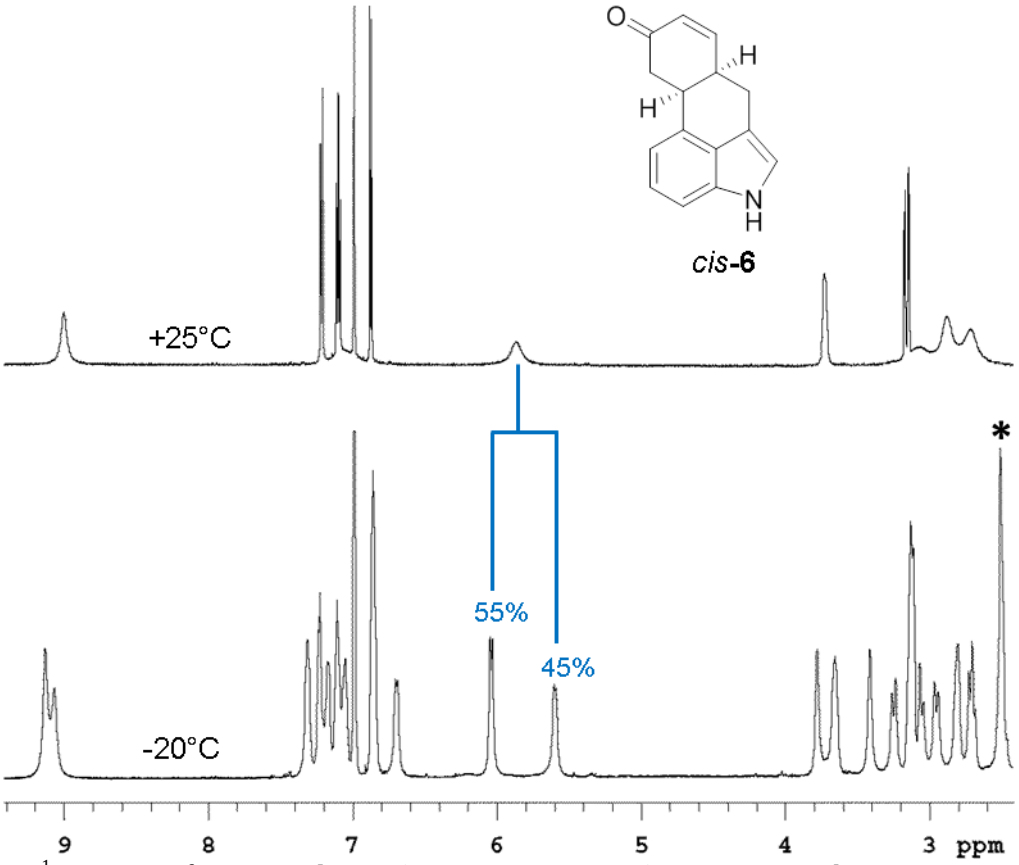

Scheme S10. ^{1}H spectra of compound *cis*-**6** (600 MHz in CD_3CN). Top trace: ambient temperature spectrum. Bottom: spectrum recorded at -20°C. The asterisk indicates the water signal of the solvent.

The two diastereoisomers *cis*-**6** and *trans*-**6** were separated by means of semi-preparative HPLC on a C18 column (Phenomenex® Synergi Hydro-RP) using Acetonitrile/H_2O 60:40 (see § "Experimental details"). The ^{1}H spectra of the first eluted peak showed very broad lines in the aliphatic part and for the two vinylic hydrogens (see Scheme S10, top trace). On lowering the temperature these lines broaden further and they eventually split at -20°C into two set of signals in a 55:45 ratio (Scheme S10, bottom). This dynamic behaviour can be explained considering the optimized structures of the two diastereoisomers. In the case of *trans*-**6** isomer a single conformation should be populated. In this conformation the two bridgehead hydrogens occupy the pseudo-axial positions. In the case of the *cis*-**6** isomer, the same hydrogens occupy one pseudo-axial and one pseudo-equatorial position, thus two conformations obtained by exchanging the positions of these hydrogens can be envisaged (Scheme S11).

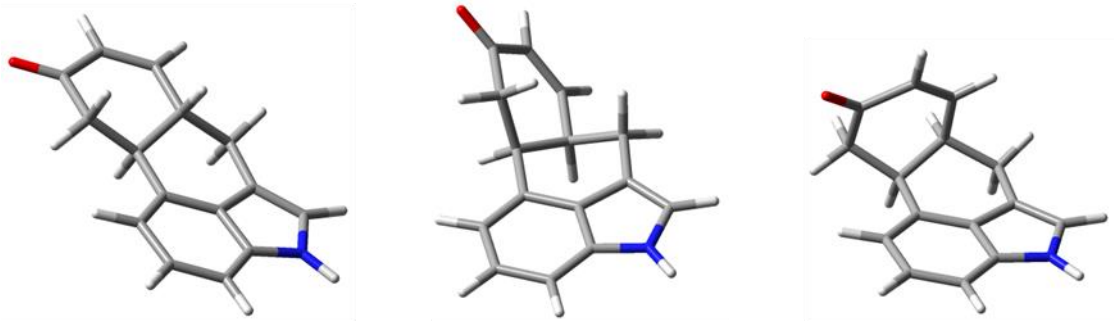

Scheme S11. Optimized structures for the ground state conformations of *trans*-**6** and *cis*-**6**

The conformational search found only one conformation for the *trans*-**6** isomer, and confirmed that both the proposed conformation of *cis*-**6** corresponded to energy minima. When optimized at the M06-2X/6-31G(d) level, the two conformations of the *cis* isomer were found to be very close in energy (0.67 kcal/mol), and the transition state for their interconversion was found to be 14.1 kcal/mol. This explains the dynamic behaviour observed in the NMR spectra of the first eluted compound, that can be thus assigned to the *cis*-**6** isomer. The *trans*-**6** isomer was calculated to be slightly more stable than the *cis* (0.33 kcal/mol). When the calculation of the two ground states of *cis*-**6** were repeated using a larger basis set and including the solvent (acetonitrile) in the calculations (PCM-M06-2X/6-31+G(d,p)), the energy difference between the two conformations reduced to 0.05 kcal/mol, thus reproducing well also the experimentally observed ratio.

As said before, compound *cis*-**6** is very rigid and the exact ratio of the two populated conformations can be provided by low-temperature NMR. For this reason the simulation of the ECD spectrum is straightforward. Having already established the absolute configuration of **3a,** a new assignment of the absolute configuration could appear an overkill, but it is not. Compound **3a** had a considerable conformational mobility while **6a** is rigid. The stereogenic centre at C5 of **3a** should be left unchanged, but the reaction conditions are severe. For these reasons the independent assignment of the absolute configuration of *cis*-**6** provides a validation about the retention of configuration at C-5. As for **3a**, the electronic excitation energies and rotational strengths have been calculated for the isolated molecule in the gas phase for the two conformations of *cis*-**6** using TD-DFT with CAM-B3LYP, BH&HLYP, 06-2X, ωB97XD and the 6-311++G(2d,p) (Scheme S13).

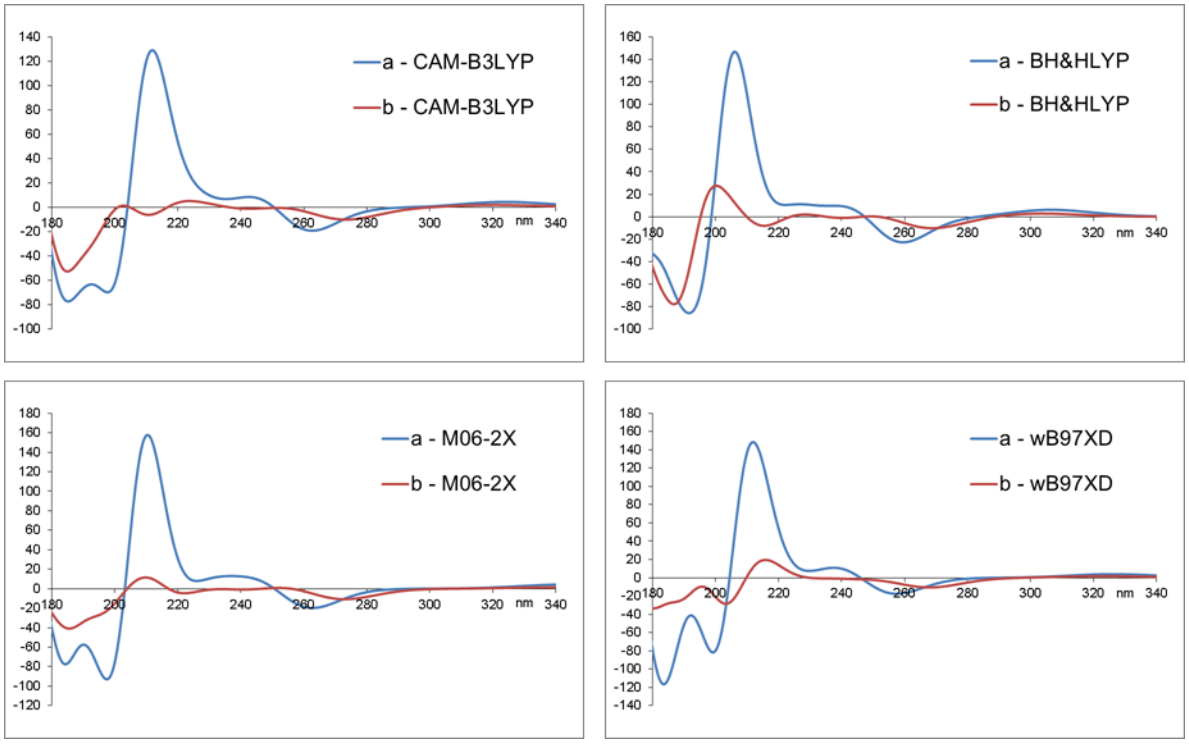

Scheme S12. TD-DFT simulated spectra calculated for the two conformations of *cis*-**6** using four different functionals (CAM-B3LYP, BH&HLYP, M06-2X, ωB97XD) and the same 6-311++G(2d,p) basis set. For each conformation the first 50 excited states were calculated, and the spectrum was obtained using a 0.40 eV line width at half height. All the simulations are for the 6a*R*,10a*S* absolute configuration.

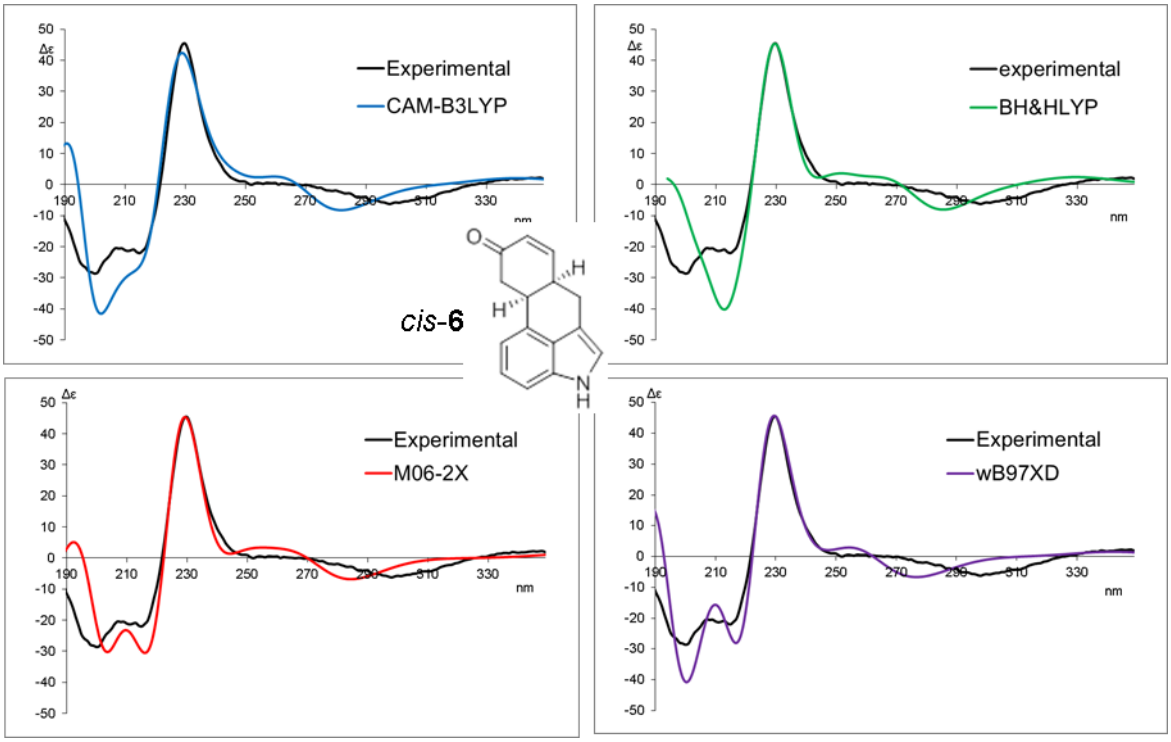

Scheme S13: Simulations of the experimental ECD spectrum of *cis*-**6** (black traces). For each section, the black line correspond to the experimental spectrum (acetonitrile solution, $1.5 \cdot 10^{-4}$M, 0.2 cm path length, Δε in Mol L^{-1} cm^{-1}). The simulated spectra were vertically scaled and red-shifted by 7-18 nm to get the best match with the experimental spectrum. All the simulations are for the 6a*R*,10a*S* absolute configuration.

Although the experimental assignment of the two conformations of *cis*-**6** is not available, the ratio is very close to 50:50. Moreover, the spectrum simulated for the **b** conformation is very weak. For these reason the spectrum resulting from Boltzmann distribution does not change on reversing the conformers population. All the simulated spectra agree well with the 6a*R*,10a*S* absolute configuration. Taking into account the different numbering of *cis*-**6**, the 10a*S* configuration matches the 5*S* configuration of the starting compound **3a**.

Compound 5: structural determination and mechanistic hypothesis

Compound **5** was surprisingly obtained by treating **3a** under Pinnick[16] (or Pinnick-Lindgren[17]) conditions. In principle, these conditions which employ chlorite as the oxidant species (the byproduct hypochlorite should be trapped by the 2-methyl-2-butene olefin) should leave the indole core untouched,[1] oxidising selectively the aldehyde moiety to a carboxylic acid. However, apparently the concomitant oxidation of the indole ring occurred in compound **3a** (Scheme S14).

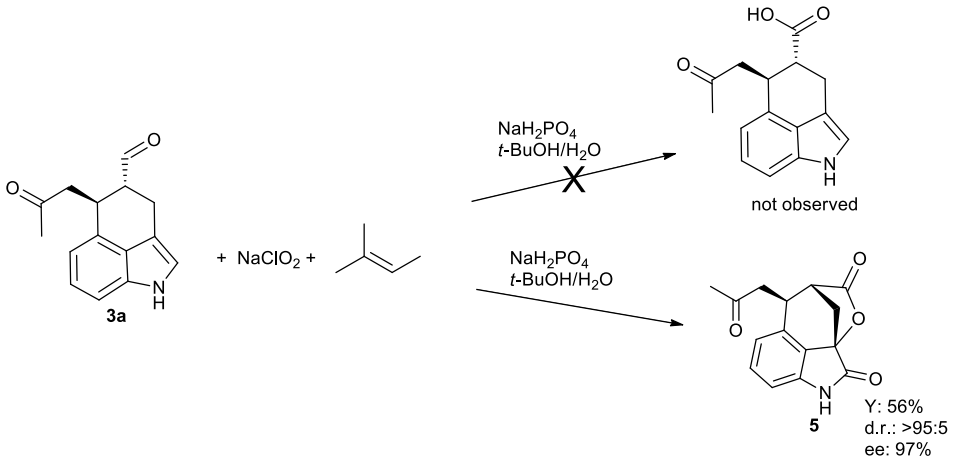

Scheme S14

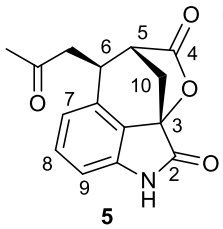

The structure of compound **5** was established by NMR experiments and mass spectrometric analysis. The ESI-mass revealed a molecular mass which was not compatible with the structure of the carboxylic acid having the indole core unaltered, but on the contrary it was perfectly consistent with compound **5** (experimental ESIMS: 271 [M+Na$^+$]). ^{1}H NMR spectrum showed only three correlated aromatic signals, no signal ascribable to the proton at C2 of indole was recognized. ^{13}C NMR revealed three signals which were compatible with C=O carbon: one carbonyl belonging to the ketone in the side

[16] B. S. Bal, W. E. Childers and H. W. Pinnick, *Tetrahedron*, 1981, **37**, 2091.
[17] B. O. Lindgren, T. Nilsson, S. Husebye, Ø. Mikalsen, K. Leander and C.-G. Swhan, *Acta Chem. Scand.*, 1973, **27**, 288.

chain (δ = 204.6 ppm), and two carboxyl (C4 and C2), one belonging to the lactone and one to the oxindole (δ = 175.0 and 169.9 ppm). The comparison between ^{13}C NMR, DEPT 1.0 and DEPT 1.5 experiments revealed the overall presence of seven quaternary carbons, five CH carbons (three of which aromatic), two CH_2 carbons and one CH_3 carbon. The chemical shifts of the carboxyl C2 (175.0 ppm), the quaternary C3 (78.0 ppm) and the lactone carboxyl C4 (169.9 ppm) are in agreement to those reported by Menéndez et al in the synthesis of oxindole and spyroxindole structures.[18]

In order to support the hypothesized structure of lactone **5**, a series of bidimensional NMR spectra (gCOSY, gHSQC and gHMBC) were recorded. It is worth nothing that in the HMBC spectra, the bridged methylene (C10) is correlated with the quaternary C3 (78.0 ppm), with C5 (43.9 ppm), with the lactone carboxyl C4 (175.0 ppm), with an aromatic quaternary carbon at 125.9 ppm and with C6 (33.1 ppm) (see pages S51-55 for the NMR spectra of lactone **5**).

The set of all these experimental data leads us to assign the proposed structure to compound **5**.

The conversion of 3-indole-propanoic acids to the corresponding spirocyclic oxindole lactones has been reported in several instances, and was found to occur under a variety of oxidative conditions (e.g. oxalyl chloride/DMSO[18], *t*-BuBr/DMSO,[19] thallium trinitrate,[20] NBS,[21] Scheme S15).

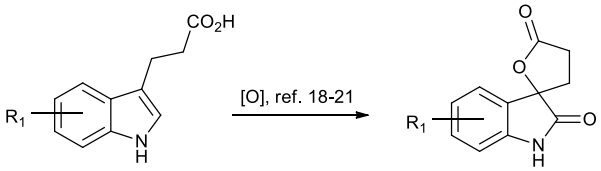

Scheme S15

On these grounds, our current interpretation for the formation of compound **5** involves a first oxidation of the aldehyde moiety to the carboxylic acid by chlorite, followed by the indole oxidation and lactone formation (Scheme S16). Given the presumed inability of chlorite in oxidising the indole ring, we hypothesise that the particular structure of compound **3a** makes its indole C2-C3 bond more efficient than 2-methyl-2-butene in trapping the hypochlorite, the by-product of the first oxidative process. Regarding the mechanism of the oxidative lactonisation reaction, it can be assumed that the reaction of the indole with hypochlorite leads to a 3-chloro

[18] P. López-Alvarado, J. Steinhoff, S. Miranda, C. Avendaño and J. C. Menéndez, *Tetrahedron*, 2009, **65**, 1660.
[19] R. B. Labroo, V. M. Labroo, M. M. King and L. A. Cohen, *J. Org. Chem.*, 1991, **56**, 3637.
[20] T. Ohnuma, Y. Kimura and Y. Ban, *Tetrahedron Lett.*, 1981, **22**, 4969.
[21] A. Patchornik, W. B. Lawson, E. Gross and B. Witkop, *J. Am. Chem. Soc.*, 1960, **82**, 5923.

indolenine, which can be easily oxidised (even by chlorite) to a 3-chloro oxindole. Then, lactonisation occurs, possibly though an *ortho*-azaxylylene intermediate.

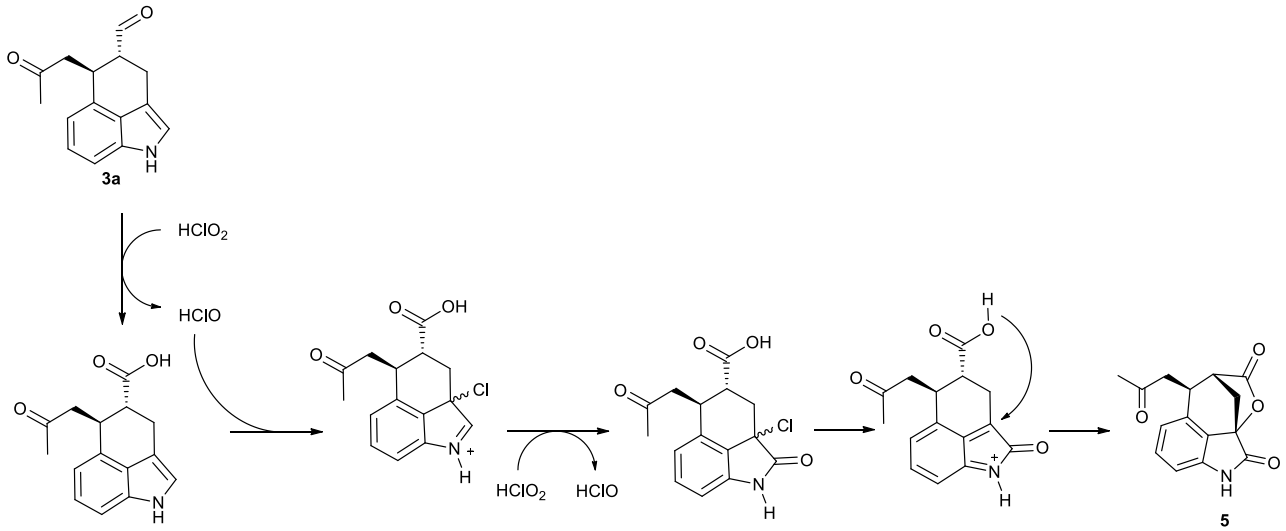

Scheme S16

Experimental Details

General Methods. ^{1}H, ^{13}C NMR spectra were recorded on a Varian AS 400 or 600 spectrometer. Chemical shifts (δ) are reported in ppm relative to residual solvent signals for ^{1}H and ^{13}C NMR.[22] ^{13}C NMR spectra were acquired with ^{1}H broad band decoupled mode. Chromatographic purifications were performed using 70-230 mesh silica. Mass spectra were recorded on a micromass LCT spectrometer using electrospray (ES) ionisation techniques or using electron impact (EI) ionisation techniques. Optical rotations were measured on a Perkin-Elmer 241 polarimeter. The Electronic Circular Dichroism spectra were recorded on a Jasco J-810 spectropolarimeter. The enantiomeric excess (ee) of the products was determined by chiral stationary phase HPLC, using a UV detector operating at 254 nm. The absolute and relative configuration of compounds **3a**, **3h** and *cis*-**6** was determined as outlined in the precedent paragraph. We assume a similar reaction pathway for the remaining compounds **3**, leading to the same relative and absolute configuration.

Materials. Analytical grade solvents and commercially available reagents were used as received, unless otherwise stated. 1*H*-Indole-4-carbaldehyde was purchased from Apollo Scientific. 2-Methyl-1*H*-indole-4-carbaldehyde[23] and 1-methyl-1H-indole-4-carbaldehyde[24] were prepared according to the literature. Indole substrates **1a-g** were synthesised through Wittig olefination, detailed as follows: the phosphonium salts, unless commercially available, were obtained by refluxing an equimolar mixture of triphenyl phosphine and the appropriate alkyl halides for a few hours in toluene or acetonitrile, and collected by filtration; the phosphorous ylides were then obtained by pouring a CH_2Cl_2 solution of the phosphonium salts in a separating funnel containing 2 N aq. NaOH; after five minutes of vigorous shaking, the organic phase was collected, dried over $MgSO_4$, filtered and evaporated affording the ylides; finally, the Wittig olefination between the indole-4-carbaldehyde and the appropriate phosphorous ylide[25] was carried out in a toluene/1,4-dioxane mixture (8:2), at reflux temperature for 18-48 h; products **1a-g** were purified by column chromatography and obtained as pure *E*-isomers. Acrolein **2a** was distilled before use, cinnamaldehyde **2c** was distilled under vacuum (11 mbar, bp = 125 °C) before use, crotonaldehyde **2b** was purchased from Sigma-Aldrich as "predominantly *trans*" with assay >99% and was used as received. 1,4-Dioxane was passed through a short pad of basic alumina before use. Racemic samples of compounds **3a-g** were prepared using racemic (±)-α,α-bis[3,5-

[22] H. E. Gottlieb, V. Kotlyar and A. Nudelman, *J. Org. Chem.*, 1997, **62**, 7512.
[23] J. M. Muchowski, *J. Heterocyclic Chem.*, 2000, **37**, 1293.
[24] M.Antoine, P. Marchand, G. Le Baut, M. Czech, S. Baasner, E. Gunther, *J. Enzyme Inhib. Med.*, 2008, **23**, 686.
[25] F. Yamada, Y. Makita and M. Somei, *Heterocycles*, 2007, **72**, 599.

bis(trifluoromethyl)phenyl]-2-pyrrolidinemethanol trimethylsilyl ether **4a** as the catalyst, in 1,4-dioxane at RT for 18-60 h. Racemic samples of compounds **3h-j** were prepared using racemic (±)-5-benzyl-2-tert-butyl-3-methyl-4-imidazolidinone **4d** as the catalyst, in a CH_2Cl_2/*i*-PrOH (8:2) mixture at RT for 18-60 h. Racemic **5** was obtained by employing racemic **3a** in the oxidation reaction. Racemic *cis*-**6** for HPLC analysis was obtained by mixing a nearly equimolar mixture of the two enantiomers, obtained from the two enantiomeric products **3a** and *ent*-**3a** using L- and -proline, respectively, in the Robinson annulation reaction.

General procedure for the catalytic reactions

Method A. To a vial equipped with a magnetic stirring bar, $MgSO_4$ (50 mg) was added, followed by the indole derivative **1a-g** (0.10 mmol), 1,4-dioxane (0.300 mL), catalyst **4b** (0.010 mmol) and trifluoroacetic acid (8 µL of a 1.33 M solution of TFA in 1,4-dioxane, 0.010 mmol). The mixture was stirred for five minutes then acrolein **2a** (0.25 mmol) was added in one portion.
After 18 h, the reaction mixture was filtered through a plug of silica gel, and the plug was washed with Et_2O (4x). After removal of solvents, the reaction crude was analysed by ^1H NMR spectroscopy to determine the diastereomeric ratio of the cycloadducts. Finally, the residue was purified by chromatography on silica gel (*n*-hexane/EtOAc mixtures).

Method B. To a vial equipped with a magnetic stirring bar, $MgSO_4$ (50 mg) was added, followed by the catalyst **4d** (0.020 mmol), a CH_2Cl_2/*i*-PrOH mixture (8:2, 0.200 mL) and trifluoroacetic acid (16 µL of a 1.33 M solution of TFA in CH_2Cl_2/*i*-PrOH 8:2, 0.020 mmol). The vial was placed in a bath at the desired temperature, stirred for five minutes, then the α,β-unsaturated aldehyde **2b-d** (0.25 mmol) was added in one portion. After stirring for additional five minutes, the indole derivative **1g** (0.10 mmol) was added. The resulting suspension was stirred at the same temperature for the appropriate time, then it was filtered through a plug of silica gel, and the plug was washed with Et_2O (4x). After removal of the solvents, the reaction crude was analysed by ^1H NMR spectroscopy to determine the diastereomeric ratio of the cycloadducts. Finally, the residue was purified by chromatography on silica gel (*n*-hexane/EtOAc mixtures).

(4*R*,5*S*)-5-(2-Oxopropyl)-1,3,4,5-tetrahydrobenzo[*cd*]indole-4-carbaldehyde (3a)

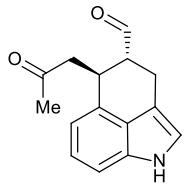

Following the method A of the general procedure, the title compound was obtained as a yellow solid in 76% yield after chromatography on silica gel (*n*-hexane/EtOAc 1:1). The diasteromeric ratio was evaluated by ^{1}H NMR of the crude mixture and was found to be >20:1. The enantiomeric excess of the product was determined by chiral stationary phase HPLC (AD-H, *n*-hexane/*i*-PrOH 80:20, 0.75 mL/min, λ = 254 nm, t_{maj} = 11.9 min, t_{min} = 13.2 min, 98% ee). $[\alpha]_D^{22}$ = -73 ° (c = 0.60 in $CHCl_3$); ^{1}H NMR ($CDCl_3$, 400 MHz) δ = 9.53 (s, 1H), 8.12 (br s, 1H), 7.15-7.08 (m, 2H), 6.93-6.87 (m, 2H), 4.16-4.10 (m, 1H), 3.37 (dd, J = 15.9, 3.0 Hz, 1H), 3.00 (ddd, J = 15.9, 5.2, 1.5 Hz, 1H), 2.93-2.89 (m, 1H), 2.84 (dd, J = 17.5, 6.5 Hz, 1H), 2.77 (dd, J = 17.3, 7.3 Hz, 1H), 2.12 (s, 3H); ^{13}C NMR ($CDCl_3$, 100 MHz) δ = 207.3, 204.1, 133.9, 131.1, 126.0, 123.0, 118.8, 116.4, 109.2, 109.0, 50.9, 49.0, 32.9, 30.7, 18.9; MS (EI) m/z: 241 (M^+).

(4*R*,5*S*)-5-(2-Oxo-2-phenylethyl)-1,3,4,5-tetrahydrobenzo[*cd*]indole-4-carbaldehyde (3b)

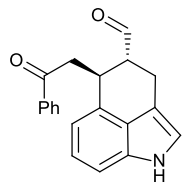

Following the method A of the general procedure, the title compound was obtained as a yellow solid in 75% yield after chromatography on silica gel (*n*-hexane/EtOAc 1:1). The diasteromeric ratio was evaluated by ^{1}H NMR of the crude mixture and was found to be >20:1. The enantiomeric excess of the product was determined by chiral stationary phase HPLC (AD-H, *n*-hexane/*i*-PrOH 80:20, 0.75 mL/min, λ = 254 nm, t_{min} = 17.7 min, t_{maj} = 20.5 min, 98% ee). $[\alpha]_D^{22}$ = -55° (c = 0.65 in $CHCl_3$); ^{1}H NMR ($CDCl_3$, 400 MHz) δ = 9.52 (s, 1H), 7.90 (br s, 1H), 7.89-7.86 (m, 2H), 7.52-7.45 (m, 1H), 7.40-7.32 (m, 2H), 7.14-7.02 (m, 2H), 6.94-6.88 (m, 2H), 4.32-4.25 (m, 1H), 3.39-3.20 (m, 3H), 3.03-2.94 (m, 2H); ^{13}C NMR ($CDCl_3$, 100 MHz) δ = 203.8, 198.4, 136.8, 133.9, 133.3, 131.4, 128.7, 128.1, 126.2, 123.1, 118.7, 116.6, 109.2, 109.1, 50.7, 44.2, 33.2, 18.7; MS (EI) m/z: 303 (M^+).

(4*R*,5*S*)-5-(2-(4-Bromophenyl)-2-oxoethyl)-1,3,4,5-tetrahydrobenzo[*cd*]indole-4-carbaldehyde (3c)

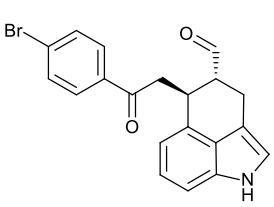

Following the method A of the general procedure, the title compound was obtained as a yellow solid in 78% yield after chromatography on silica gel (*n*-hexane/EtOAc 1:1). The diasteromeric ratio was evaluated by ^{1}H NMR of the crude mixture and was found to be >20:1. The enantiomeric excess of the product was determined by chiral stationary phase HPLC (AD-H, *n*-hexane/*i*-PrOH 80:20, 0.75 mL/min, λ = 254 nm, t_{min} = 24.1 min, t_{maj} = 27.9 min, 91% ee). $[\alpha]_D^{22}$ = -80° (c = 0.50 in CH_2Cl_2); ^{1}H NMR ($CDCl_3$, 400 MHz) δ = 9.58 (s, 1H), 7.99 (br s, 1H), 7.77 (d, J = 8.6 Hz, 2H), 7.57 (d, J =

8.4 Hz, 2H), 7.20-7.09 (m, 2H), 6.99-6.93 (m, 2H), 4.37-4.28 (m, 1H), 3.45-3.39 (m, 1H), 3.35 (dd, J = 5.3 , 17.1 Hz, 1H), 3.26 (dd, J = 8.6 , 17.4 Hz, 1H), 3.09-3.01 (m, 2H); ^{13}C NMR ($CDCl_3$, 100 MHz) δ =203.7, 197.4, 135.6, 133.9, 132.0, 129.6, 128.5, 126.1, 123.2, 118.8, 116.6, 109.3, 109.1, 50.7, 44.1, 33.2, 18.8; ESIMS: 404-406 [M+Na$^+$].

(4*R*,5*S*)-5-(2-(4-Methoxyphenyl)-2-oxoethyl)-1,3,4,5-tetrahydrobenzo[*cd*]indole-4-carbaldehyde (3d)

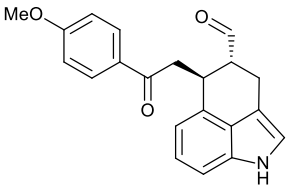

Following the method A of the general procedure, but using (*S*)-α,α-bis[3,5-bis(trifluoromethyl)phenyl]-2-pyrrolidinemethanol trimethylsilyl ether **4a** as catalyst, the title compound was obtained as a yellow solid in 70% yield after chromatography on silica gel (*n*-hexane/EtOAc 2:1). The diasteromeric ratio was evaluated by ^{1}H NMR of the crude mixture and was found to be >20:1. The enantiomeric excess of the product was determined by chiral stationary phase HPLC (AD-H, *n*-hexane/*i*-PrOH 80:20, 0.75 mL/min, λ = 254 nm, t_{maj} = 38.5 min, t_{min} = 30.9 min, >99% ee); $[\alpha]_D^{22}$ = -86° (c = 0.65 in CH_2Cl_2); ^{1}H NMR ($CDCl_3$, 400 MHz) δ = 9.59 (s, 1H), 8.01 (br s, 1H), 7.92 (d, J = 8.7 Hz, 2H), 7.20-7.10 (m, 2H), 6.99-6.88 (m, 4H), 4.37-4.30 (m, 1H), 3.86 (s, 3H), 3.45-3.35 (m, 1H), 3.33 (dd, J = 5.7, 17.1 Hz, 1H), 3.26 (dd, J = 8.5, 17.2 Hz, 1H), 3.10-3.01 (m, 2H);^{13}C NMR ($CDCl_3$, 100 MHz) δ = 204.0, 196.9, 163.6, 133.9, 131.6, 130.4, 130.0, 126.2, 123.1, 118.7, 116.6, 113.8, 109.3, 109.1, 55.5, 50.7, 43.8, 33.4, 18.6; ESIMS: 356 [M + Na$^+$].

(4*R*,5*S*)-5-(2-(4-Nitrophenyl)-2-oxoethyl)-1,3,4,5-tetrahydrobenzo[*cd*]indole-4-carbaldehyde (3e)

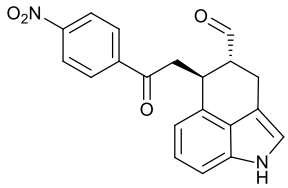

Following the method A of the general procedure, the title compound was obtained as an orange solid in 71% yield after chromatography on silica gel (*n*-hexane/EtOAc 2:1). The diasteromeric ratio was evaluated by ^{1}H NMR of the crude mixture and was found to be >20:1. Since every attempts to separate the enantiomers by chiral stationary phase HPLC failed, the enantiomeric ratio of this compound was evaluated by ^{1}H NMR spectroscopy, using (*S*)-1-anthracen-9-yl-2,2,2-trifluoroethanol (Pirkle's alcohol) as chiral shift reagent: in a NMR tube, 5 mg of compound **3e** were dissolved in 0.75 mL of CD_2Cl_2 then the ^{1}H NMR spectrum (600 MHz) was recorded at -15 °C. When 100 equiv. of Pirkle's alcohol were added, the doublet at 6.94 ppm (J = 7.1 Hz) split into two doublets centred at 6.95 and 6.93 ppm (J = 7.1 Hz), integration of those peaks furnished the enantiomeric ratio that was equal to 98 : 2. $[\alpha]_D^{22}$ = -125° (c = 0.35 in CH_2Cl_2); ^{1}H NMR ($CDCl_3$, 400 MHz) δ = 9.59 (s, 1H), 8.26 (d, J = 8.8 Hz, 2H), 8.06-8.00 (m, 3H), 7.19 (d, J = 8.5 Hz, 1H), 7.11 (t, J = 7.6 Hz, 1H), 6.98 (br s, 1H), 6.94 (d, J = 7.1 Hz, 1H), 4.39-4.30 (m, 1H), 3.50-3.40 (m,

2H), 3.33 (dd, J = 7.9, 17.6 Hz, 1H), 3.12-3.03 (m, 2H); ^{13}C NMR ($CDCl_3$, 100 MHz) δ = 202.4, 195.9, 149.4, 140.2, 133.0, 129.7, 128.1, 125.0, 122.8, 122.2, 117.9, 115.7, 108.4, 107.9, 49.8, 43.7, 32.2, 17.9; ESIMS: 347 [M - H].

(4*R*,5*S*)-2-Methyl-5-(2-oxopropyl)-1,3,4,5-tetrahydrobenzo[*cd*]indole-4-carbaldehyde (3f)

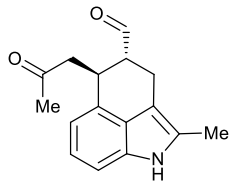

Following the method A of the general procedure, the title compound was obtained as a white solid in 81% yield after chromatography on silica gel (*n*-hexane/EtOAc 3:2). The diasteromeric ratio was evaluated by ^{1}H NMR of the crude mixture and was found to be >20:1. The enantiomeric excess of the product was determined by chiral stationary phase HPLC (OJ-H, *n*-hexane/*i*-PrOH 80:20, 0.75 mL/min, λ = 254 nm, t_{maj} = 32.2 min, t_{min} = 30.3 min, >99% ee). $[\alpha]_D^{22}$ = -33° (c = 0.700 in CH_2Cl_2); ^{1}H NMR ($CDCl_3$, 400 MHz) δ = 9.51 (s, 1H), 7.73 (br s, 1H), 7.09-6.99 (m, 2H), 6.87 (d, J = 7.0 Hz, 1H), 4.12-4.06 (m, 1H), 3.30-3.20 (m, 1H), 2.92-2.69 (m, 4H), 2.38 (s, 3H), 2.13 (s, 3H); ^{13}C NMR ($CDCl_3$, 100 MHz) δ = 207.2, 204.0, 133.5, 130.0, 128.9, 127.1, 121.9, 116.4, 108.3, 105.1, 58.8, 49.0, 33.0, 30.7, 19.2, 11.7; MS (EI) m/z: 255 (M^+).

(4*R*,5*S*)-1-Methyl-5-(2-oxopropyl)-1,3,4,5-tetrahydrobenzo[*cd*]indole-4-carbaldehyde (3g)

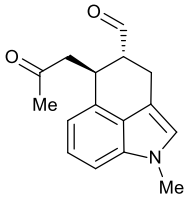

Following the method A of the general procedure, but using 20 mol% of catalyst **4b** and running the reaction for 48 h, the title compound was obtained as a yellow solid in 67% yield after chromatography on silica gel (*n*-hexane/EtOAc 3:2). The diasteromeric ratio was evaluated by ^{1}H NMR of the crude mixture and was found to be >20:1. The enantiomeric excess of the product was determined by chiral stationary phase HPLC (AD-H, *n*-hexane/*i*-PrOH 80:20, 0.75 mL/min, λ = 254 nm, t_{maj} = 15.3 min, t_{min} = 11.7 min, 99% ee). $[\alpha]_D^{22}$ = -38° (c = 0.50 in CH_2Cl_2) ^{1}H NMR ($CDCl_3$, 400 MHz) δ = 9.54 (s, 1H), 7.19-7.09 (m, 2H), 6.92-6.87 (m, 1H), 6.80 (s, 1H), 4.17-4.09 (m, 1H), 3.74 (s, 3H), 3.37 (dd, J = 15.9, 2.9 Hz, 1H), 3.05-2.70 (m, 4H), 2.17 (s, 3H); ^{13}C NMR ($CDCl_3$, 100 MHz) δ = 206.1, 202.9, 133.9, 130.2, 125.3, 122.4, 121.7, 114.9, 106.7, 106.4, 49.9, 48.0, 31.9, 31.8, 29.7, 17.2; MS (EI) m/z: 255 (M^+).

(3*S*,4*S*,5*R*)-1,3-Dimethyl-5-(2-oxopropyl)-1,3,4,5-tetrahydrobenzo[*cd*]indole-4-carbaldehyde (3h)

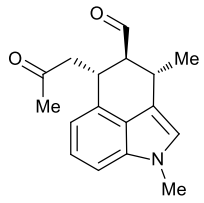

Following the method B of the general procedure (-30 °C, 65 h reaction time), the title compound was obtained as a yellow solid in 71% yield after chromatography on silica gel (*n*-hexane/EtOAc 3:2). The diasteromeric ratio was evaluated by ^{1}H

NMR of the crude mixture and was found to be >20:1. The enantiomeric excess of the product was determined by chiral stationary phase HPLC (AD-H, *n*-hexane/*i*-PrOH 80:20, 0.75 mL/min, λ = 254 nm, t_{maj} = 13.2 min, t_{min} = 12.0 min, 86% ee). $[\alpha]_D^{22}$ = +30° (c = 0.333 in $CHCl_3$) ^{1}H NMR ($CDCl_3$, 400 MHz) δ = 9.66 (d, J = 4.6 Hz, 1H), 7.19-7.11 (m, 2H), 6.80 (d, J = 1.6 Hz, 1H), 6.76 (d, J = 6.8 Hz, 1H), 4.10 (dt, J = 5.7.; 9.1 Hz, 1H), 3.77 (s, 3H), 3.57-3.49 (m, 1H), 3.09 (dd, J = 18.3; 5.9 Hz, 1H), 2.86 (dd, J = 18.3; 5.9 Hz, 1H), 2.36 (td, J = 4.6; 9.1 Hz, 1H), 2.24 (s, 3H), 1.36 (d, J = 6.9 Hz, 3H); ^{13}C NMR ($CDCl_3$, 100 MHz) δ = 207.4, 205.3, 134.8, 131.4, 125.8, 122.6, 115.1, 113.9, 107.2, 61.3, 46.5, 32.9, 32.8, 30.5, 28.4, 19.4; MS (EI) m/z: 269 (M^+).

(3*R*,4*R*,5*R*)-1-Methyl-5-(2-oxopropyl)-3-phenyl-1,3,4,5-tetrahydrobenzo[*cd*]indole-4-carbaldehyde (3i)

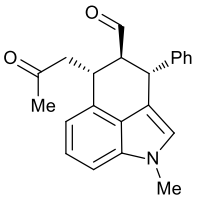

Following the method B of the general procedure (0 °C, 65 h reaction time), the title compound was obtained as white solid in 74% yield after chromatography on silica gel (*n*-hexane/EtOAc 8:2). The diasteromeric ratio was evaluated by ^{1}H NMR of the crude mixture and was found to be > 20:1. The enantiomeric excess of the product was determined by chiral stationary phase HPLC (AD-H, *n*-hexane/*i*-PrOH 80:20, 0.75 mL/min, λ = 254 nm, t_{maj} = 12.7 min, t_{min} = 14.0 min, 83% ee). The product was crystalized from *n*-hexane/EtOAc/CH_2Cl_2 (7:1:2), and the mother liquor contained the product in 98% ee. $[\alpha]_D^{22}$ = -101° (c = 0.60 in CH_2Cl_2) ^{1}H NMR ($CDCl_3$, 400 MHz) δ = 9.58 (s, 1H), 7.32-7.16 (m, 7H), 6.86-6.82 (m, 1H), 6.73 (s, 1H), 4.88 (d, J = 5.0 Hz, 1H), 4.21-4.11 (m, 1H), 3.78 (s, 3H), 3.23 (dt, J = 1.7, 5.2 Hz, 1H), 2.67 (dd, J = 5.7, 18.6 Hz, 1H), 2.57 (dd, J = 8.0, 18.6 Hz, 1H), 1.73 (s, 3H); ^{13}C NMR ($CDCl_3$, 100 MHz) δ = 207.4, 203.9, 143.6, 135.0, 131.4, 128.7, 128.1, 126.7, 126.6, 125,0, 122.7, 115.2, 111.1, 107.3, 58.6, 47.5, 38.7, 33.2, 30.9, 29.9; MS (EI) m/z: 331 (M^+).

(3*R*,4*R*,5*R*)-1-Methyl-3-(4-nitrophenyl)-5-(2-oxopropyl)-1,3,4,5-tetrahydrobenzo[*cd*]indole-4-carbaldehyde (3j)

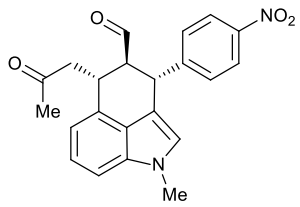

Following the method B of the general procedure (RT, 18 h reaction time), the title compound was obtained as a yellowish solid in 77% yield after chromatography on silica gel (*n*-hexane/EtOAc 7:3). The diasteromeric ratio was evaluated by ^{1}H NMR of the crude mixture and was found to be >20:1. The enantiomeric excess of the product was determined by chiral stationary phase HPLC (AD-H, *n*-hexane/*i*-PrOH 70:30, 0.75 mL/min, λ = 254 nm, t_{maj} = 21.3 min, t_{min} = 25.5 min, 95% ee). $[\alpha]_D^{22}$ = -41° (c = 0.467 in $CHCl_3$) ; ^{1}H NMR ($CDCl_3$, 400 MHz) δ = 9.58 (d, J = 2.0 Hz, 1H), 8.14 (d, J = 8.7 Hz, 2H), 7.40 (d, J = 9.0 Hz, 2H), 7.23-7.18 (m, 2H), 6.87 (d, J = 6.1 Hz, 1H), 6.71

(br s, 1H), 4.97 (d, J = 5.3 Hz, 1H), 4.22-4.15 (m, 1H), 3.80 (s, 3H), 3.25 (dt, J = 1.9, 5.3 Hz, 1H), 2.74 (dd, J = 5.2, 18.3 Hz, 1H), 2.50 (dd, J = 7.9, 18.3 Hz, 1H), 1.82 (s, 3H); ^{13}C NMR ($CDCl_3$, 100 MHz) δ = 205.8, 201.8, 150.6, 145.8, 134.1, 129.8, 128.1, 125.1, 124.0, 122.8, 122.0, 114.5, 109.0, 106.7, 57.7, 46.5, 37.8, 32.3, 32.0, 29.1; ESIMS: 399 [M + Na^+].

Elaboration of product 3a

(2a*S*,5*R*,6*S*)-6-(2-Oxopropyl)-5,6-dihydro-1H-2a,5-methanooxepino[2,3,4-cd]indole-2,4-dione (5)

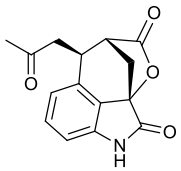

To a round bottomed flask equipped with a magnetic stirring bar, compound **3a** (0.07 mmol) was dissolved in *tert*-butyl alcohol (2.5 mL) and 2-methyl-2-butene (470 µL) and subsequently stirred for a few minutes. To this solution was added an aqueous solution of NaH_2PO_4 (120 µL of a 0.833 M solution, 0.10 mmol) and $NaClO_2$ (80 µL of a 1.11 M solution, 0.09 mmol). The mixture was stirred at room temperature for 90 minutes, then the organic solvents were removed by concentrating in vacuo. The residue was diluted with 2 mL of water, then the mixture was extracted with EtOAc twice. After drying over $MgSO_4$, filtration and evaporation of the solvents, the crude product was purified by column chromatography (*n*-hexane / EtOAc 1 : 2) to give the title compound as a brown solid in 56% yield. A single diastereoisomer was observed in the crude mixture, thus indicating that epimerisation did not occur. The enantiomeric excess of the product was determined by chiral stationary phase HPLC (AD-H, *n*-hexane/*i*-PrOH 70:30, 0.75 mL/min, λ = 254 nm, t_{maj} = 11.3 min, t_{min} = 12.2 min, 97% ee) a single enantiomer was recognized in the HPLC trace thus indicating that racemisation did not occur. ^{1}H NMR (CD_2Cl_2, 600 MHz) δ = 7.51 (br s, 1H), 7.21 (t, J = 8.3 Hz, 1H), 6.77 (d, J = 8.2 Hz, 1H), 6.68 (d, J = 8.2 Hz, 1H), 3.71 (dd, J = 2.7; 8.2 Hz 1H), 3.08 (dd, J = 2.2, 5.4 Hz, 1H), 2.80 (dd, J = 4.8; 18.4 Hz, 1 H) 2.68-2.61 (m, 2H), 2.12 (s, 3H); 2.05-2.01 (m, 1H) ^{13}C NMR (CD_2Cl_2, 100 MHz) δ =204.6, 175.0, 169.9, 137.6, 134.2, 131.4, 125.9, 120.4, 107.7, 78.0, 47.1, 43.9, 33.1, 31.1, 29.2; ^{13}C NMR DEPT 1.5 ($CDCl_3$, 100 MHz) δ = 131.4 (CH), 120.4 (CH), 107.7 (CH), 47.1 (CH_2), 43.9 (CH), 33.1 (CH), 31.1 (CH_2), 29.2 (CH_3); $[\alpha]_D^{22}$ = +123° (c = 0.100 in CH_3CN); ESIMS: 294 [M + Na^+].

(6a*S*,10a*S*)-6,6a,10,10a-Tetrahydronaphtho[3,2,1-*cd*]indol-9(4*H*)-one and (6a*R*,10a*S*)-6,6a,10,10a-tetrahydronaphtho[3,2,1-*cd*]indol-9(4*H*)-one (6)

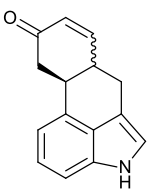

To a round bottomed flask equipped with a magnetic stirring bar, L-proline (0.07 mmol) was added, followed by 1 mL of acetonitrile, and finally $HClO_4$ was added in one portion (38 µL of 1.80 M solution of $HClO_4$ in acetonitrile, 0.07 mmol) and subsequently stirred for few minutes to allow the complete solubilisation of L-proline. To this solution was added compound **3a** (0.21 mmol) and the mixture was stirred for 16 hours at 55 °C, then it was filtered on plug of silica gel and the plug was washed several times with DCM and Et_2O. The diasteromeric ratio was evaluated by ^{1}H NMR of the crude mixture and was found to be 59:41; the yield was also determined by ^{1}H NMR of the crude mixture by using 1,1,2,2-

tetrachloroethane as internal standard and was found to be 64% referred to both diasteroisomers. The diasteroisomers were isolated by means of semi-preparative HPLC on a C18 column (Phenomenex® Synergi Hydro-RP) using Acetonitrile/H_2O 60:40.

The minor diasteroisomer was obtained in analytically pure form and was fully characterized. The enantiomeric excess of this product was determined by chiral stationary phase HPLC (AD-H, *n*-hexane/*i*-PrOH 80:20, 0.75 mL/min, λ = 254 nm, t_{maj} = 12.5 min, t_{min} = 13.7 min, 99% ee), a single enantiomer was recognized in the HPLC trace thus indicating that racemisation did not occur. Full assignment of the ^{1}H and ^{13}C spectra was achieved by bi-dimensional experiments (gHSQC, gHMBC and gCOSY taken in CD_3CN solutions at 45 °C) that confirms the proposed structure for compound *cis*-**6**. ^{1}H NMR (CD_3CN, 400 MHz, 60 °C) δ = 8.93 (br s, 1H), 7.23 (d, J = 7.8 Hz, 1H), 7.12 (t, J = 7.8 Hz, 1H), 7.05 (dd, J = 3.4, 9.8 Hz, 1H), 7.00 (br s, 1H), 6.89 (d, J = 7.5 Hz, 1H), 5.88 (d, J = 10.4 Hz, 1H), 3.78-3.71 (m, 1H), 3.19 (dd, J = 5.0, 15.2 Hz, 1H), 3.10 (br s, 1H), 2.95-2.69 (m, 3H); ^{13}C NMR (CD_3CN, 100 MHz, 45 °C) δ = 203.8, 154.5, 134.2, 132.0, 126.5, 122.6, 118.5, 115.3, 111.1, 103.0, 41.6, 37.0, 37.3, 29.4; $[\alpha]_D^{22}$ = +20° (c = 0.35 in CH_2Cl_2); ESIMS: 246 [M + Na^+].

The major isomer was not obtained in analytically pure form. GC/MS analysis however confirmed the identity of this compound, as a major peak was observed with molecular mass compatible with the expected Robinson's cycloadduct: MS (EI) m/z: 223 (M^+) (see chromatogram below). The structure of this latter compound was thus reasonably assigned as the diastereomeric form *trans*, while the *cis* isomer assignment is detailed above (see also § "Determination of relative and absolute configuration of the adducts **3** and **6**")

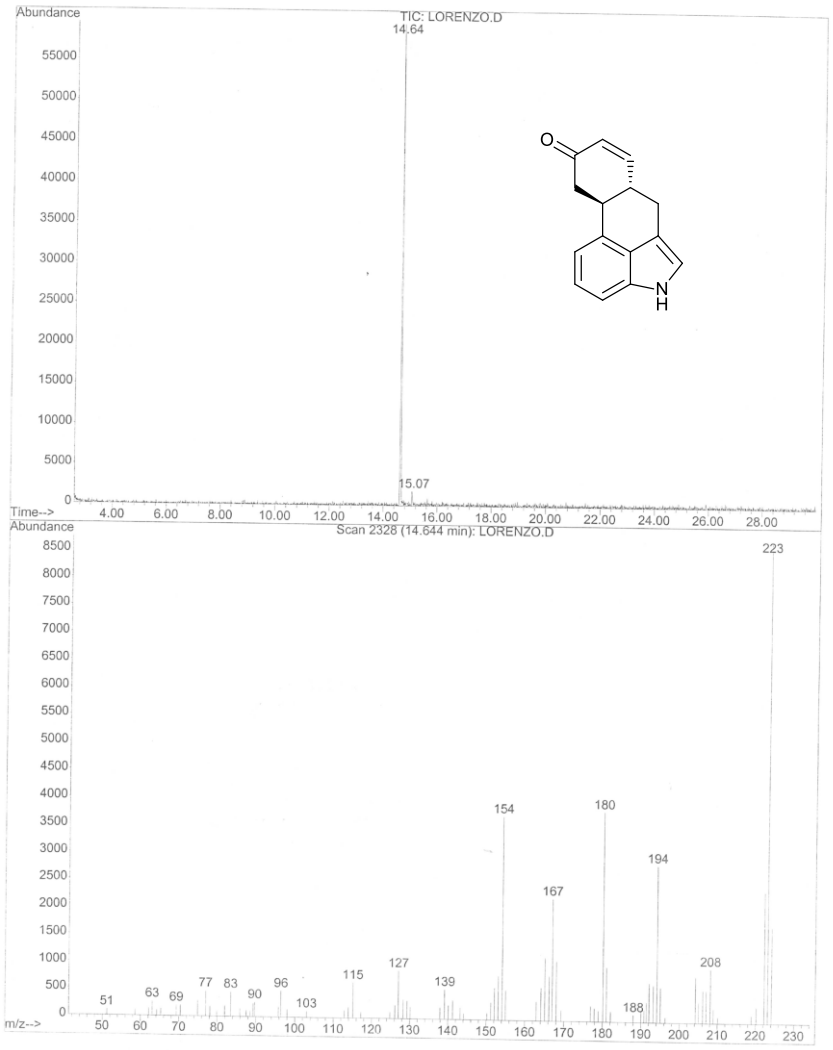
Abundance
TIC: LORENZO.D
14.64
15.07
Time-->
Abundance
Scan 2328 (14.644 min): LORENZO.D
223
154
180
194
167
208
188
127
115
139
m/z-->

Copies of the ^{1}H and ^{13}C NMR spectra and HPLC traces

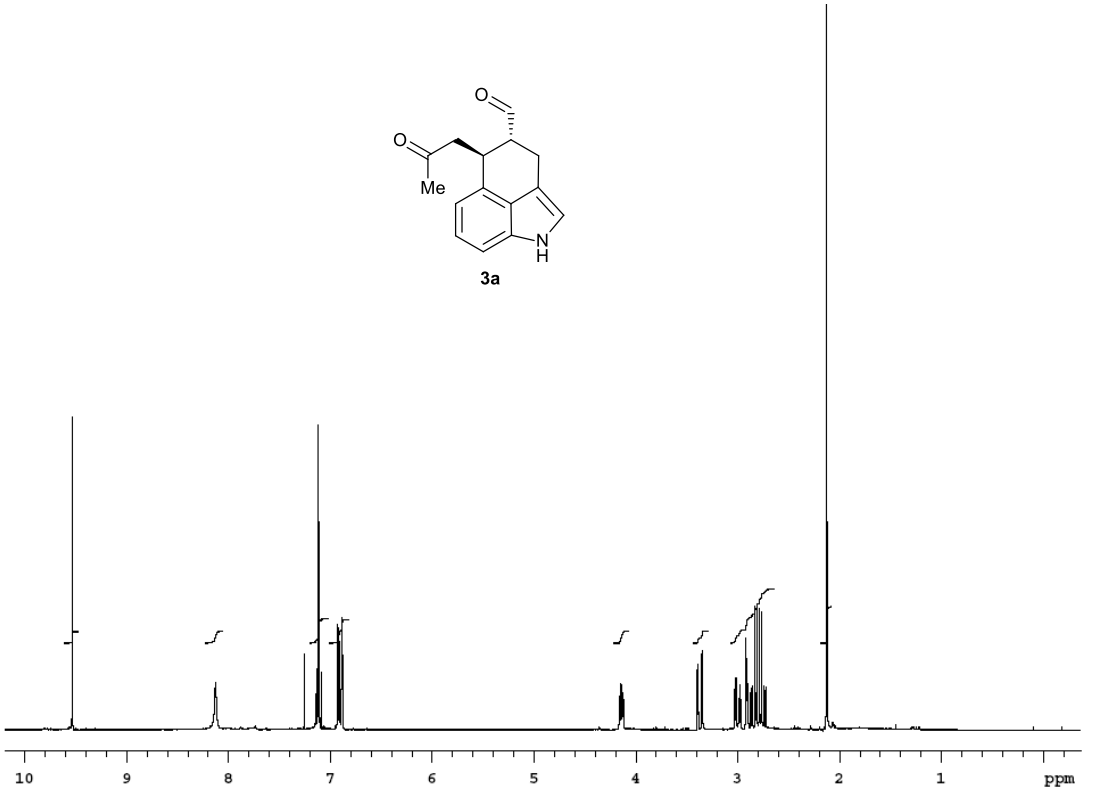

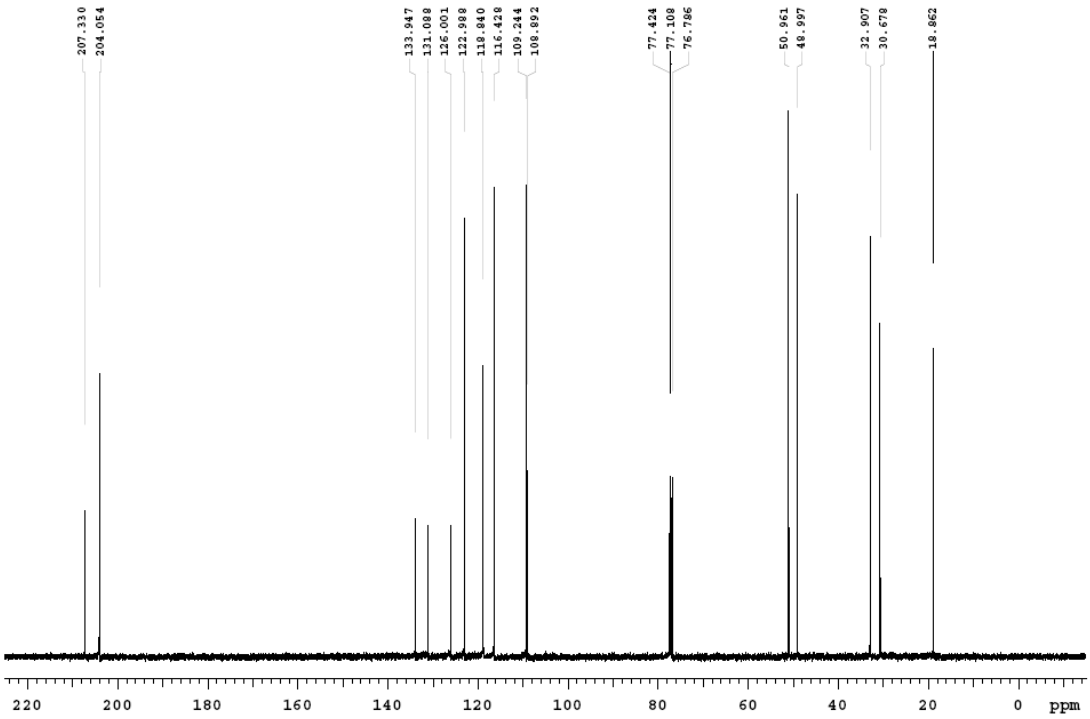

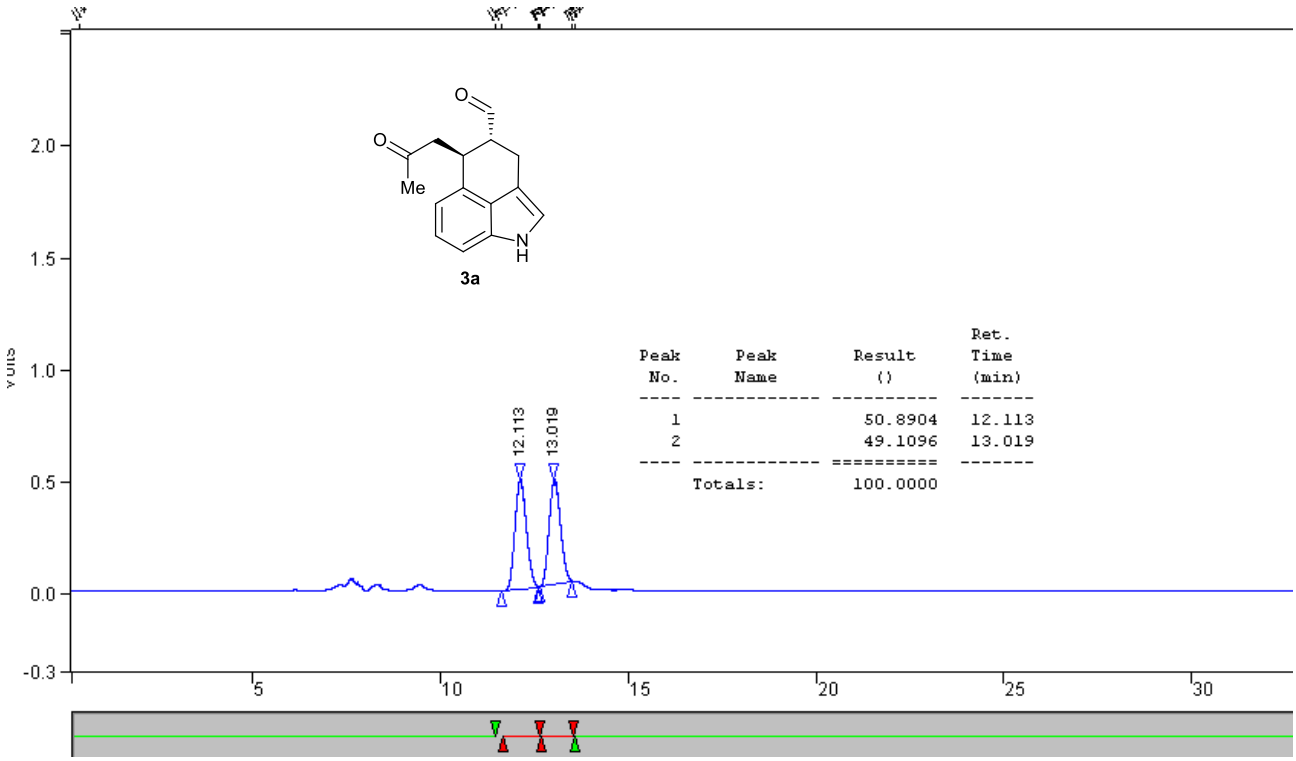
O
O
Me
N
H
3a
Peak No. | Peak Name | Result () | Ret. Time (min)
1 | | 50.8904 | 12.113
2 | | 49.1096 | 13.019
Totals: 100.0000
12.113
13.019
2.0
1.5
1.0
0.5
0.0
-0.3
5
10
15
20
25
30

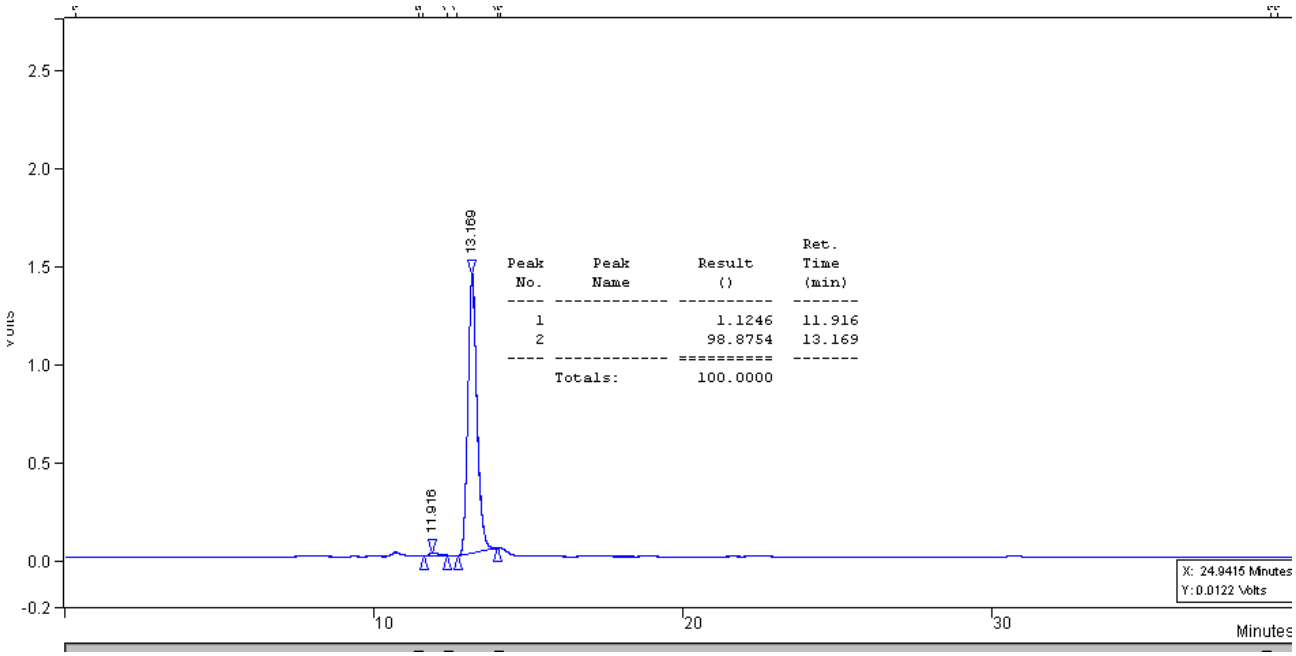
Peak No. | Peak Name | Result () | Ret. Time (min)
1 | | 1.1246 | 11.916
2 | | 98.8754 | 13.169
Totals: 100.0000
13.169
11.916
2.5
2.0
1.5
1.0
0.5
0.0
-0.2
10
20
30
Minutes
X: 24.9415 Minutes
Y: 0.0122 Volts

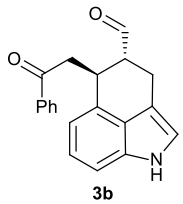

3b

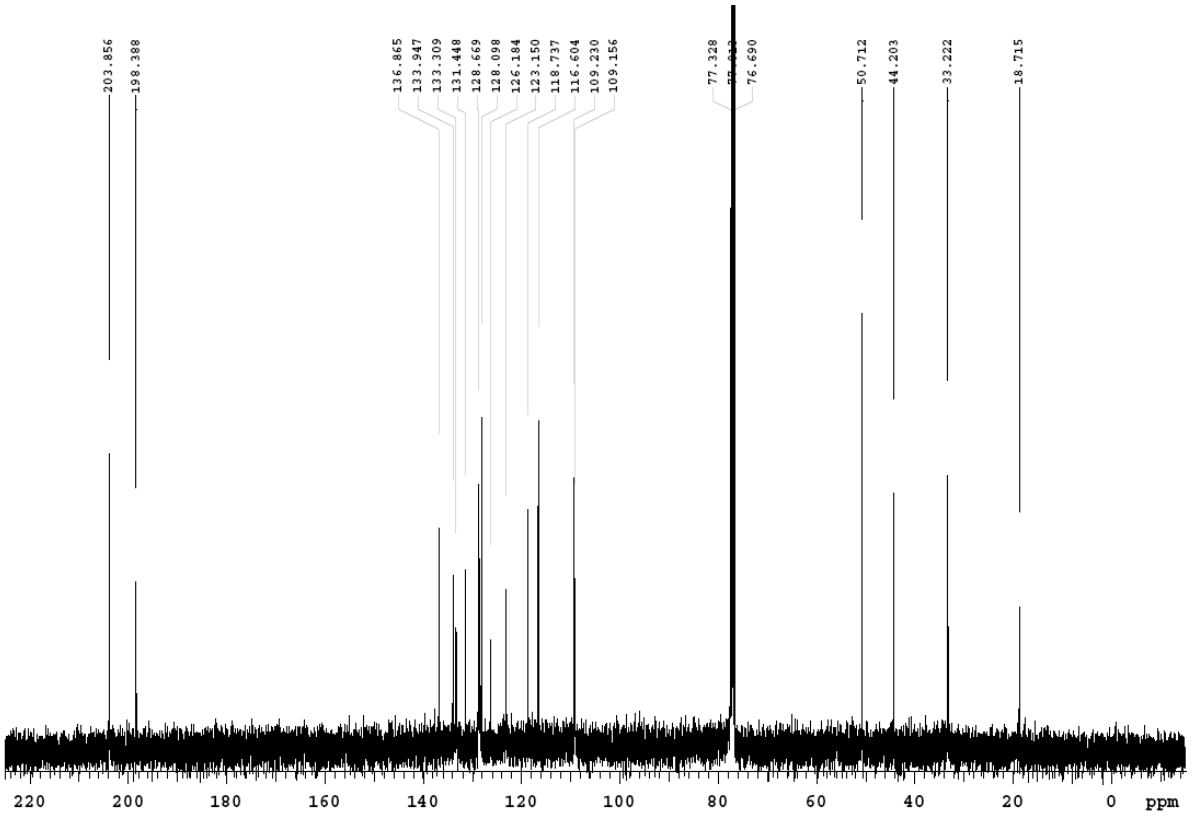

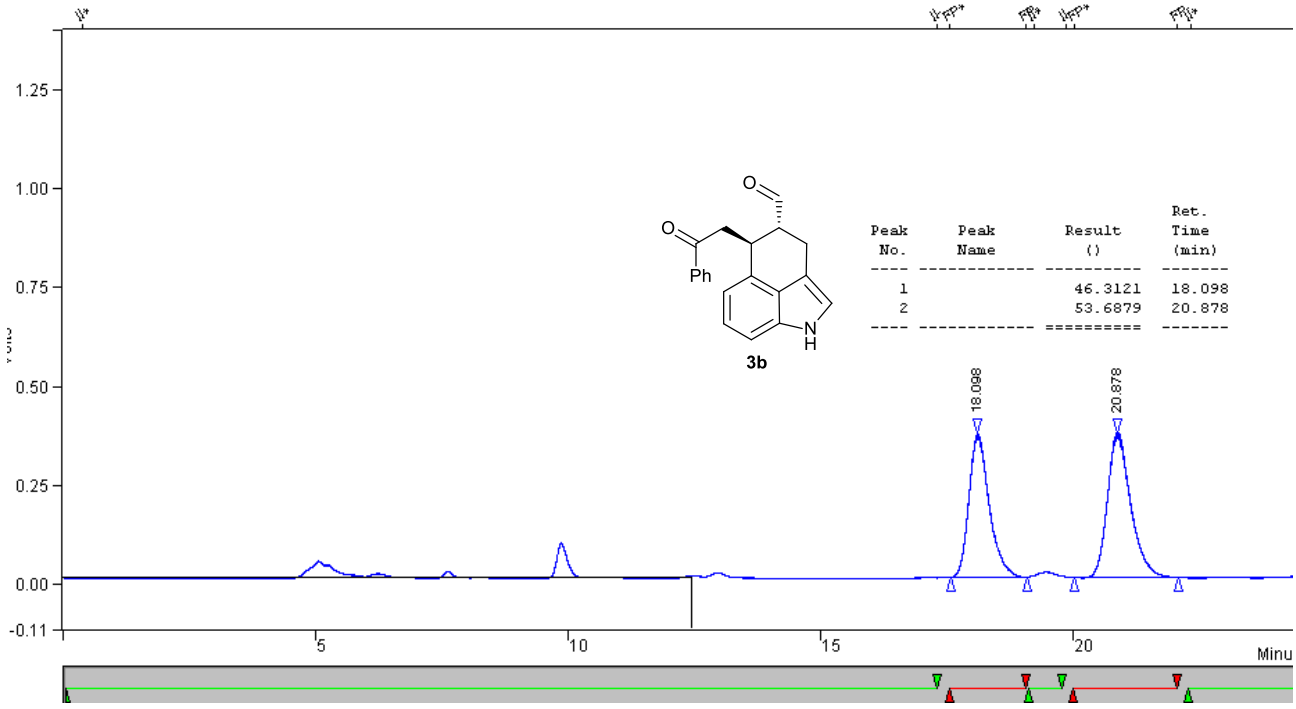
1.25
1.00
0.75
0.50
0.25
0.00
-0.11
5
10
15
20
Minu
18.098
20.878
O
O
Ph
N
H
3b
Peak No. | Peak Name | Result () | Ret. Time (min)
1 | | 46.3121 | 18.098
2 | | 53.6879 | 20.878

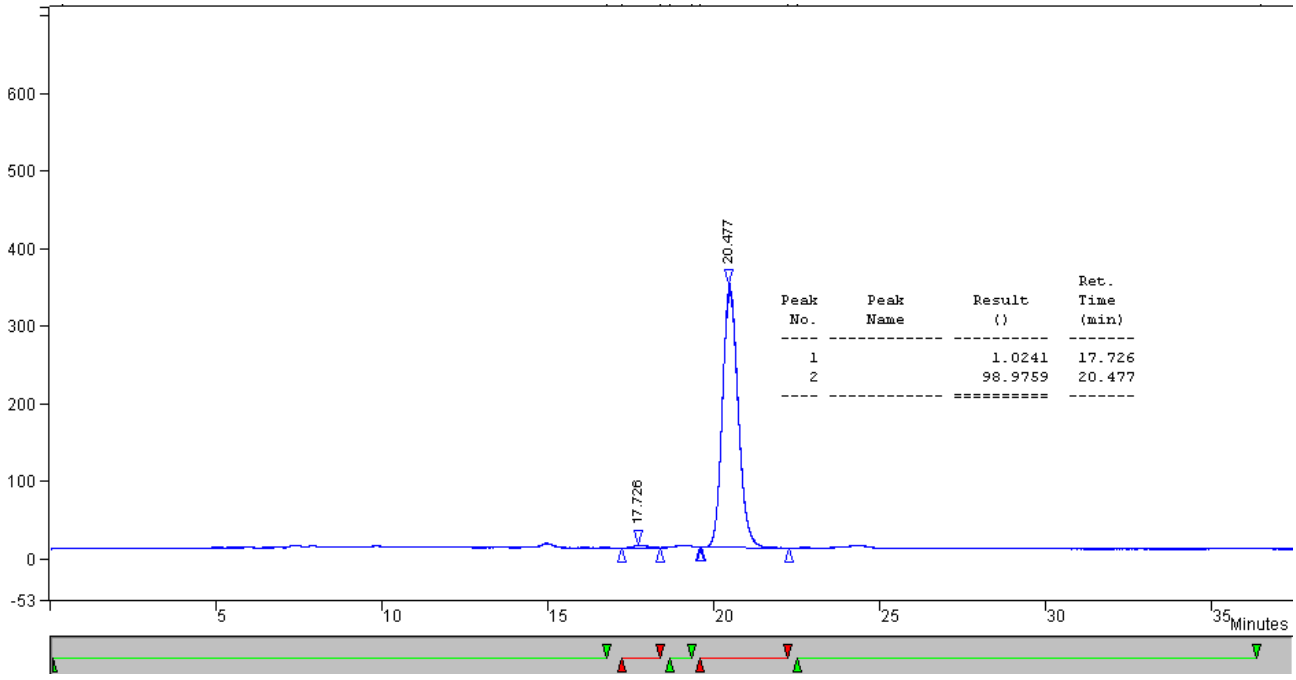
600
500
400
300
200
100
0
-53
5
10
15
20
25
30
35
Minutes
17.726
20.477
Peak No. | Peak Name | Result () | Ret. Time (min)
1 | | 1.0241 | 17.726
2 | | 98.9759 | 20.477

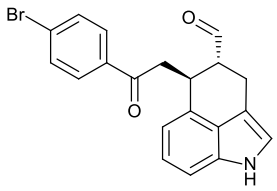

3c

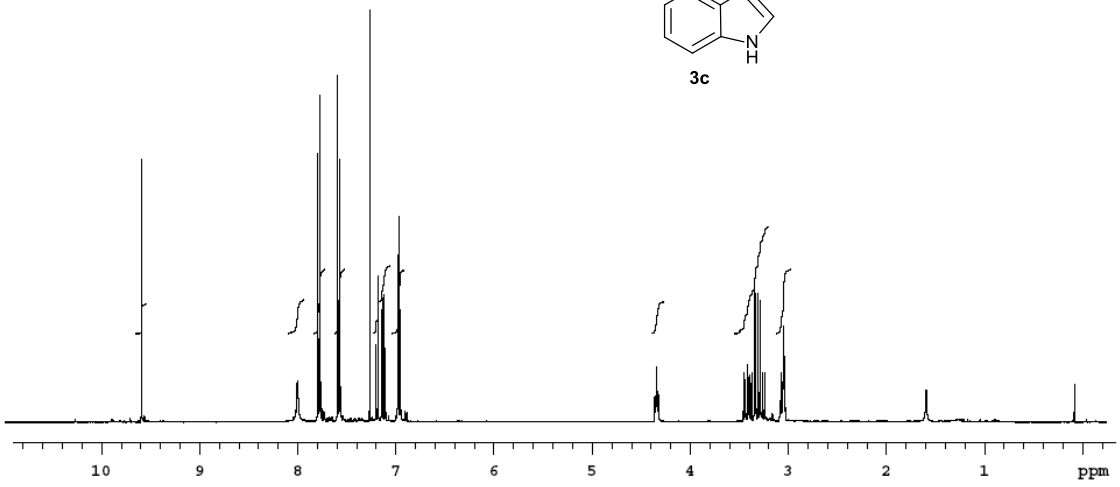

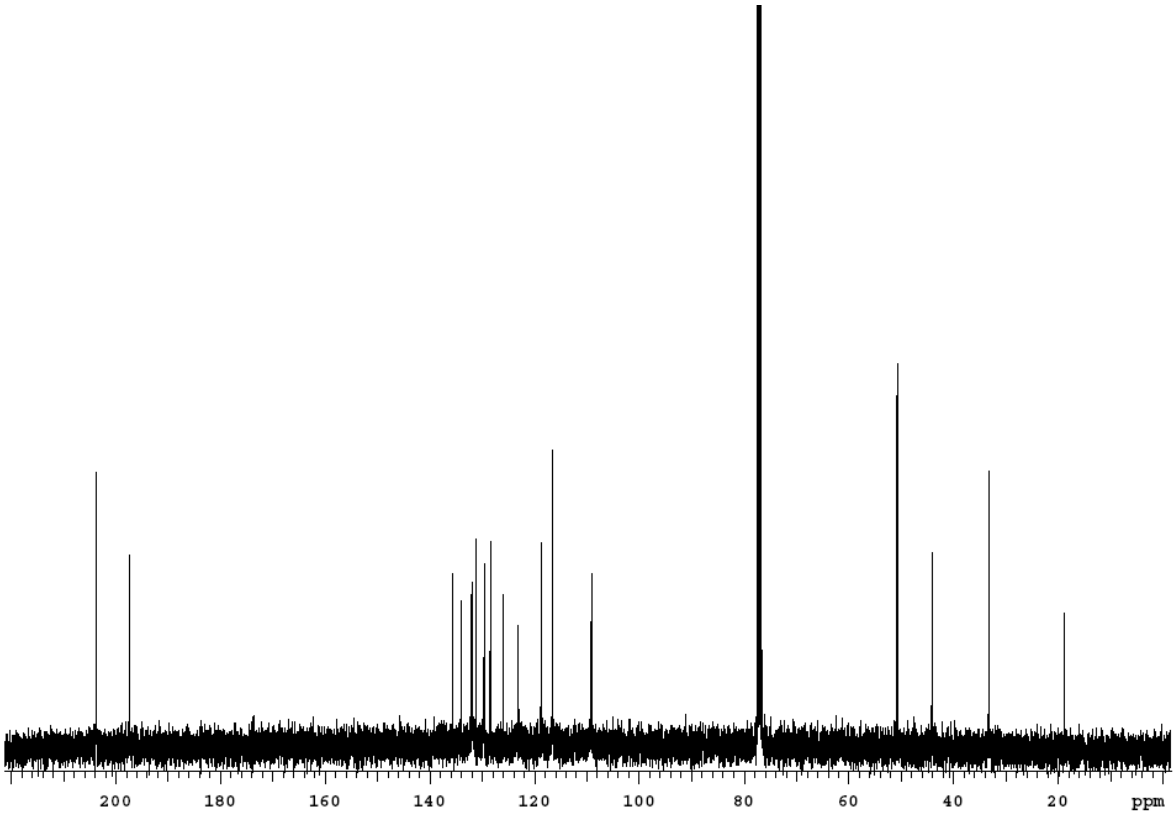

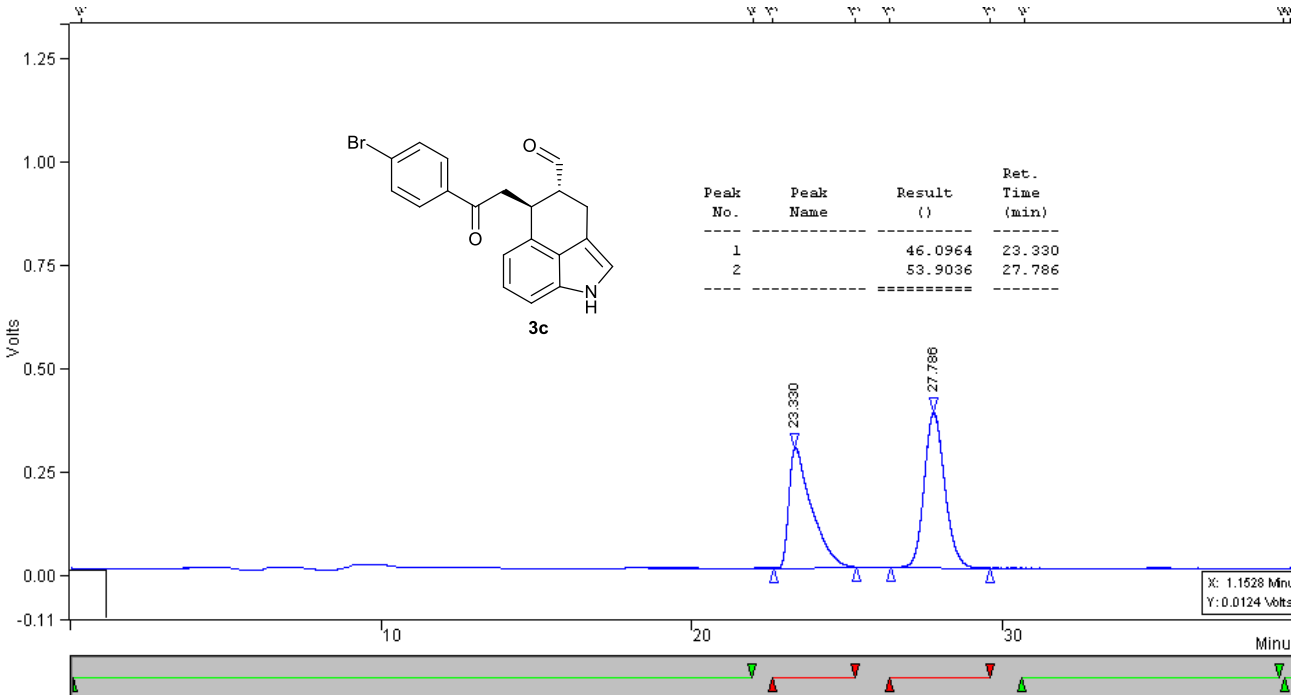
Br
O
O
N
H
3c
Peak No. | Peak Name | Result () | Ret. Time (min)
1 | | 46.0964 | 23.330
2 | | 53.9036 | 27.786
Volts
1.25
1.00
0.75
0.50
0.25
0.00
-0.11
23.330
27.786
10
20
30
Minu

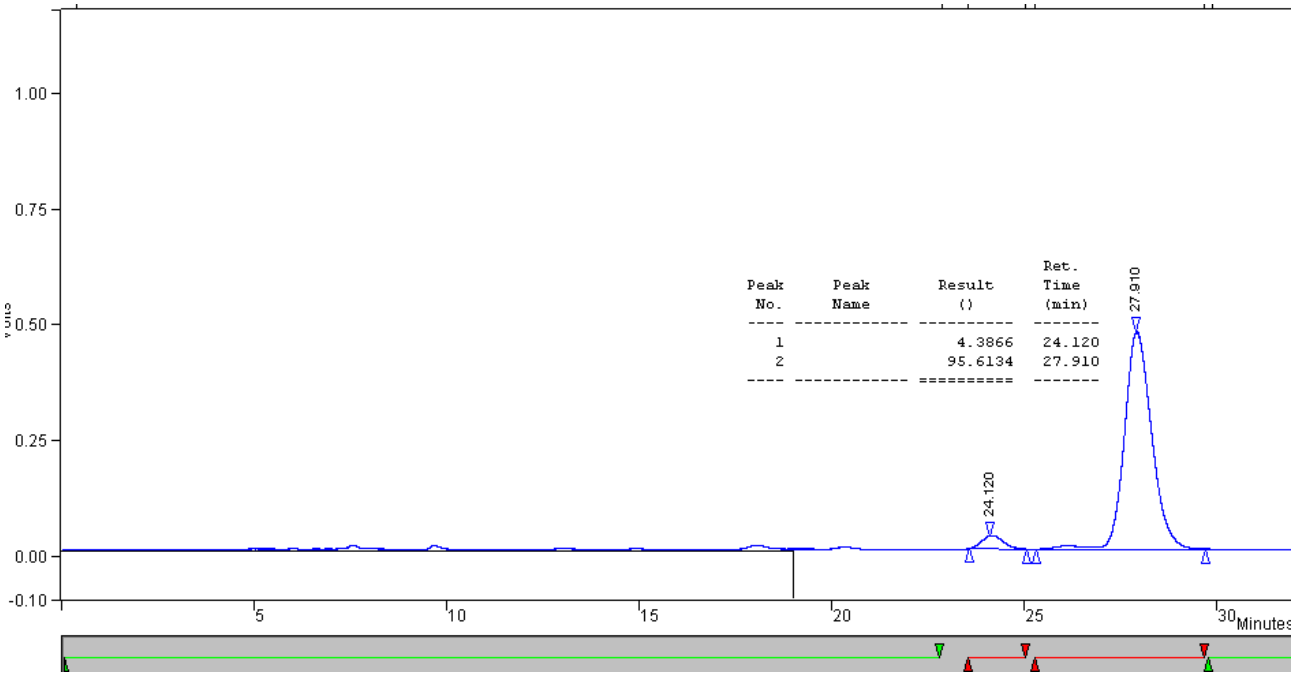
Peak No. | Peak Name | Result () | Ret. Time (min)
1 | | 4.3866 | 24.120
2 | | 95.6134 | 27.910
1.00
0.75
0.50
0.25
0.00
-0.10
24.120
27.910
5
10
15
20
25
30
Minutes

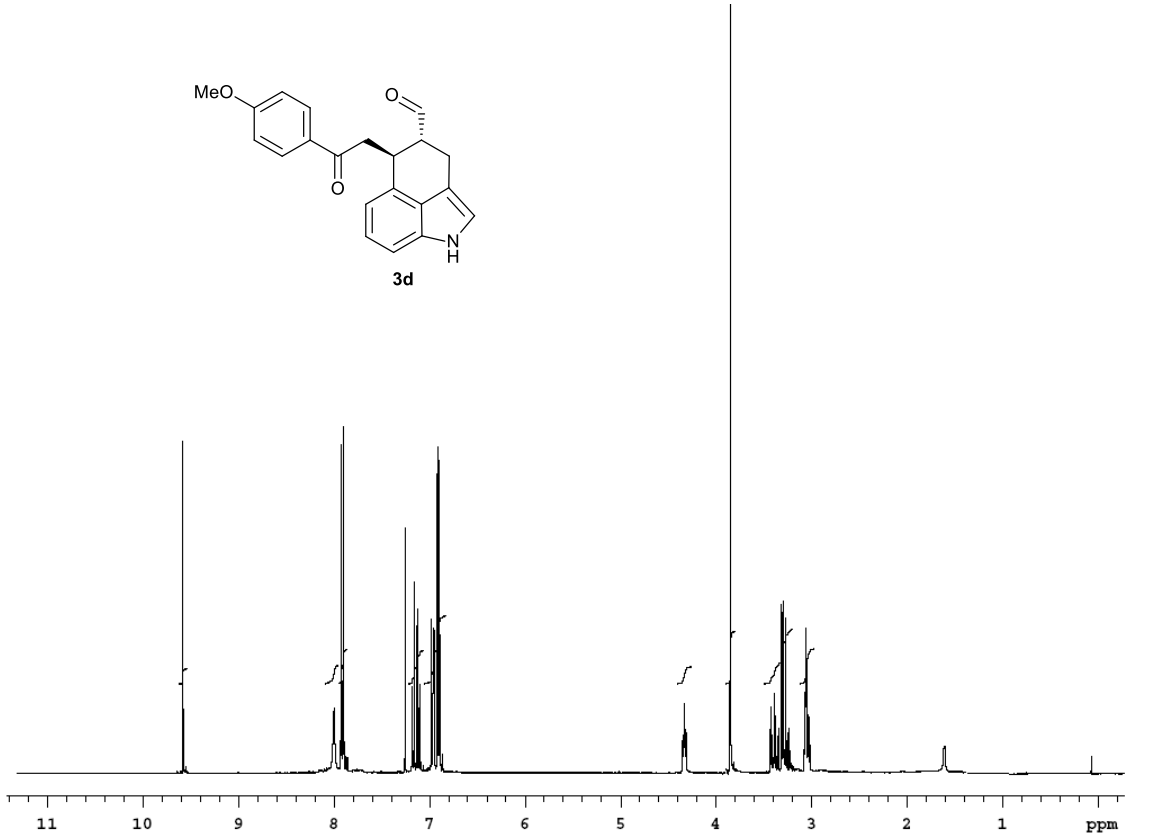

3d

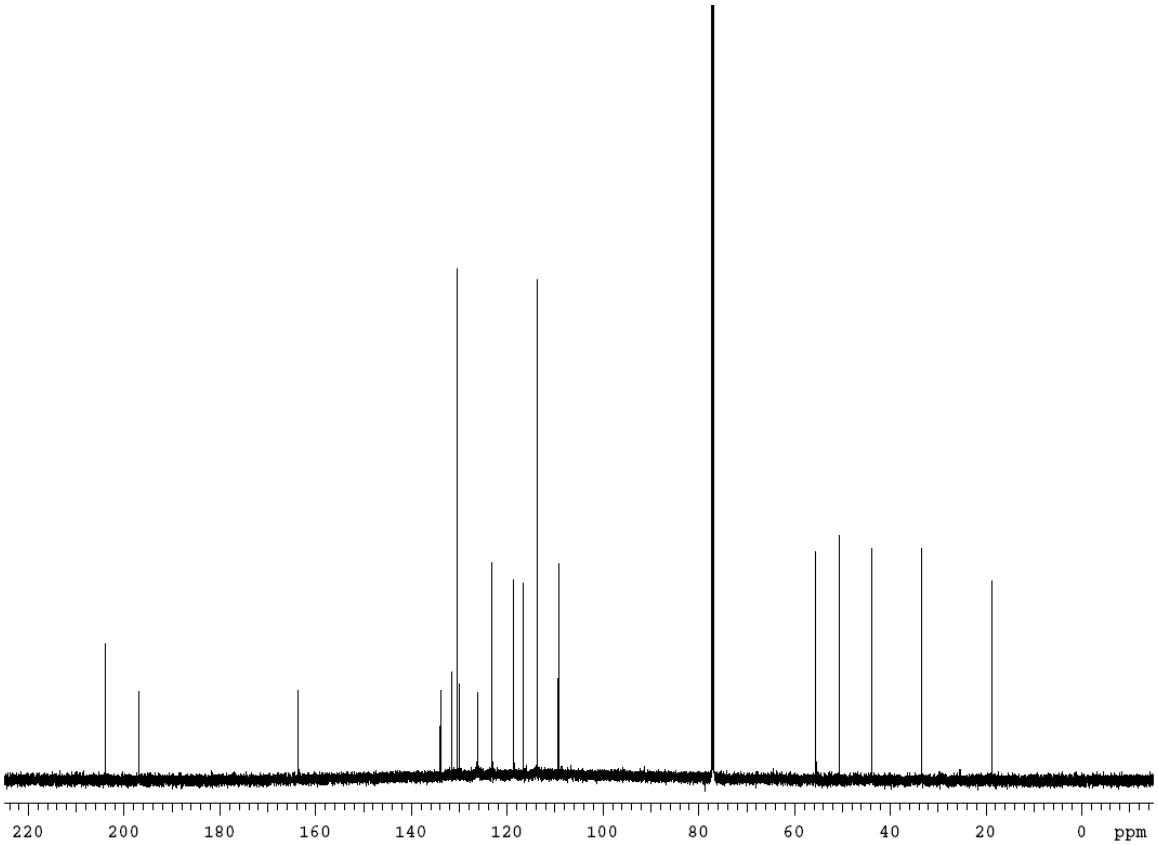

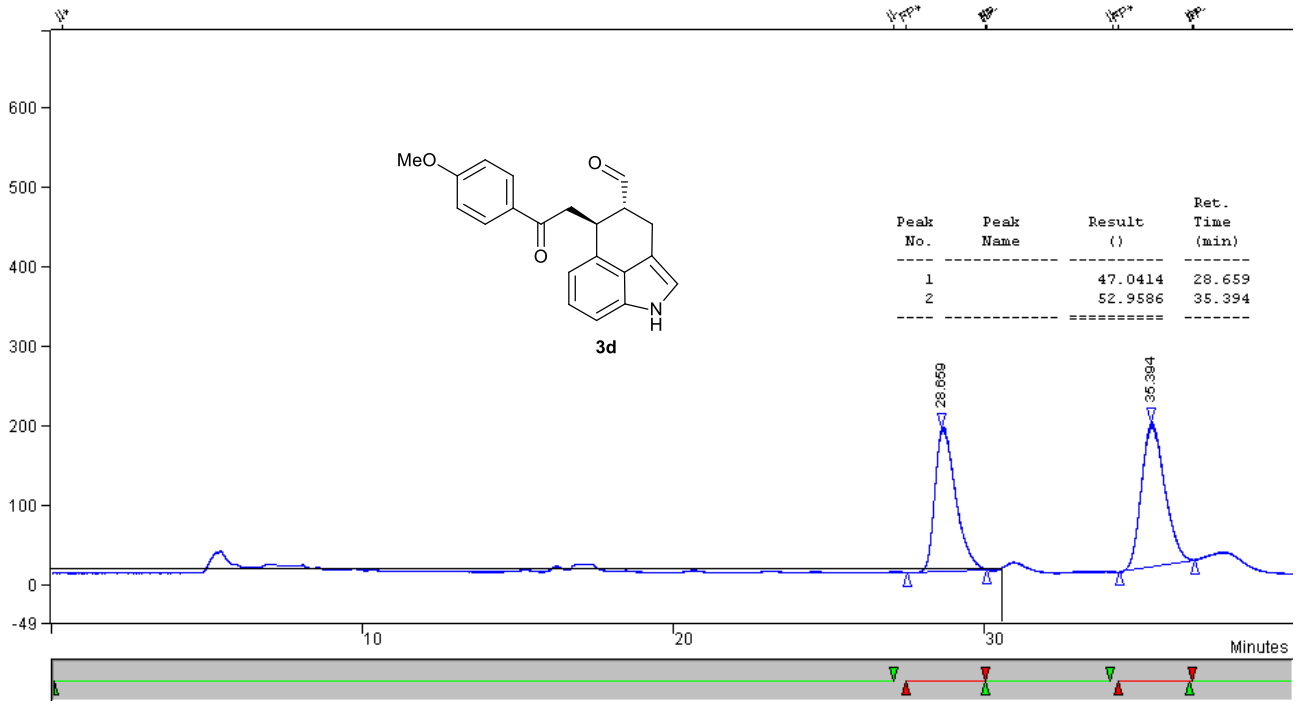
MeO
O
O
N
H
3d
Peak No. | Peak Name | Result () | Ret. Time (min)
1 | | 47.0414 | 28.659
2 | | 52.9586 | 35.394
28.659
35.394
600
500
400
300
200
100
0
-49
10
20
30
Minutes

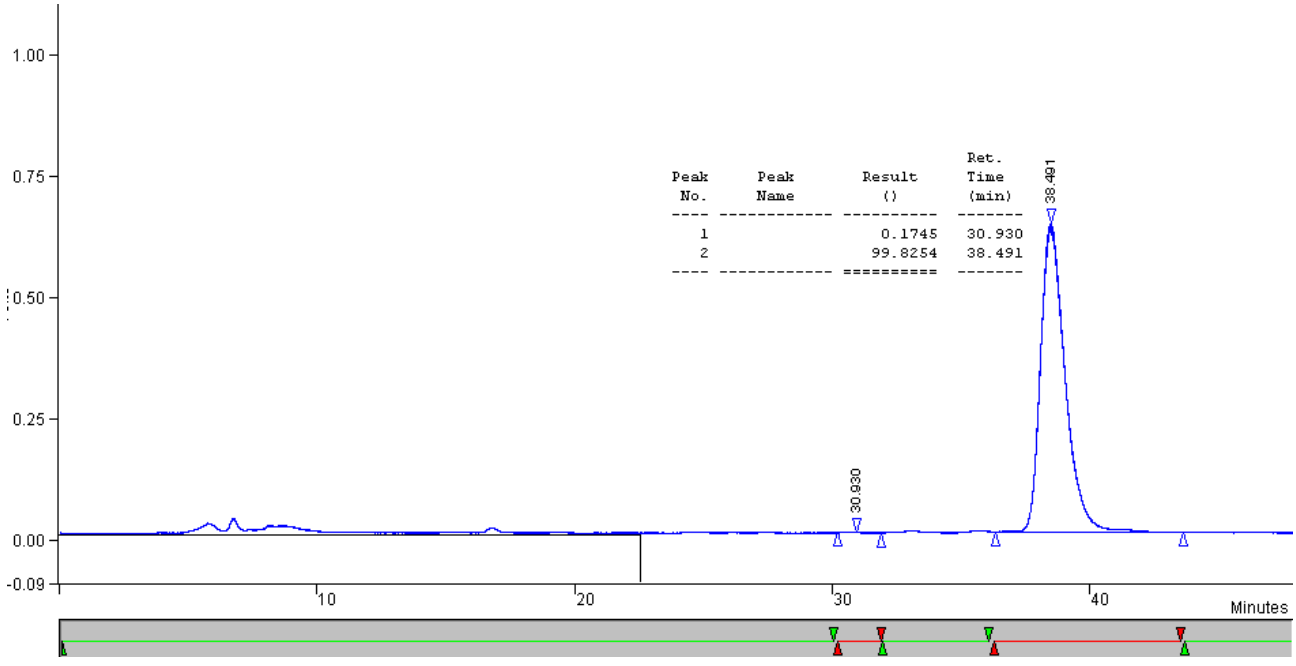
Peak No. | Peak Name | Result () | Ret. Time (min)
1 | | 0.1745 | 30.930
2 | | 99.8254 | 38.491
30.930
38.491
1.00
0.75
0.50
0.25
0.00
-0.09
10
20
30
40
Minutes

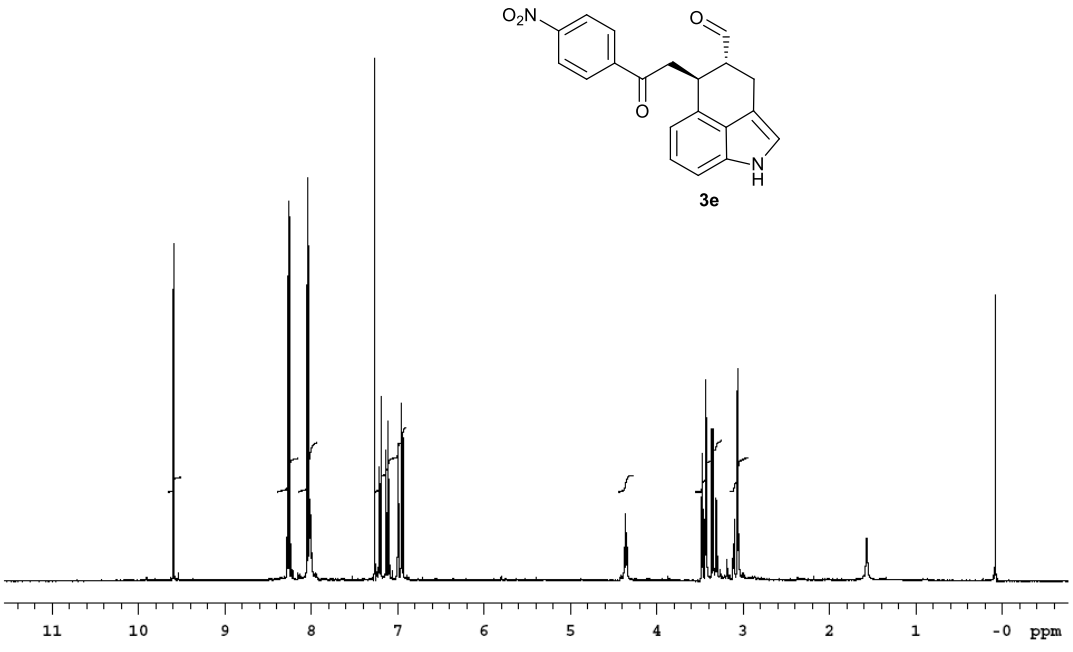
O2N
O
O
N
H
11
10
9
8
7
6
5
4
3
2
1
-0
ppm

3e

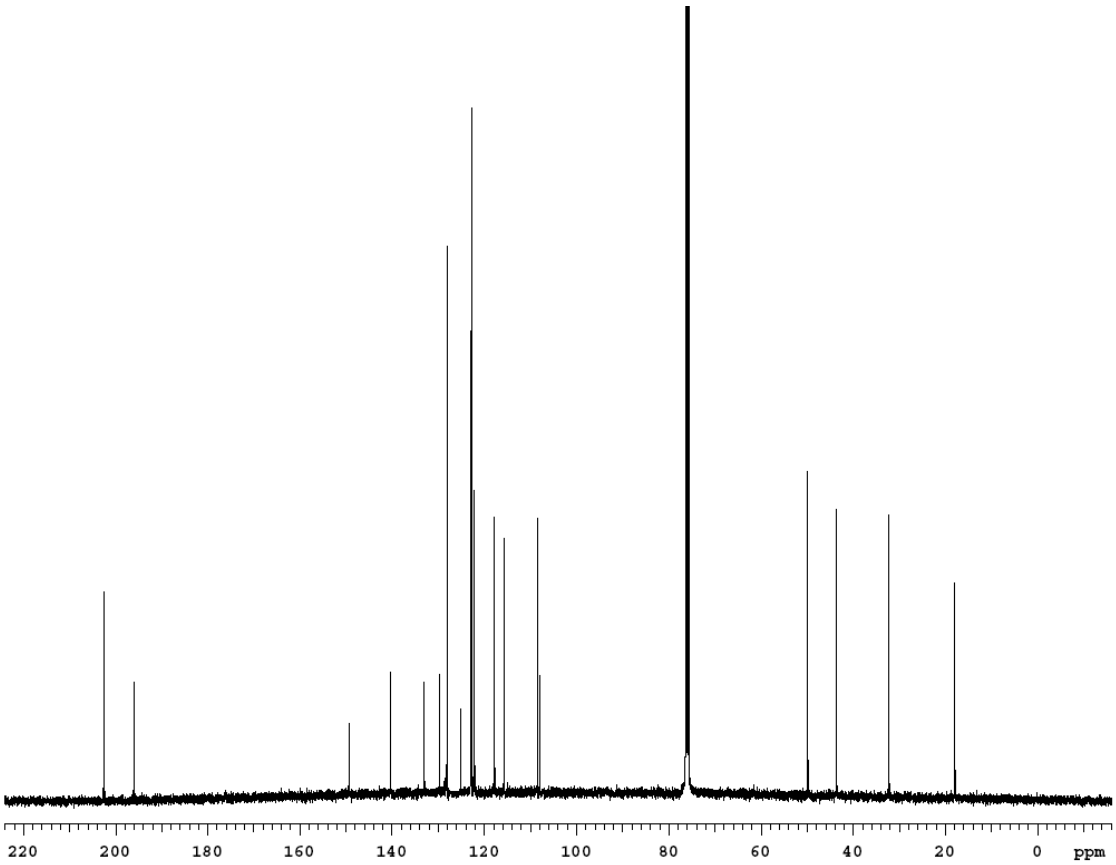
220
200
180
160
140
120
100
80
60
40
20
0
ppm

Enantiomeric ratio of compound **3e** was evaluated by means ^{1}H NMR by using Pirkle's alcohol as chiral shift reagent:

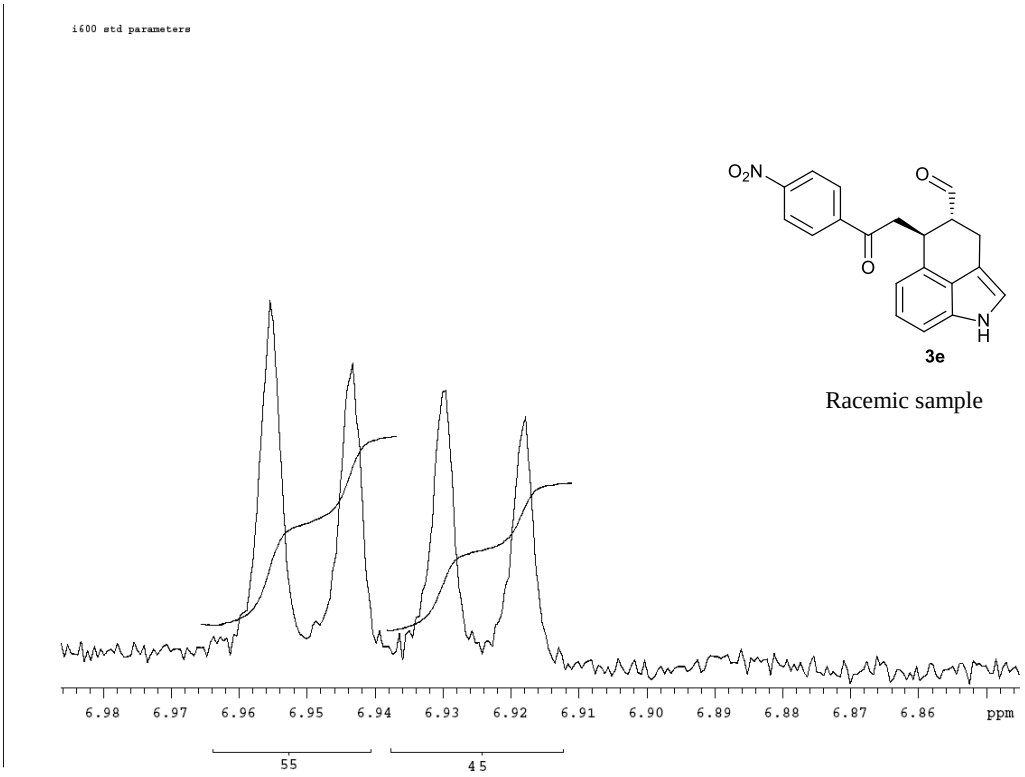

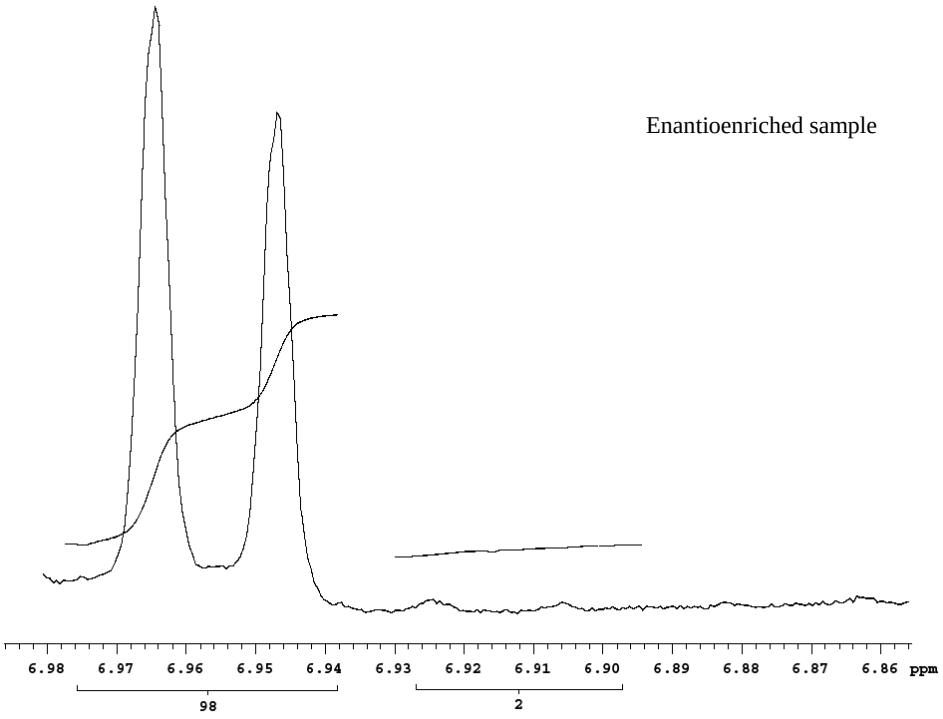

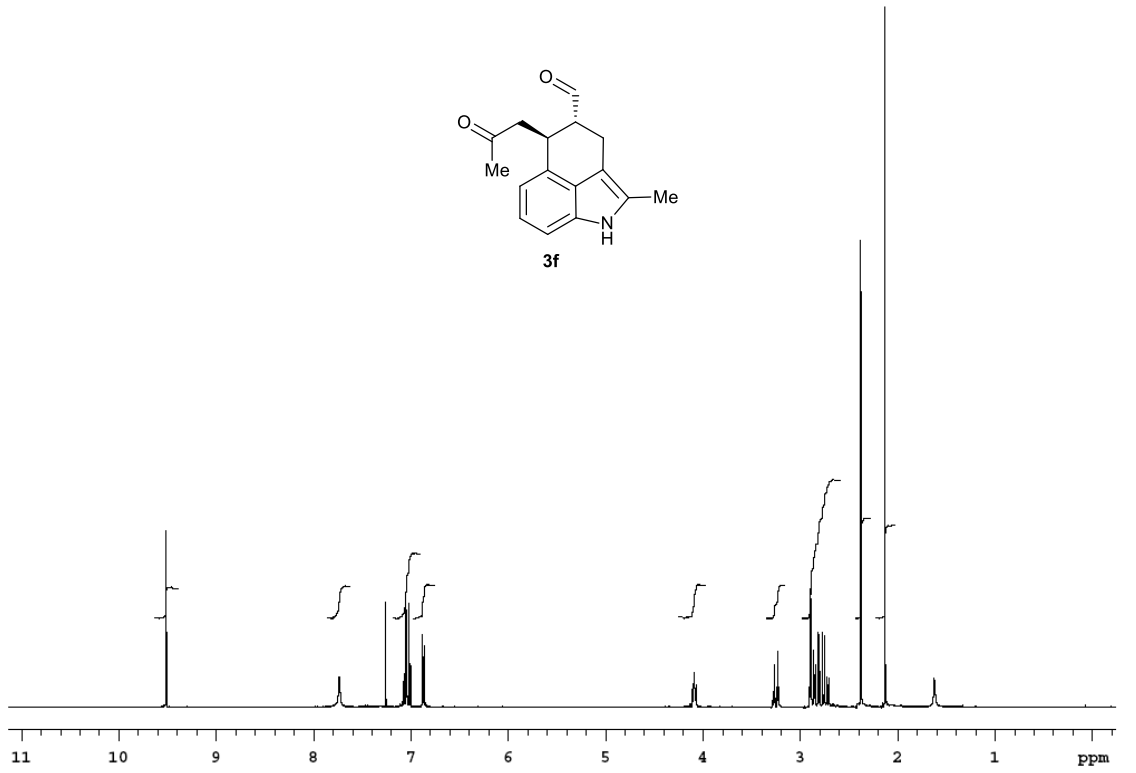

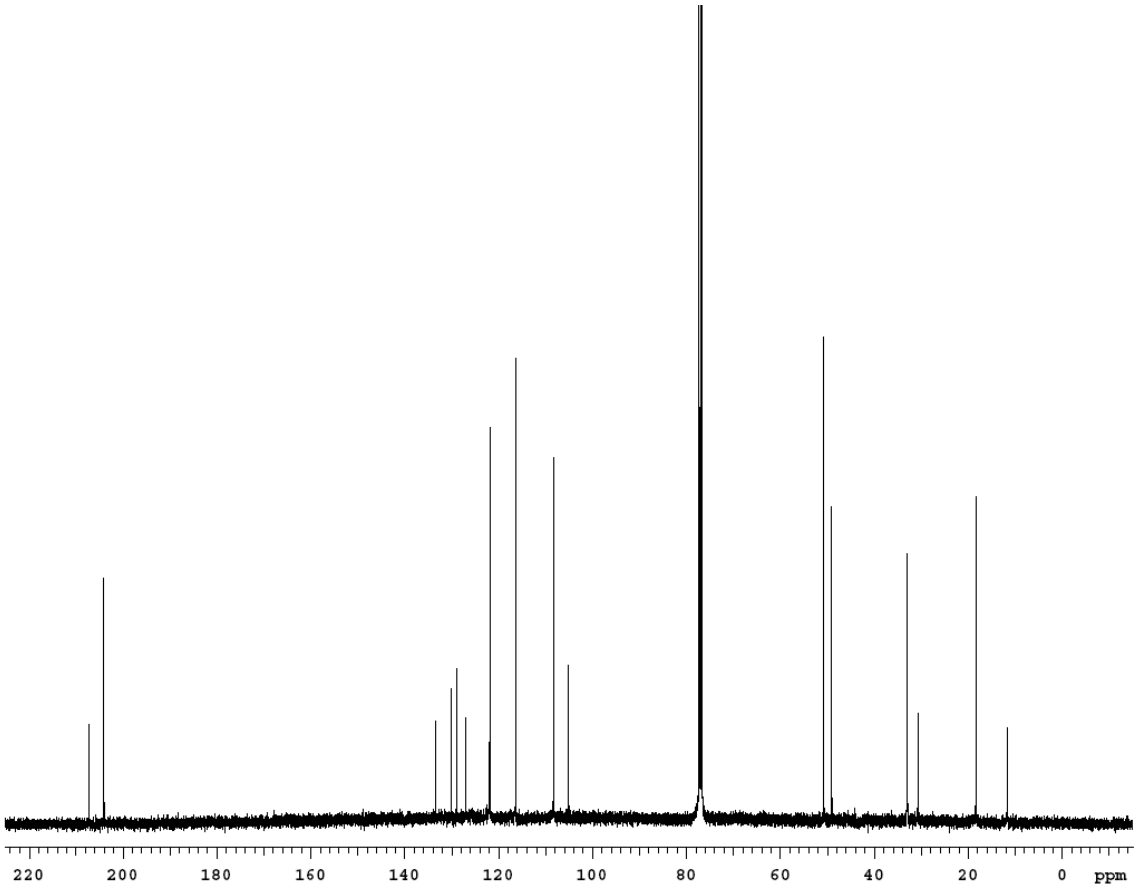

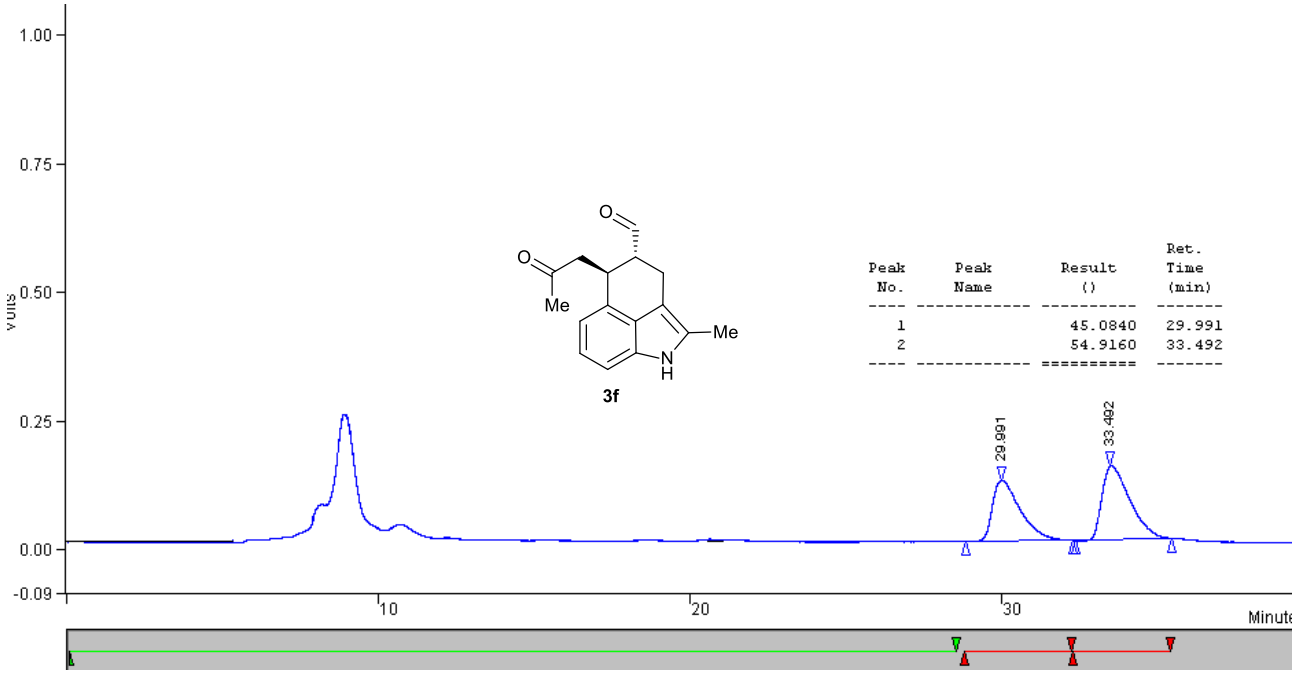
1.00
0.75
0.50
0.25
0.00
-0.09
VOLTS
10
20
30
Minute
O
O
Me
Me
N
H
3f
Peak No. | Peak Name | Result () | Ret. Time (min)
1 | | 45.0840 | 29.991
2 | | 54.9160 | 33.492
29.991
33.492

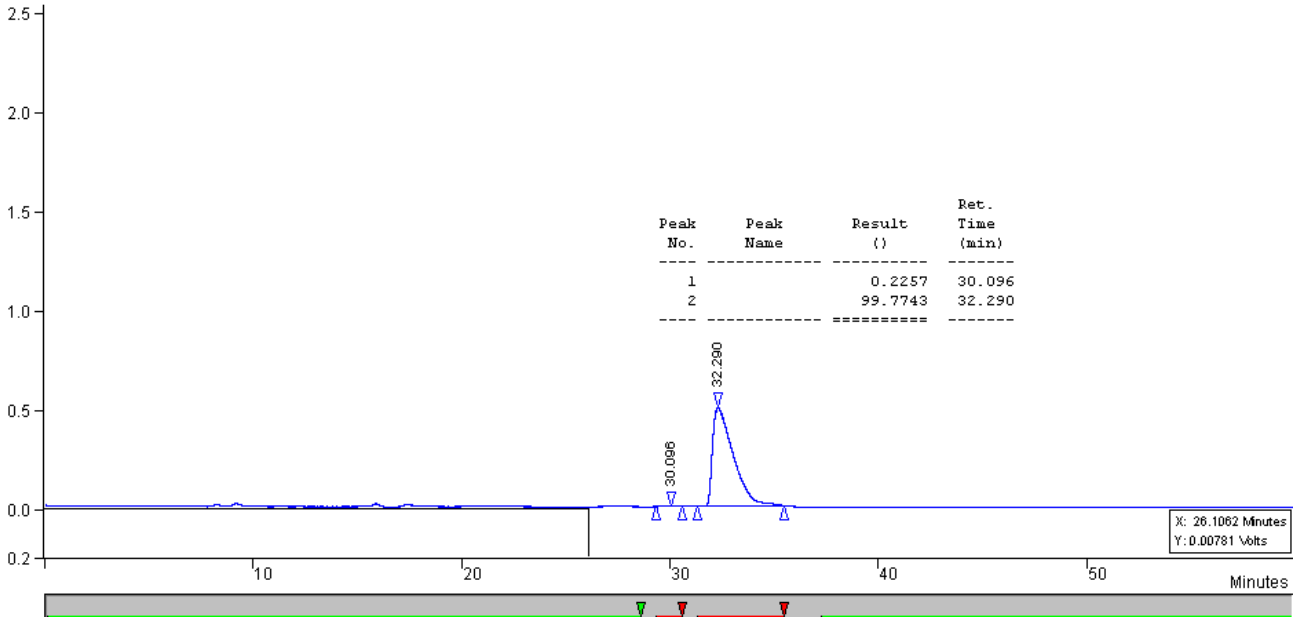
2.5
2.0
1.5
1.0
0.5
0.0
0.2
10
20
30
40
50
Minutes
Peak No. | Peak Name | Result () | Ret. Time (min)
1 | | 0.2257 | 30.096
2 | | 99.7743 | 32.290
30.096
32.290
X: 26.1062 Minutes
Y: 0.00781 Volts

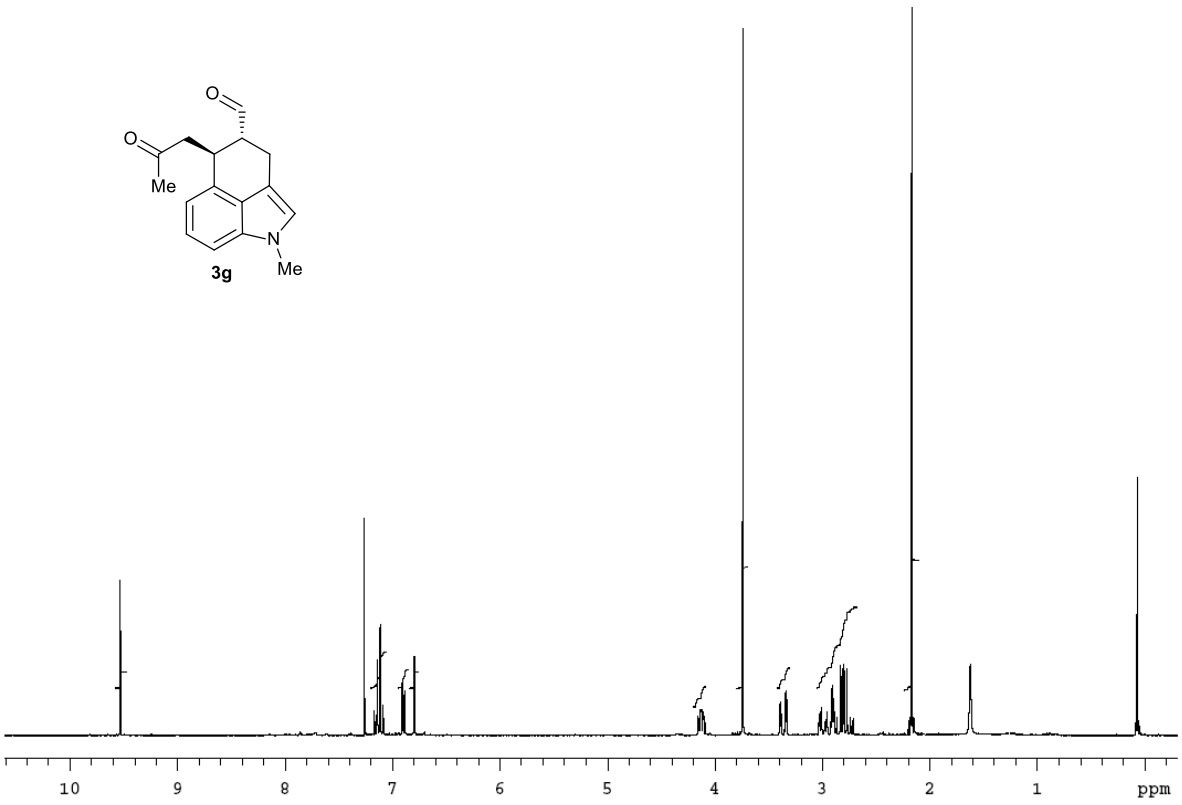

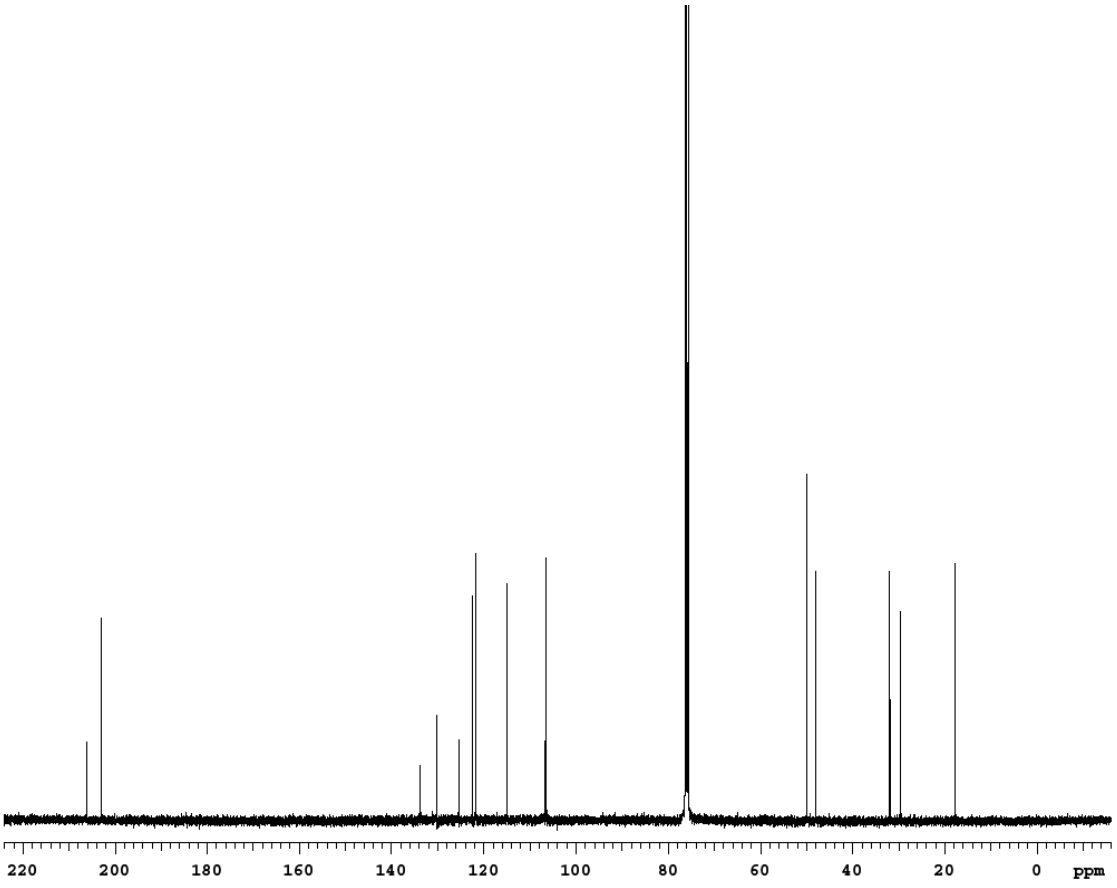

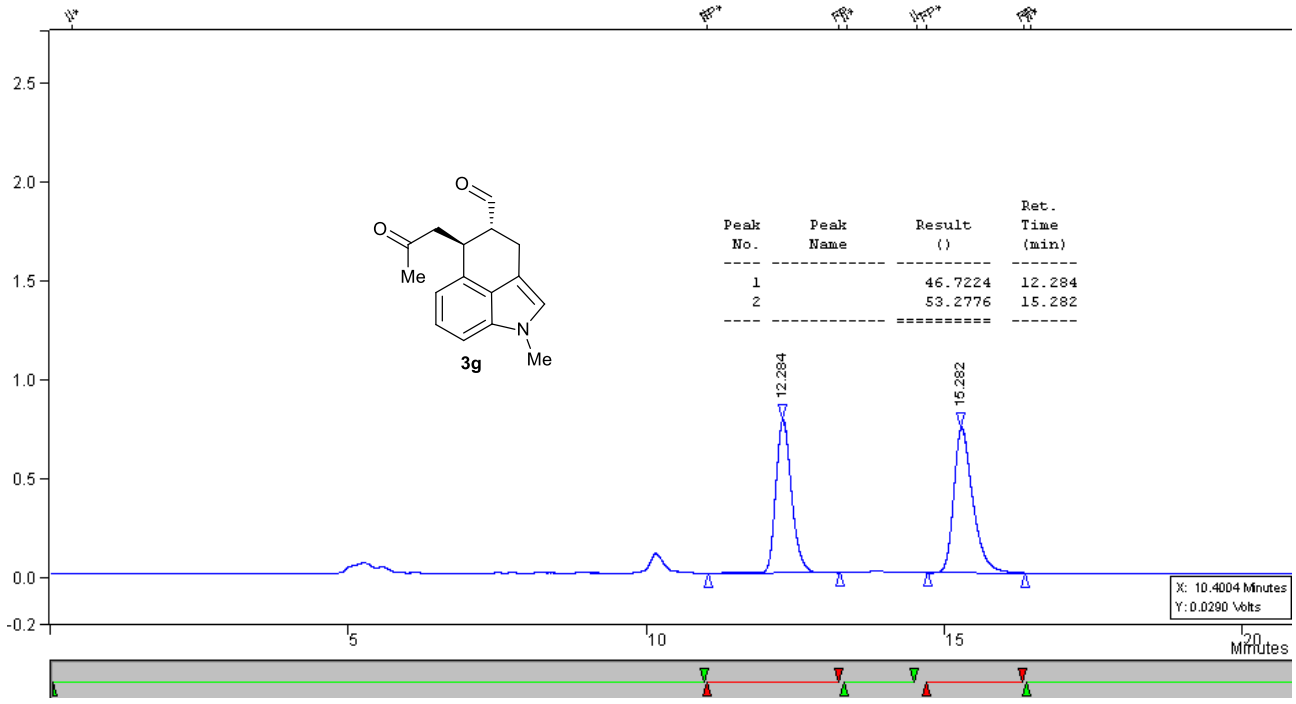
3g
Peak No. | Peak Name | Result () | Ret. Time (min)
1 | | 46.7224 | 12.284
2 | | 53.2776 | 15.282
12.284
15.282
X: 10.4004 Minutes
Y: 0.0290 Volts
Minutes

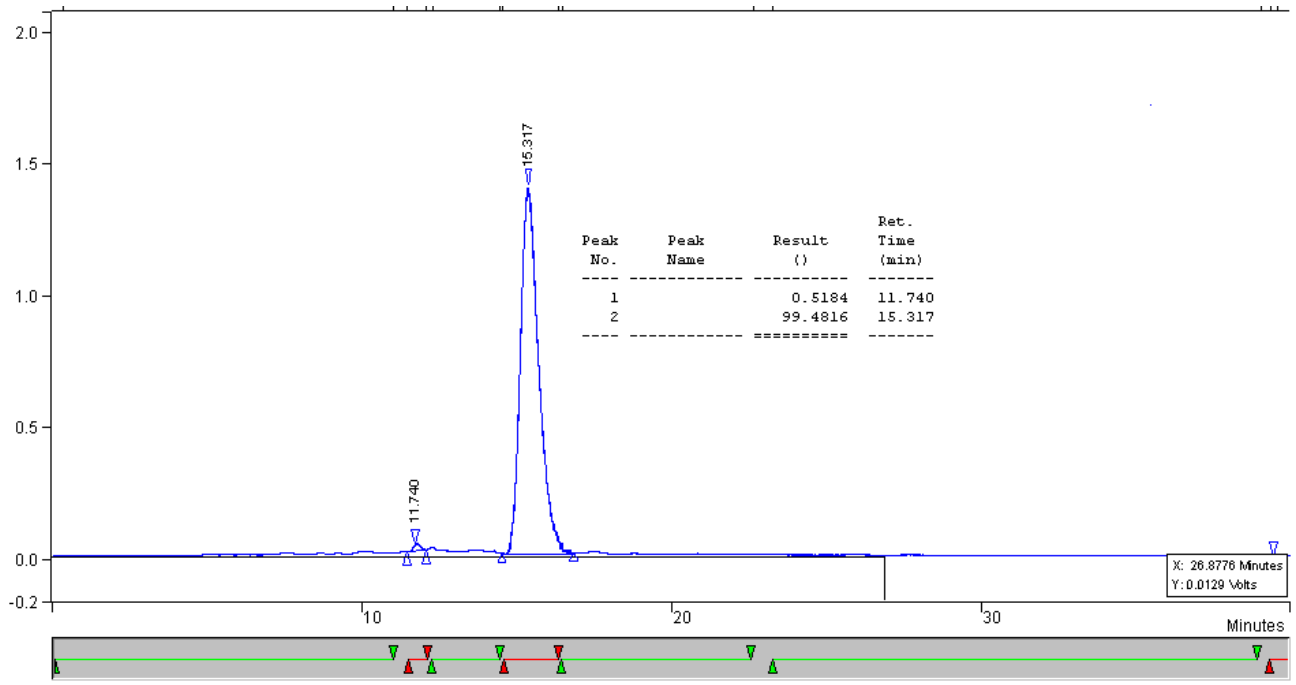
Peak No. | Peak Name | Result () | Ret. Time (min)
1 | | 0.5184 | 11.740
2 | | 99.4816 | 15.317
15.317
11.740
X: 26.8776 Minutes
Y: 0.0129 Volts
Minutes

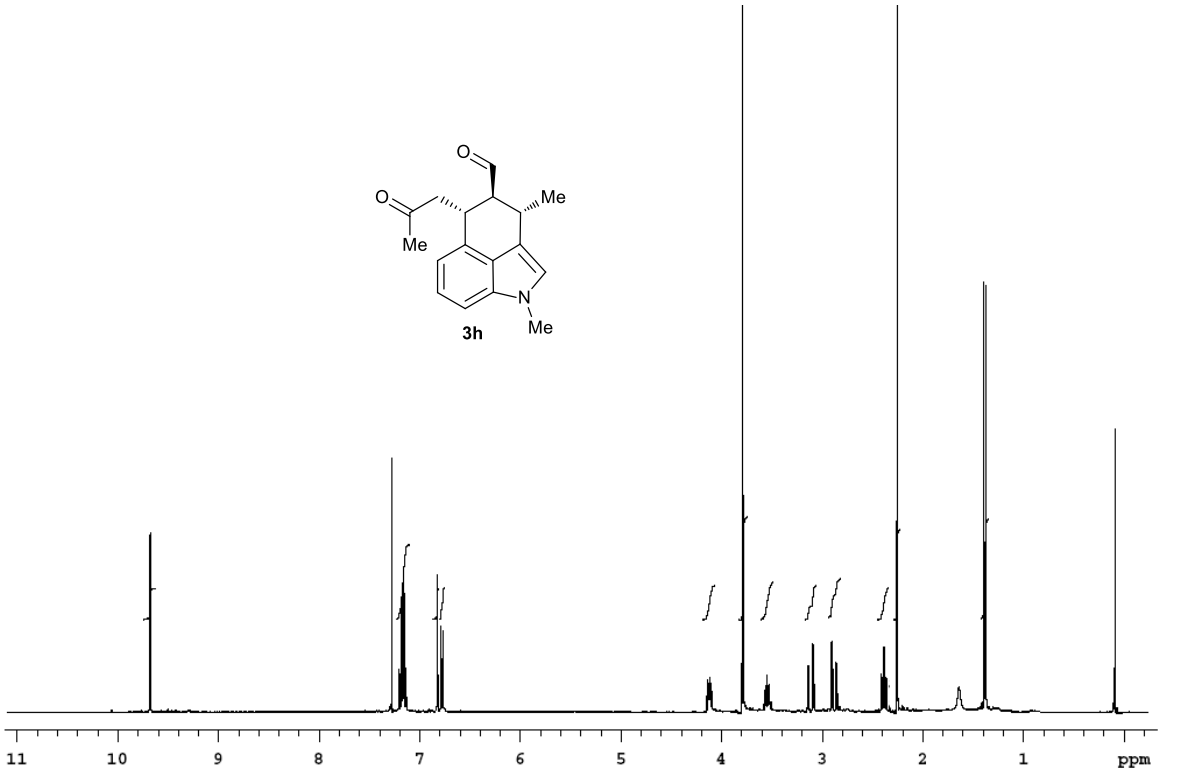

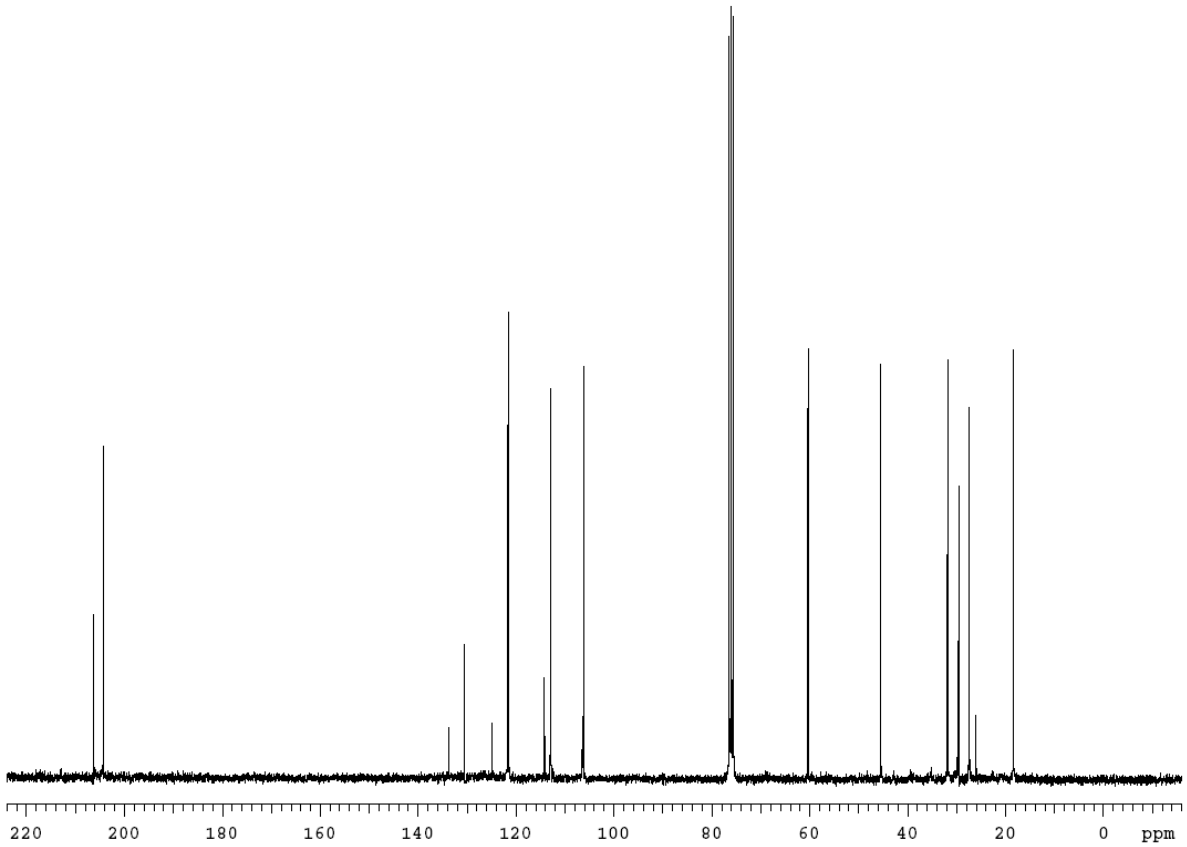

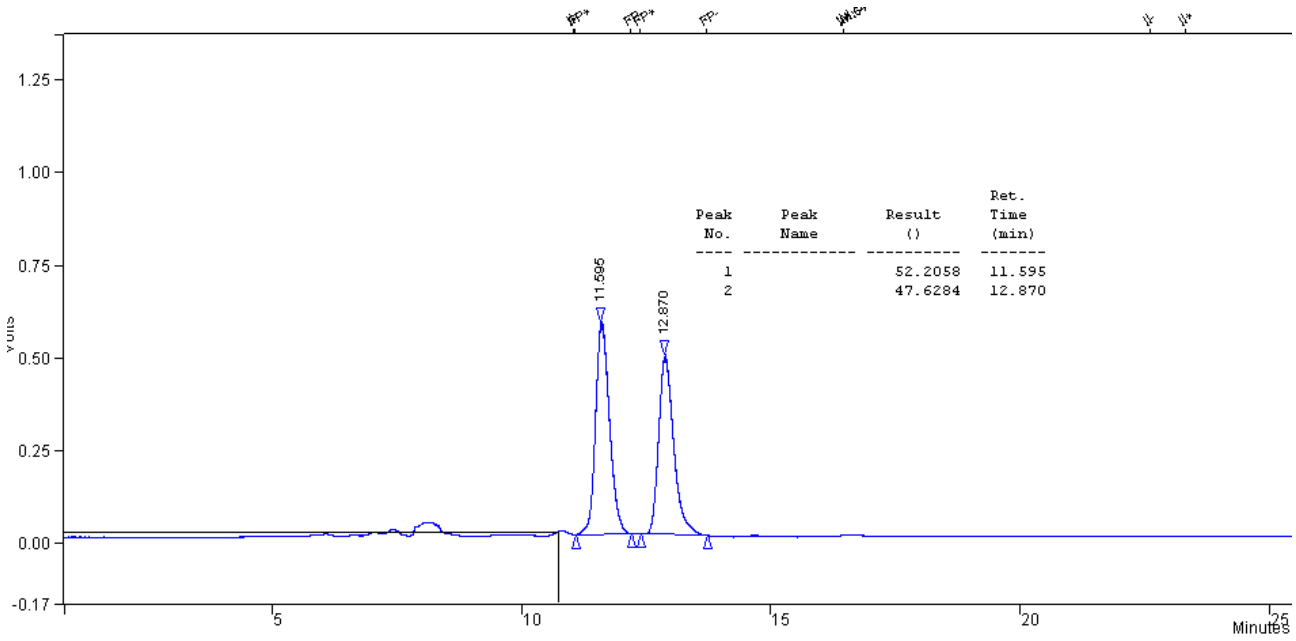
Peak No. | Peak Name | Result () | Ret. Time (min)
1 | | 52.2058 | 11.595
2 | | 47.6284 | 12.870
11.595
12.870
Volts
1.25
1.00
0.75
0.50
0.25
0.00
-0.17
5
10
15
20
25
Minutes

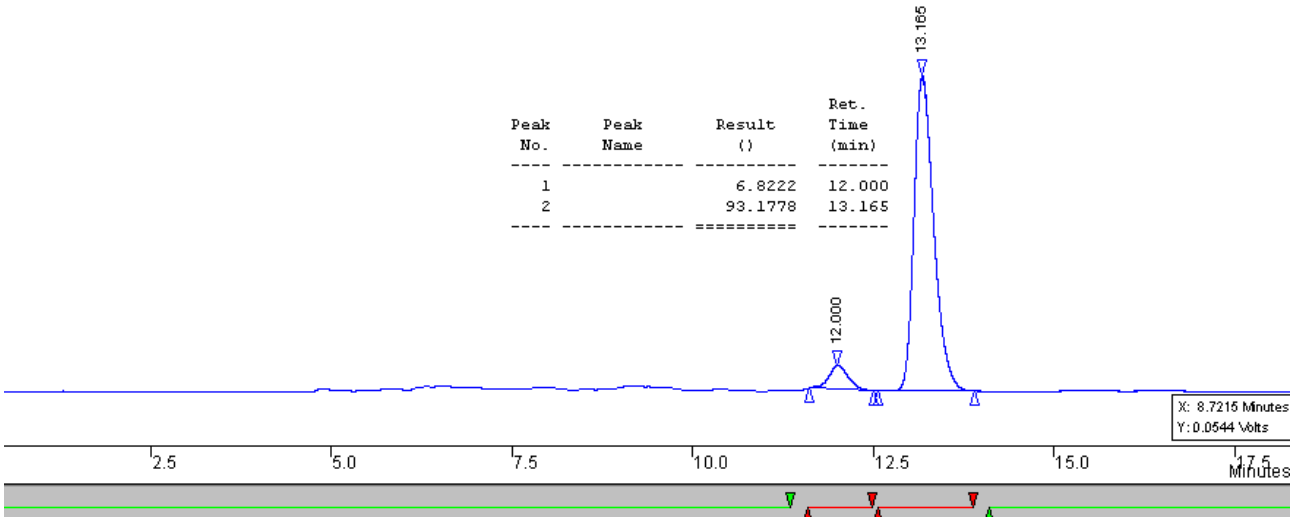
Peak No. | Peak Name | Result () | Ret. Time (min)
1 | | 6.8222 | 12.000
2 | | 93.1778 | 13.165
13.165
12.000
X: 8.7215 Minutes
Y: 0.0544 Volts
2.5
5.0
7.5
10.0
12.5
15.0
17.5
Minutes

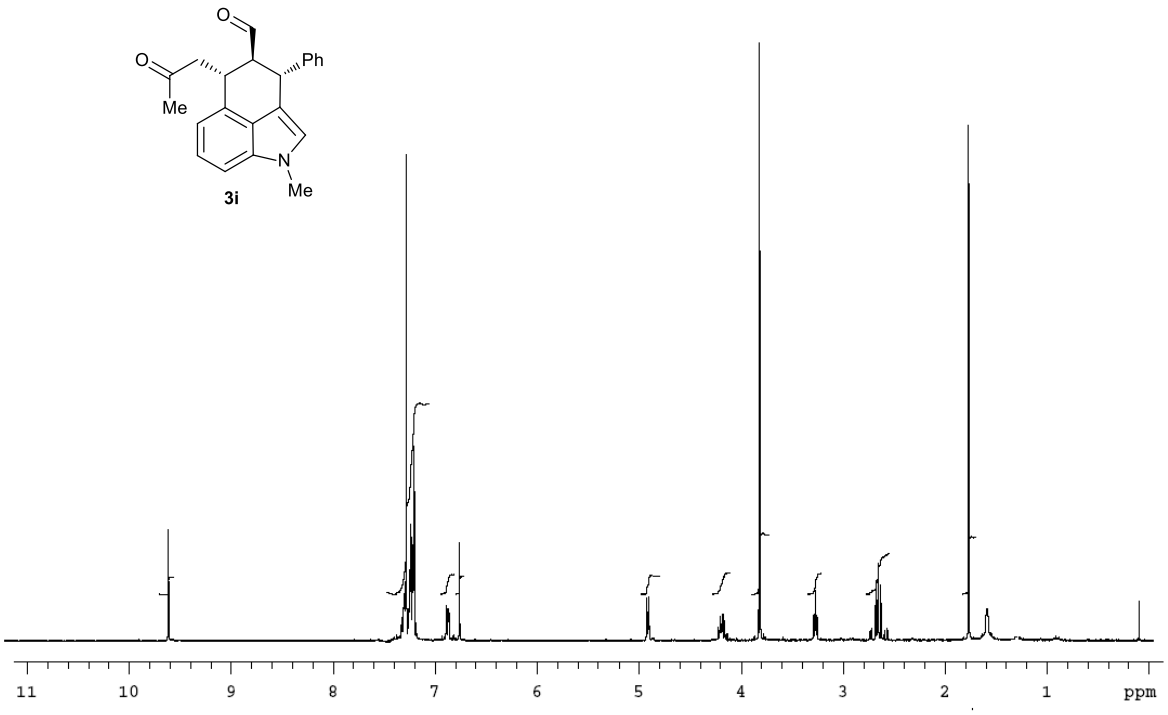

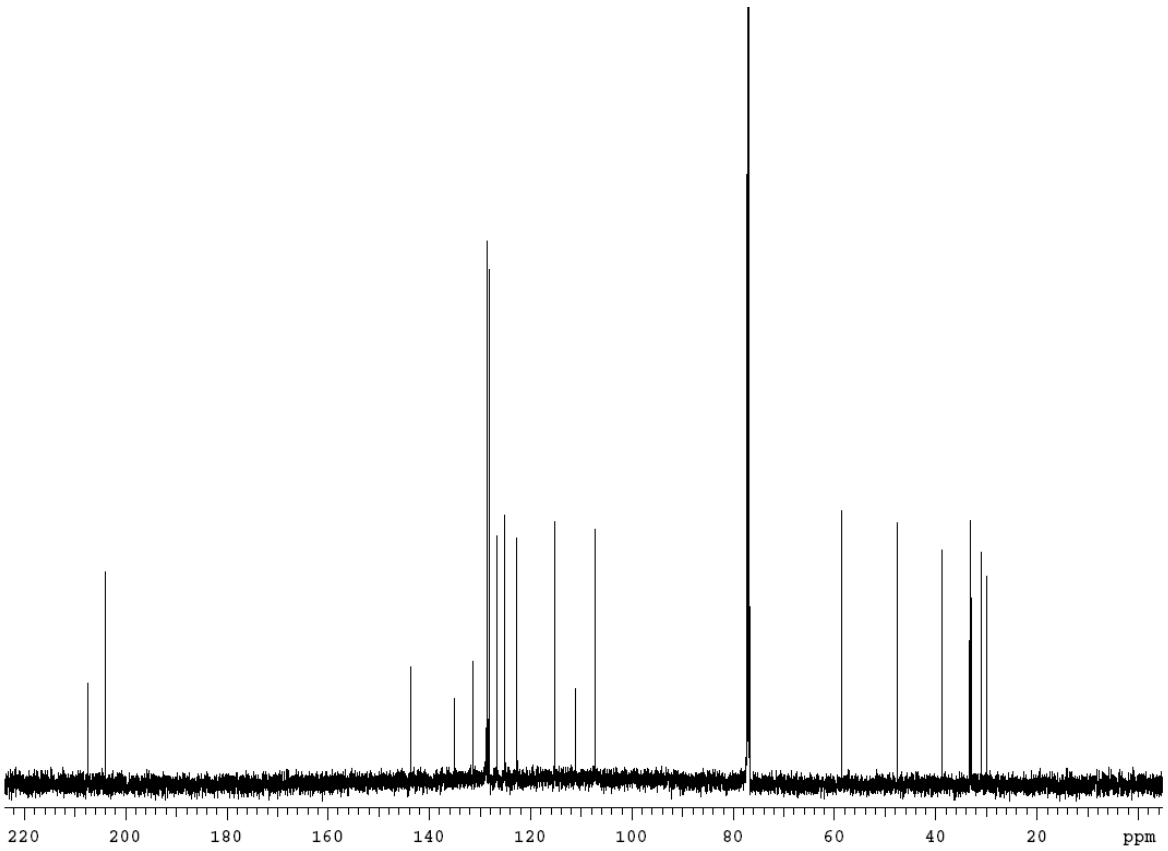

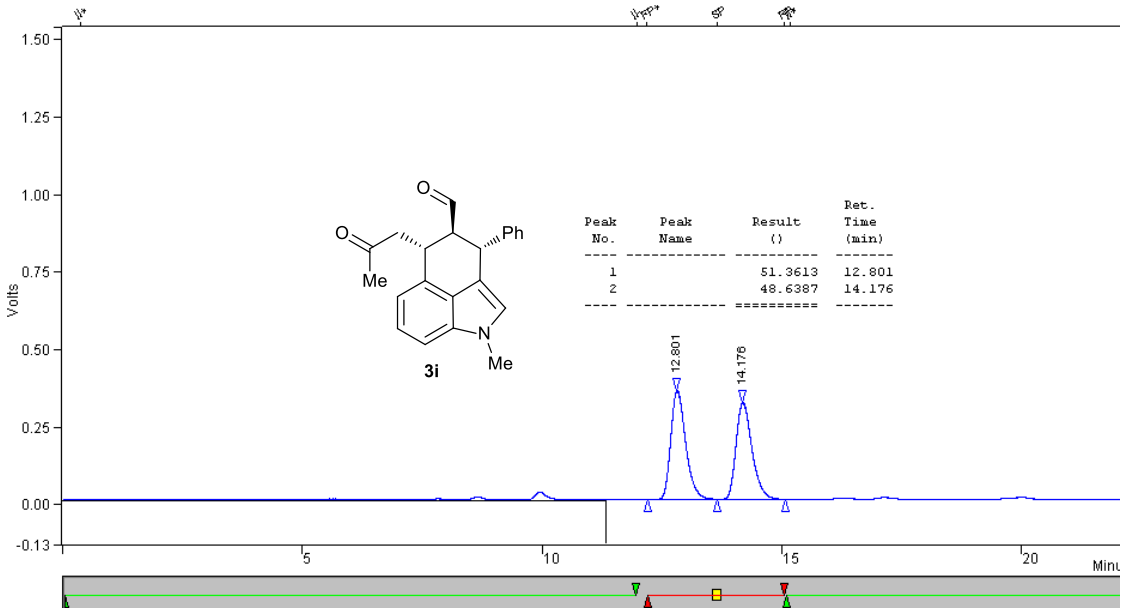
O
O
Me
Ph
N
Me
3i
Peak No. | Peak Name | Result () | Ret. Time (min)
1 | | 51.3613 | 12.801
2 | | 48.6387 | 14.176
Volts
12.801
14.176
Minu

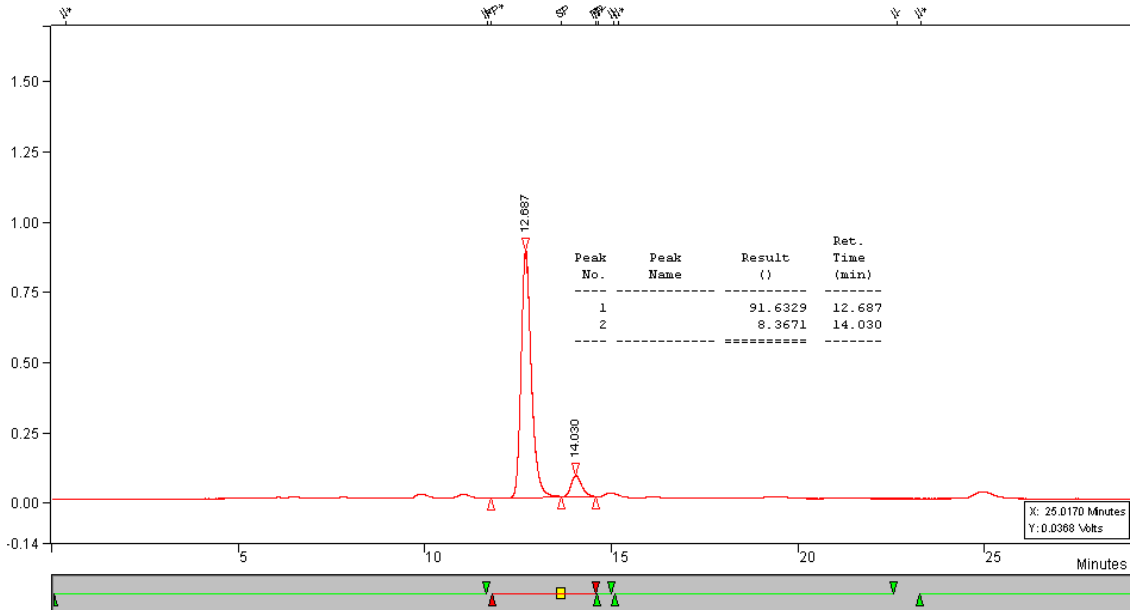
Peak No. | Peak Name | Result () | Ret. Time (min)
1 | | 91.6329 | 12.687
2 | | 8.3671 | 14.030
12.687
14.030
X: 25.0170 Minutes
Y: 0.0368 Volts
Minutes

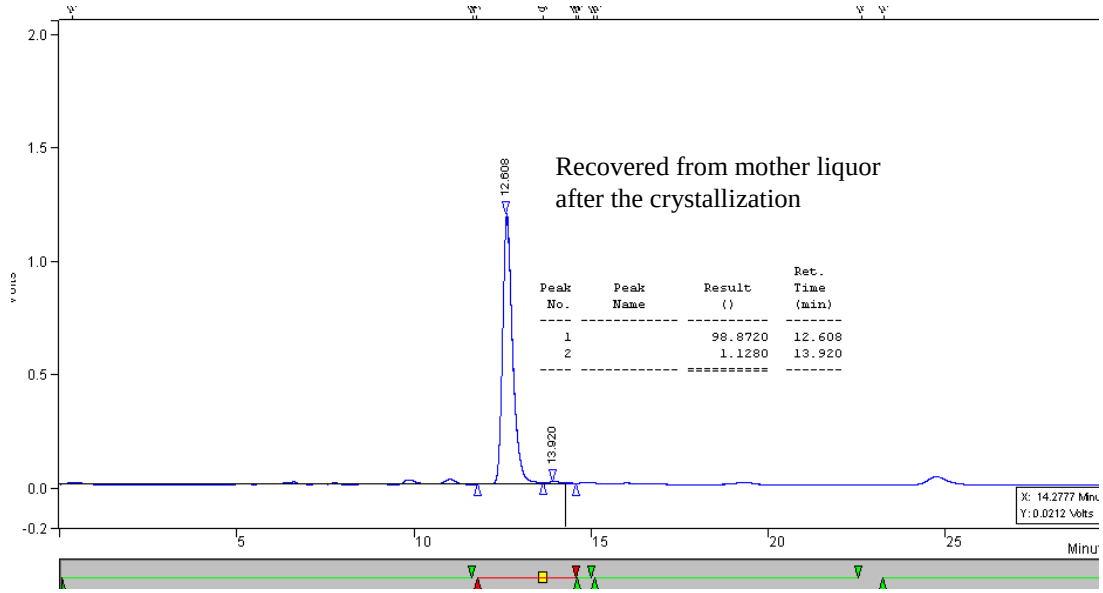
Recovered from mother liquor after the crystallization
Peak No. | Peak Name | Result () | Ret. Time (min)
1 | | 98.8720 | 12.608
2 | | 1.1280 | 13.920
12.608
13.920
X: 14.2777 Minu
Y: 0.0212 Volts

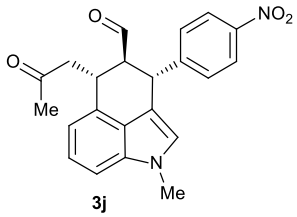

3j

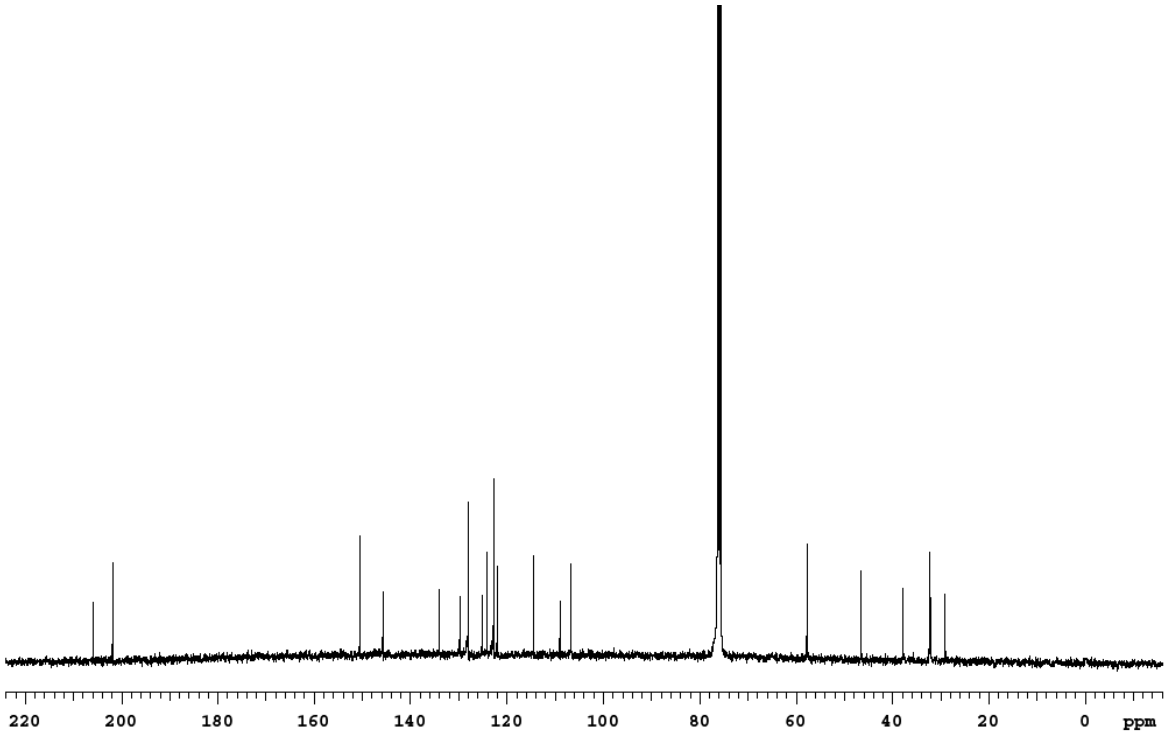

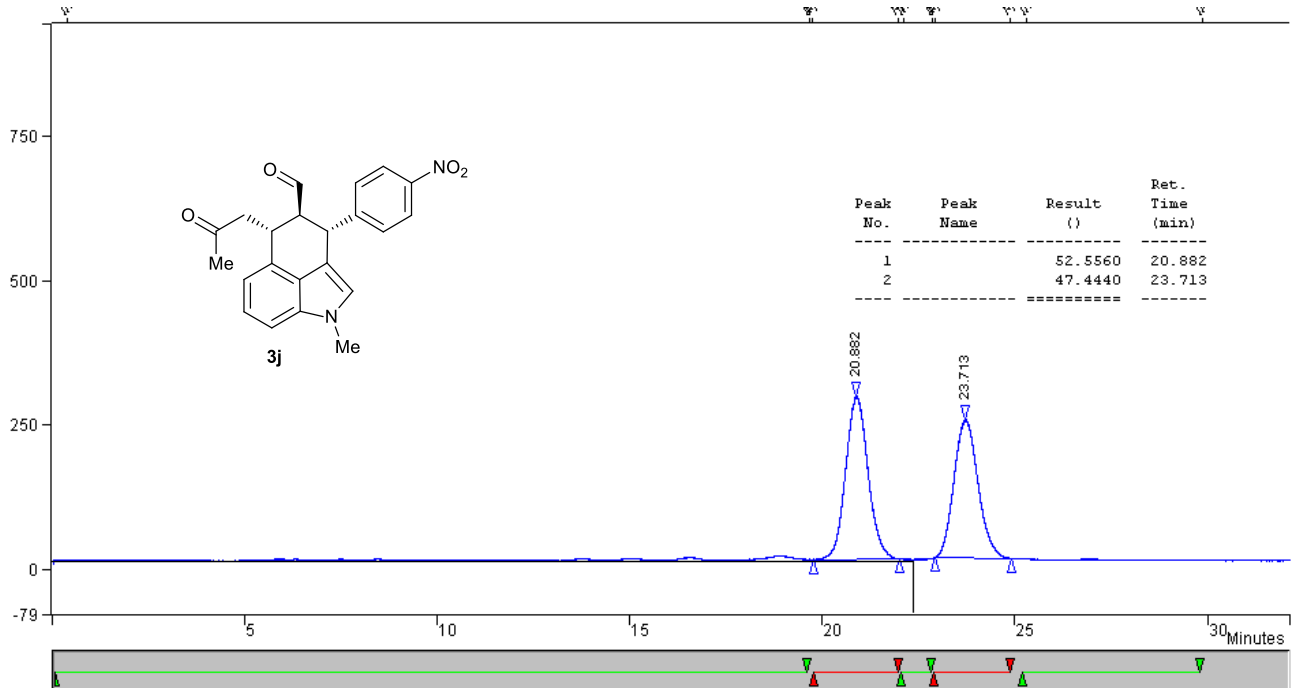

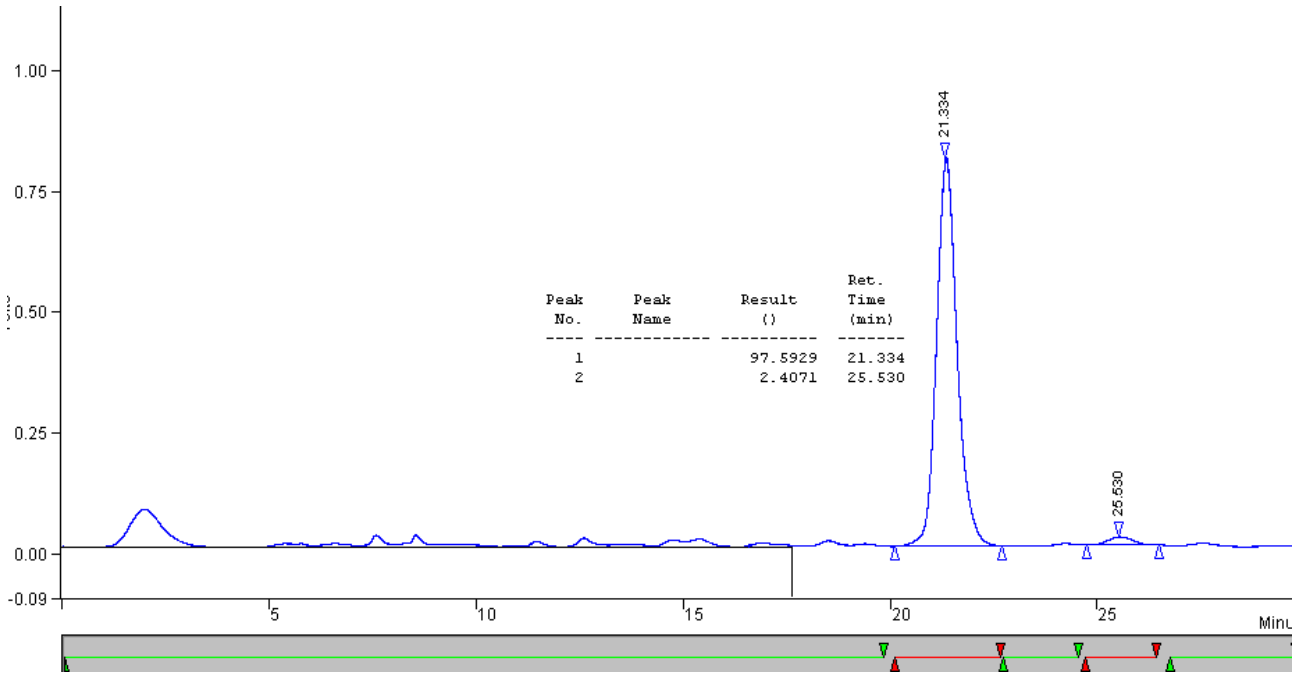

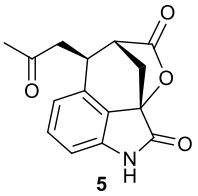

5

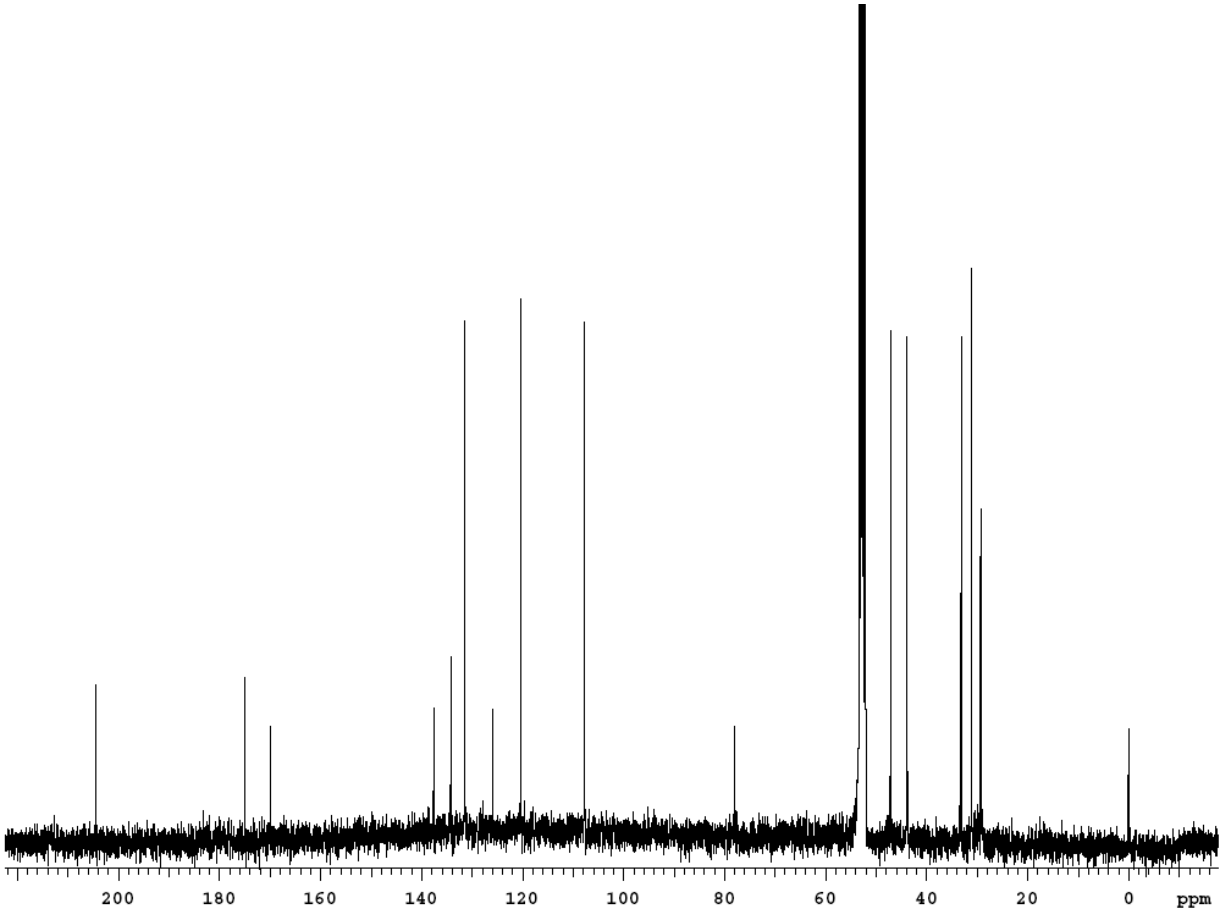

DEPT 1.5

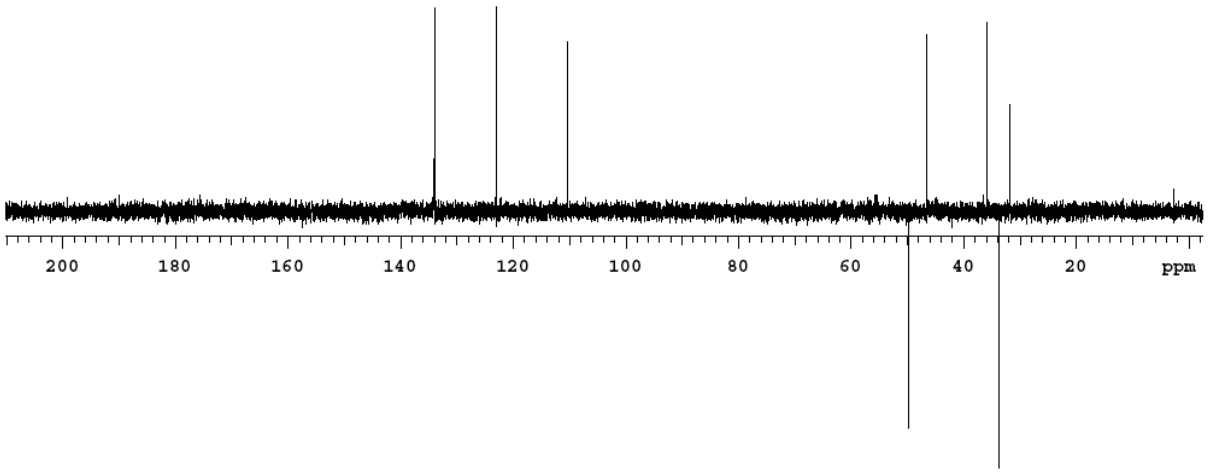

gCOSY

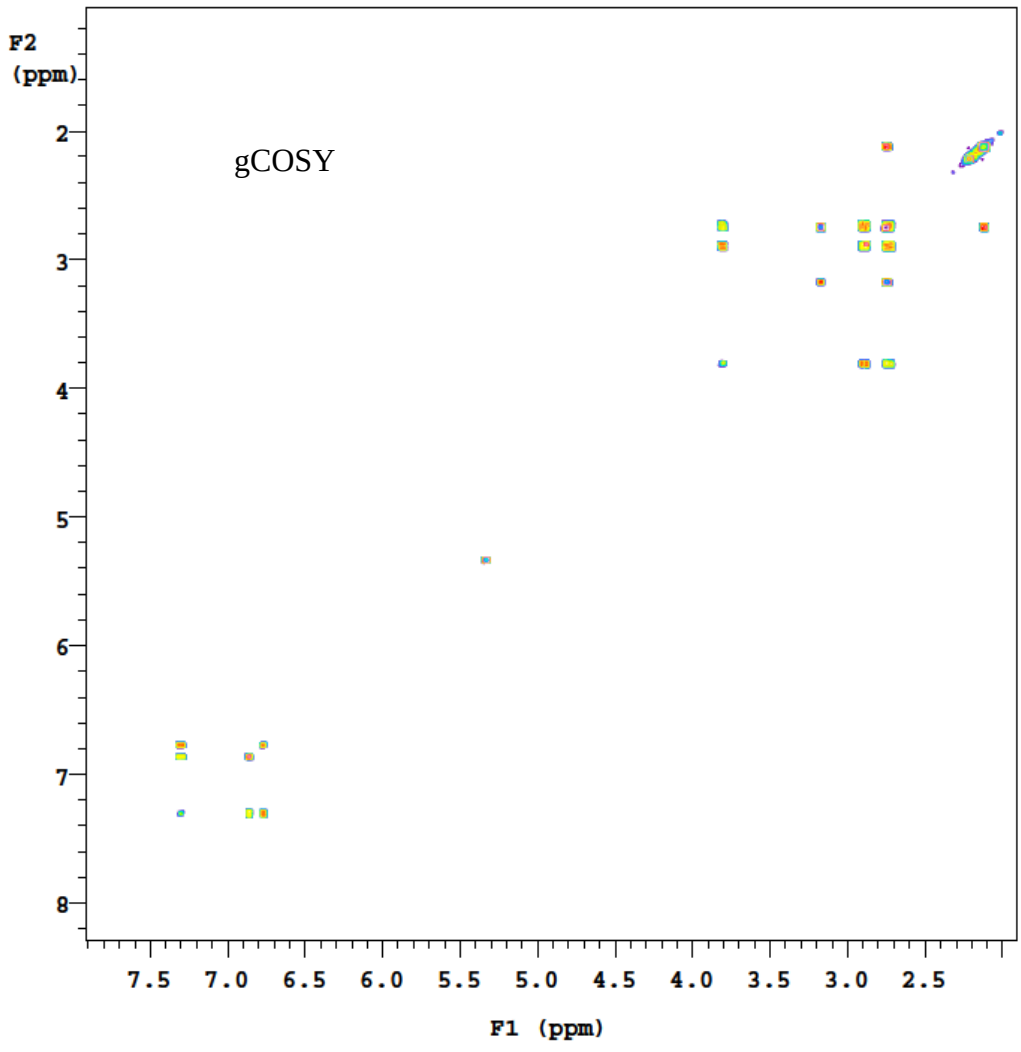

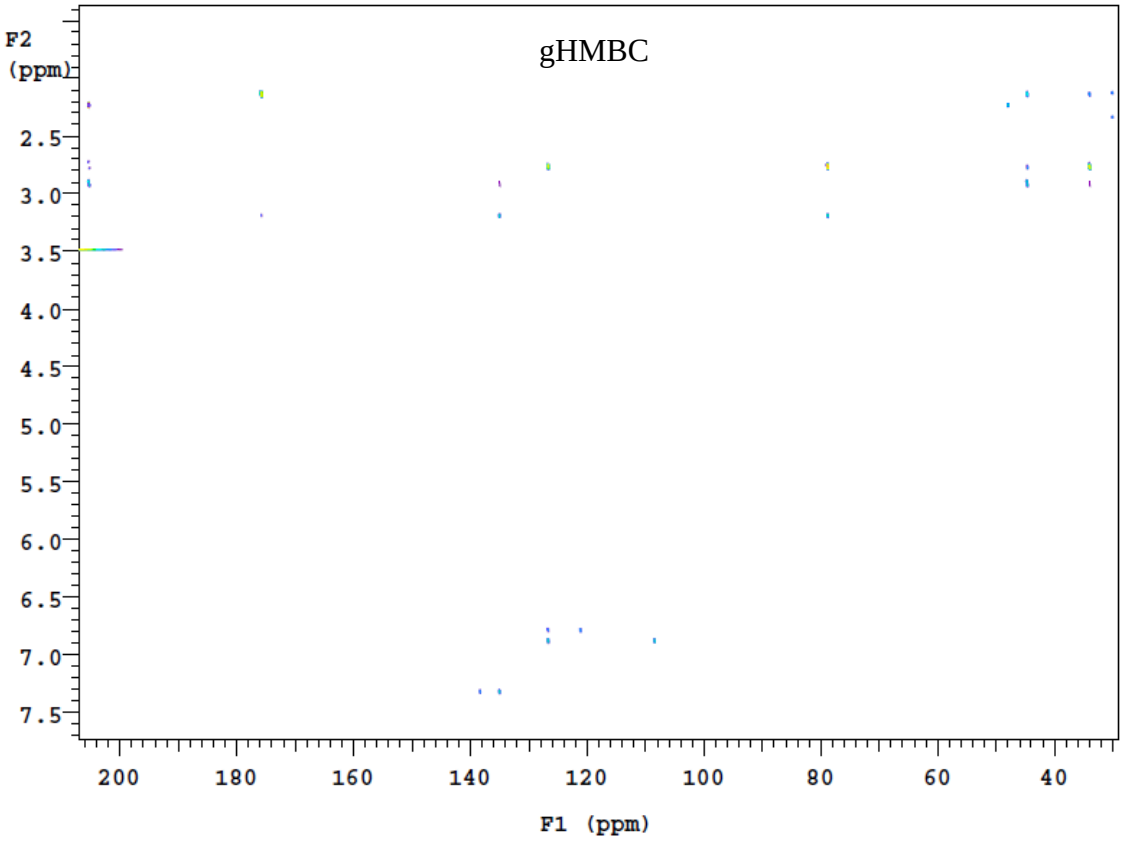
gHMBC
F2 (ppm)
2.5
3.0
3.5
4.0
4.5
5.0
5.5
6.0
6.5
7.0
7.5
200
180
160
140
120
100
80
60
40
F1 (ppm)

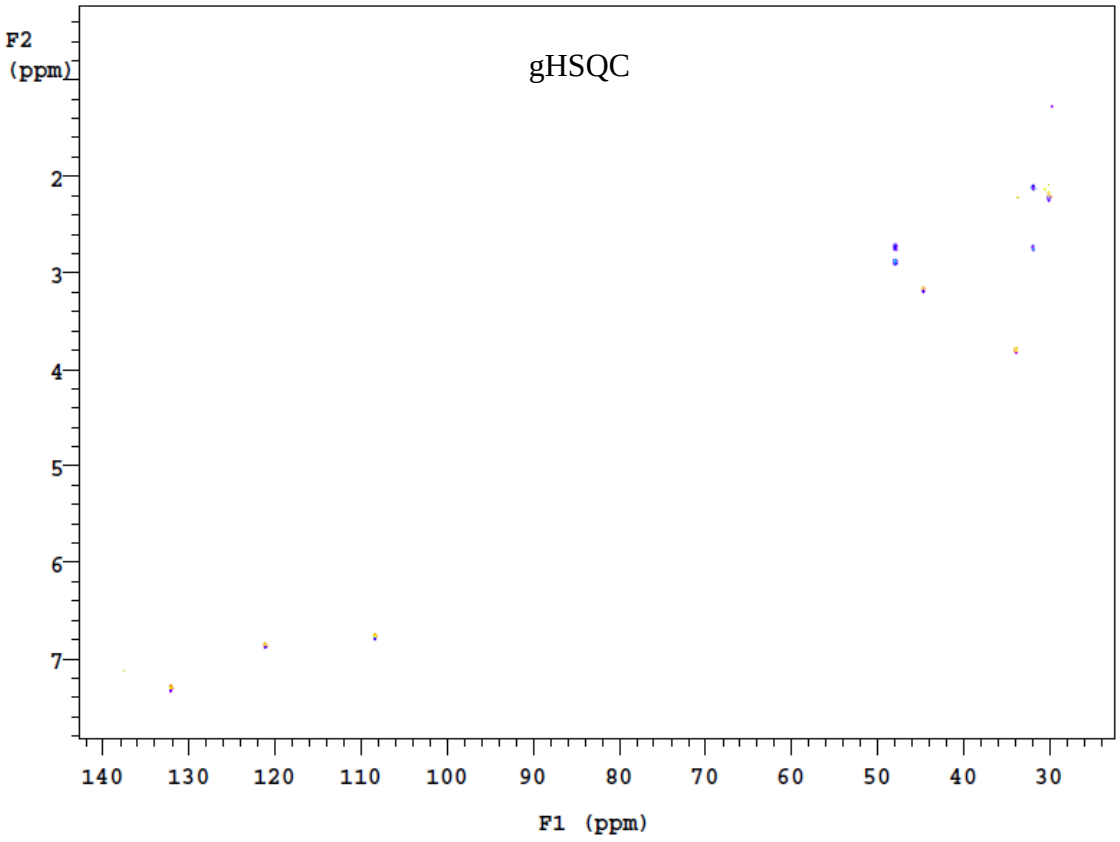
gHSQC
F2 (ppm)
2
3
4
5
6
7
140
130
120
110
100
90
80
70
60
50
40
30
F1 (ppm)

Expansion of the aliphatic region in the gHMBC spectrum

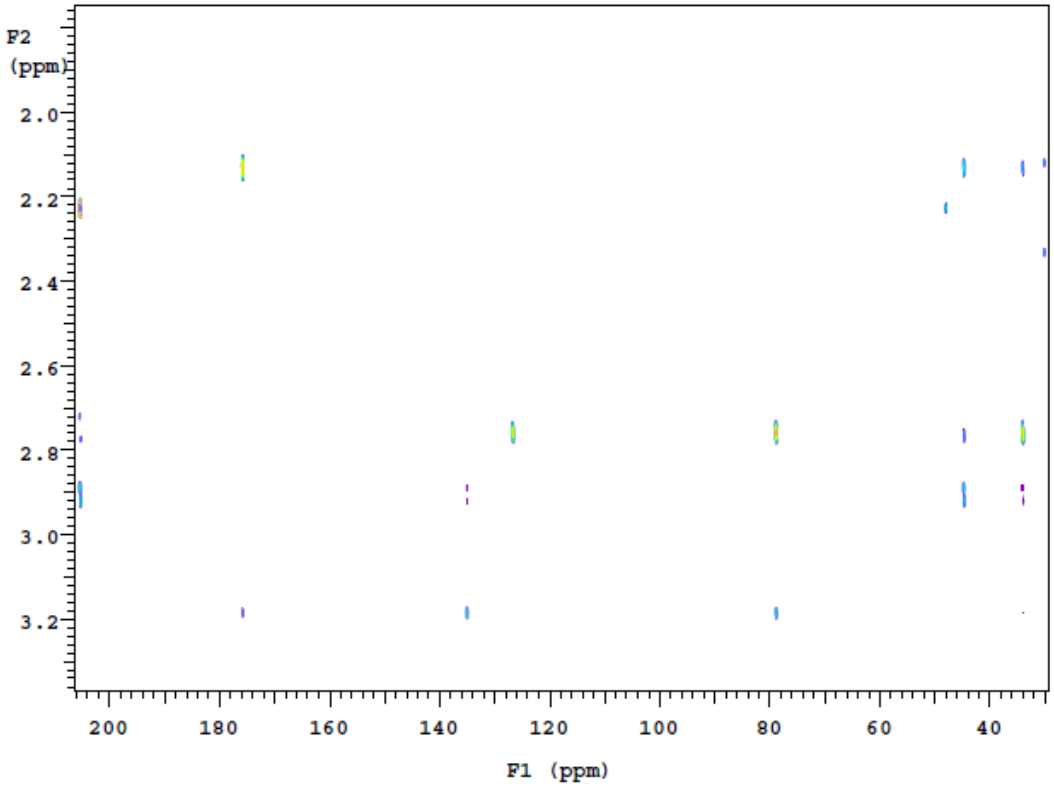

Expansion of the aliphatic region in the gHSQC spectrum

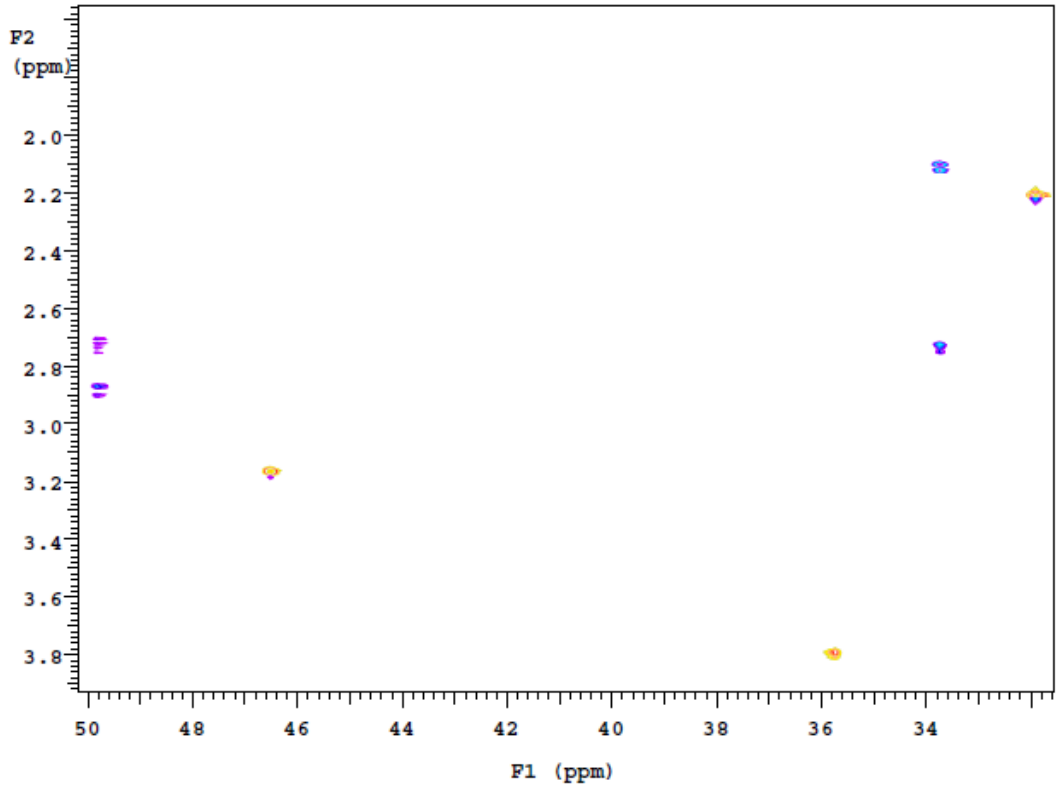

Expansion of the aromatic region in the gHSQC spectrum

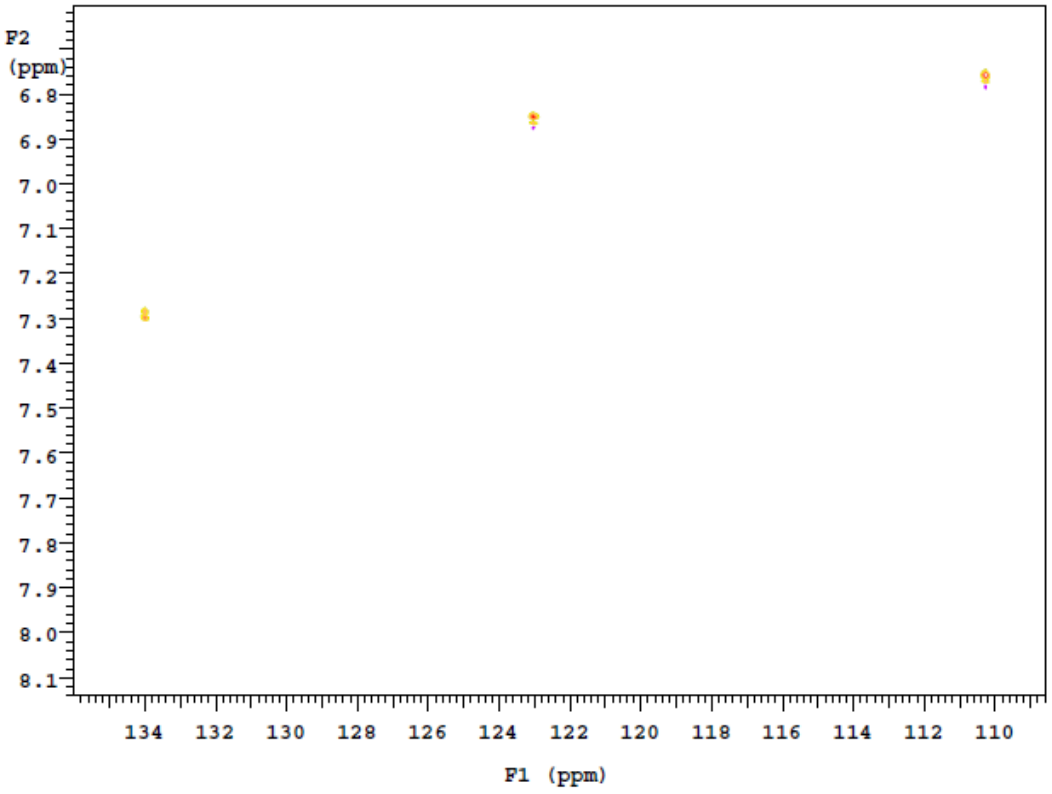

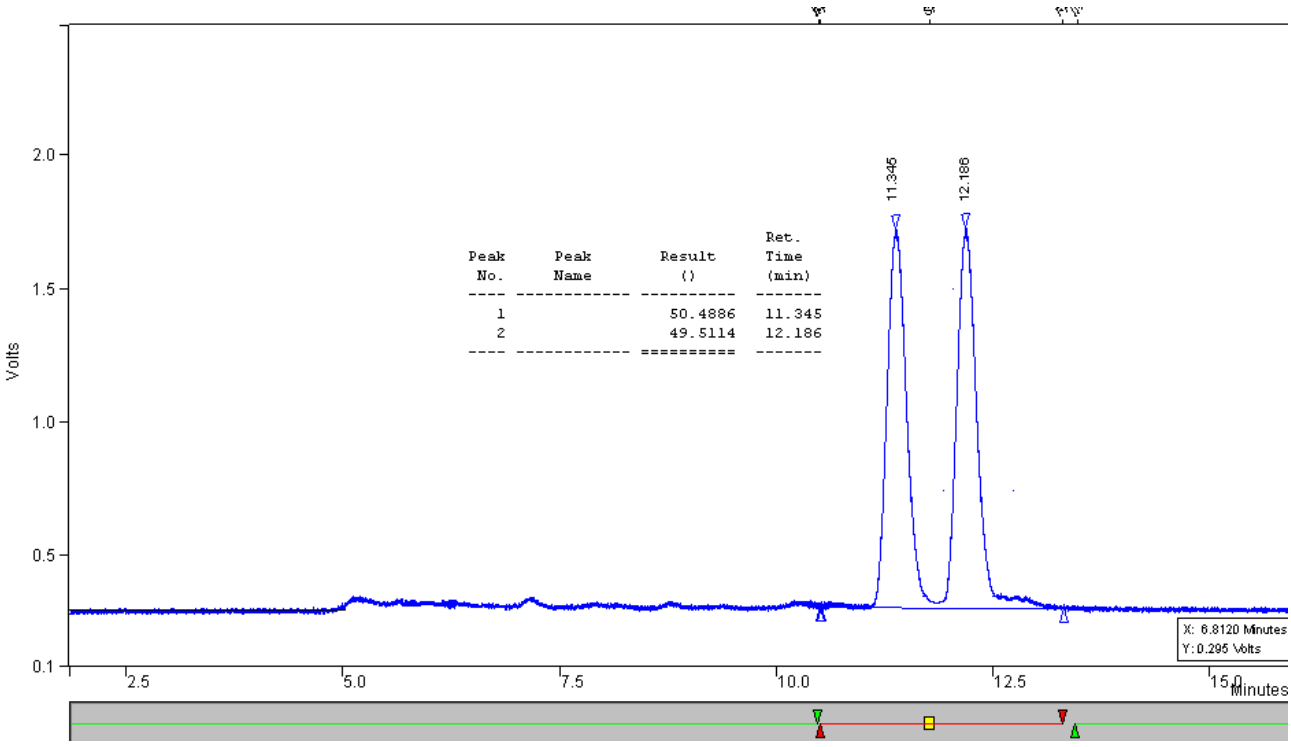
Volts
2.0
1.5
1.0
0.5
0.1
11.345
12.186
Peak No. | Peak Name | Result () | Ret. Time (min)
1 | | 50.4886 | 11.345
2 | | 49.5114 | 12.186
X: 6.8120 Minutes
Y: 0.295 Volts
2.5
5.0
7.5
10.0
12.5
15.0
Minutes

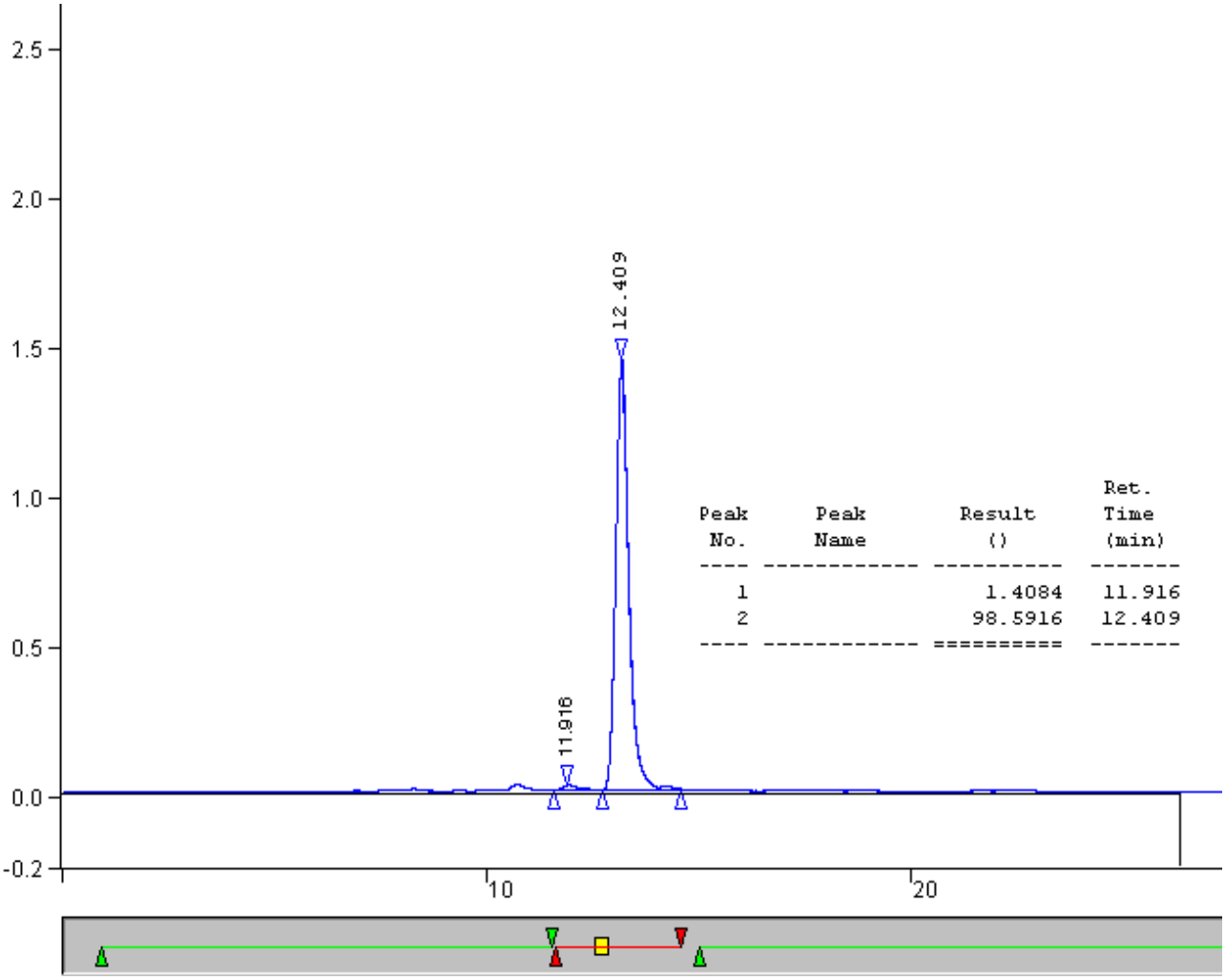
2.5
2.0
1.5
1.0
0.5
0.0
-0.2
12.409
11.916
Peak No. | Peak Name | Result () | Ret. Time (min)
1 | | 1.4084 | 11.916
2 | | 98.5916 | 12.409
10
20

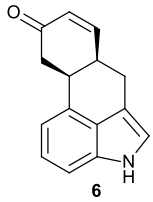

6

^{1}H NMR recorded at RT in CD_3CN

^{1}H NMR recorded at -20 °C in CD_3CN

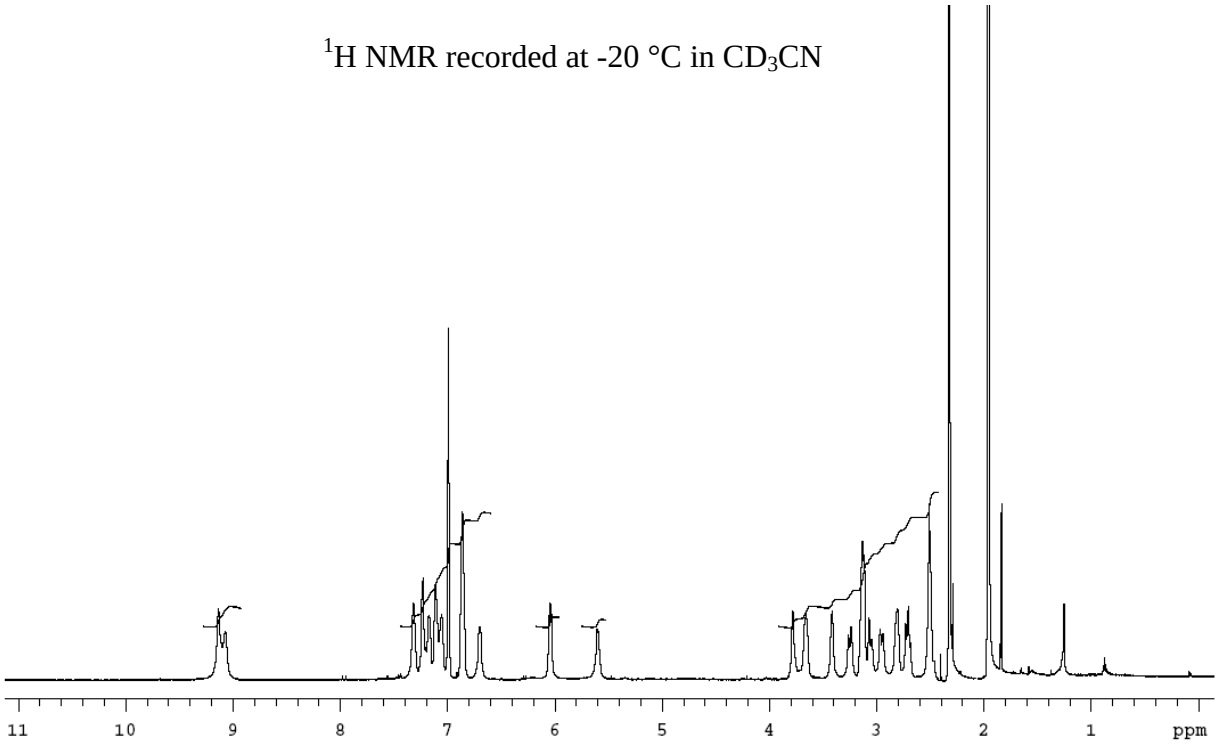

^{1}H NMR recorded at 60 °C in CD_3CN

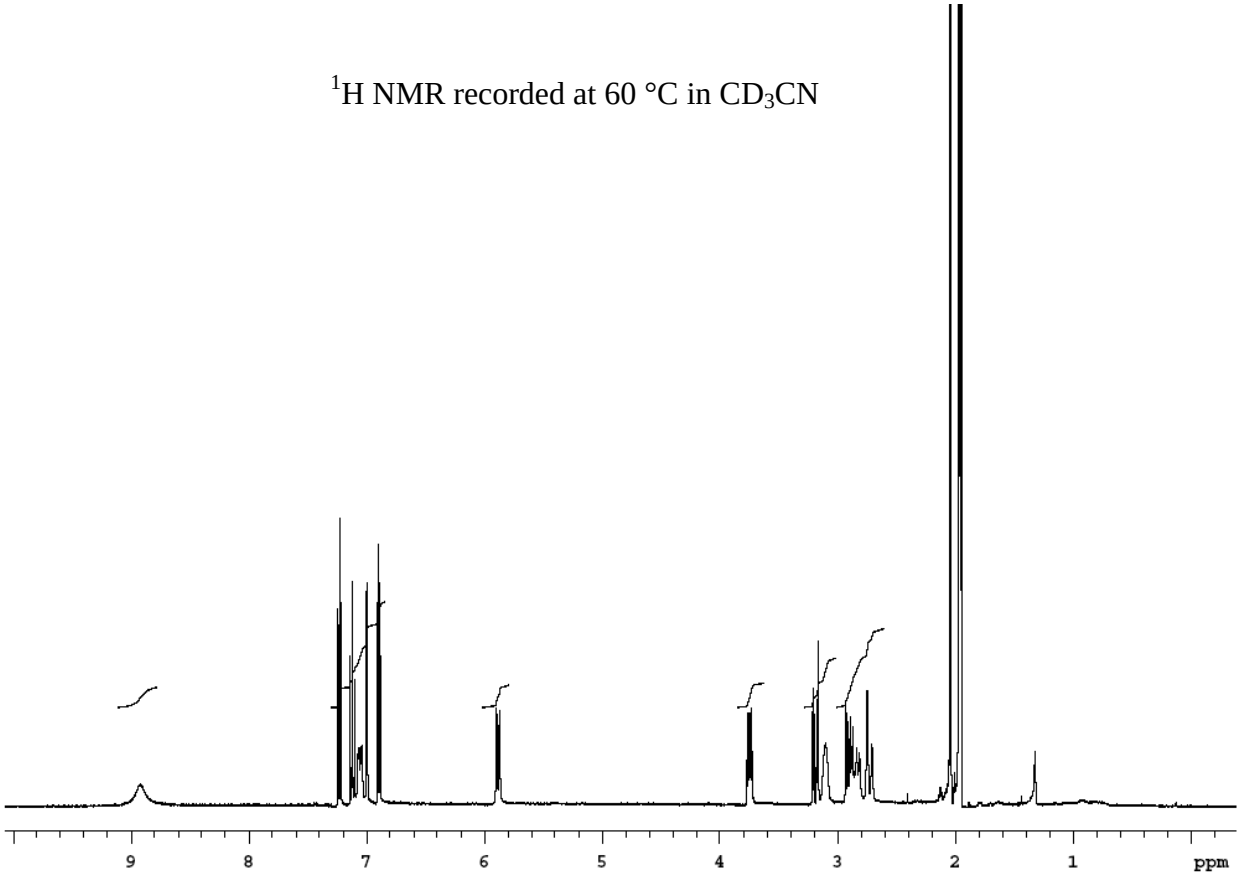

^{13}C NMR recorded at RT in C_6D_6

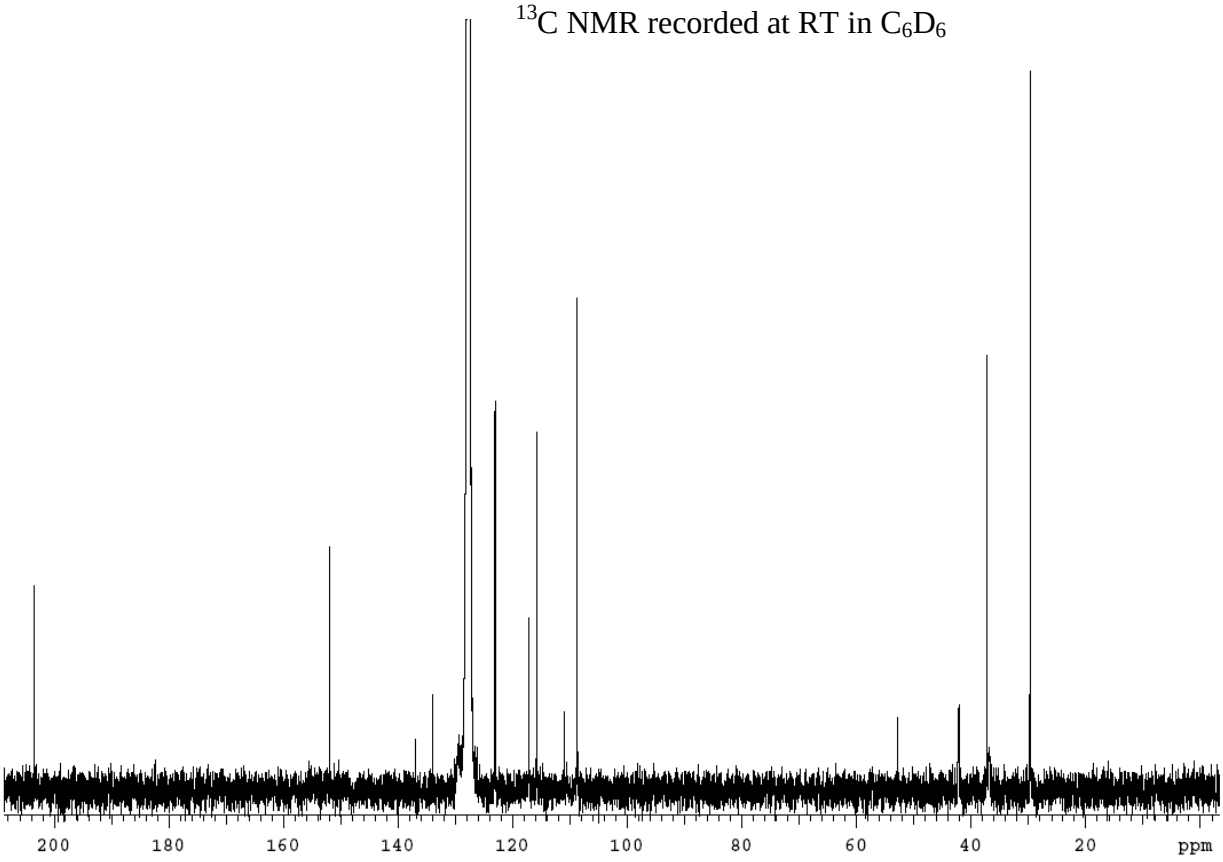

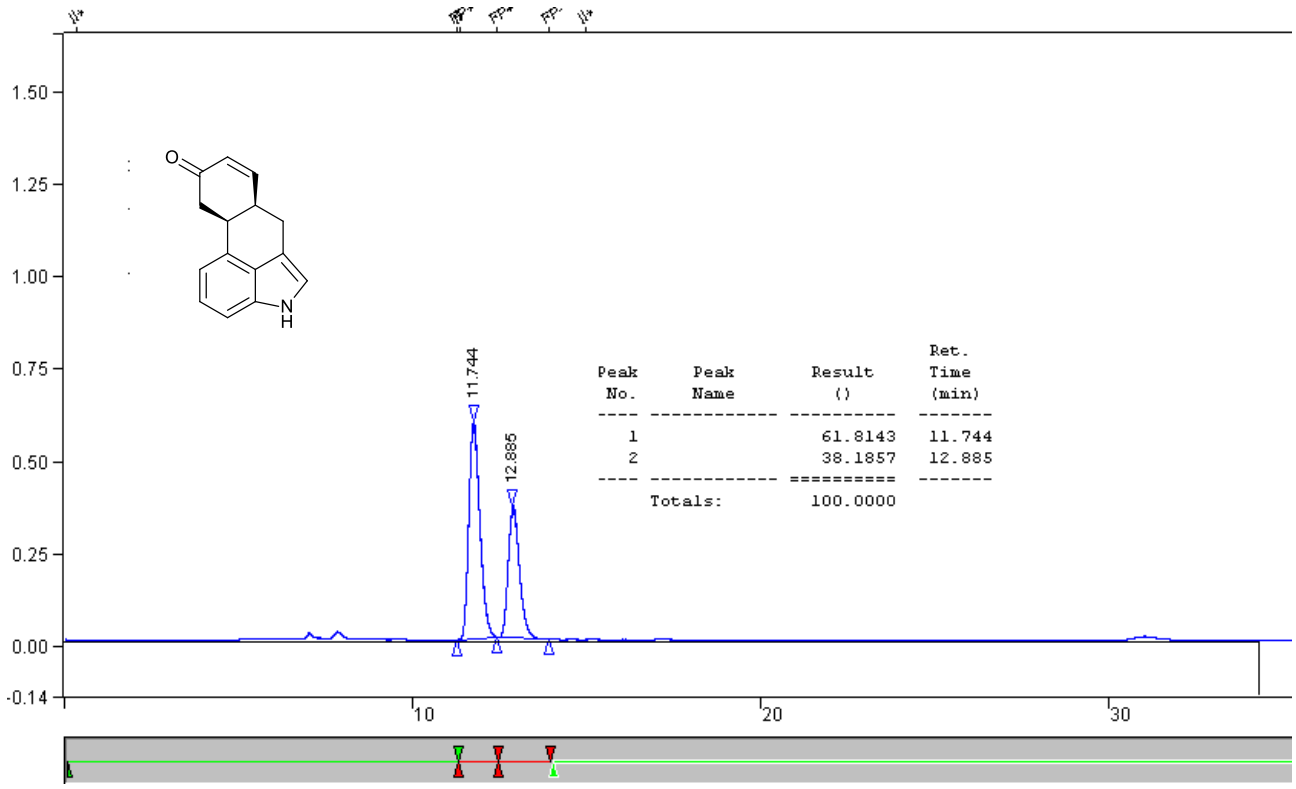

Peak No.	Peak Name	Result ()	Ret. Time (min)
1		61.8143	11.744
2		38.1857	12.885
	Totals:	100.0000	

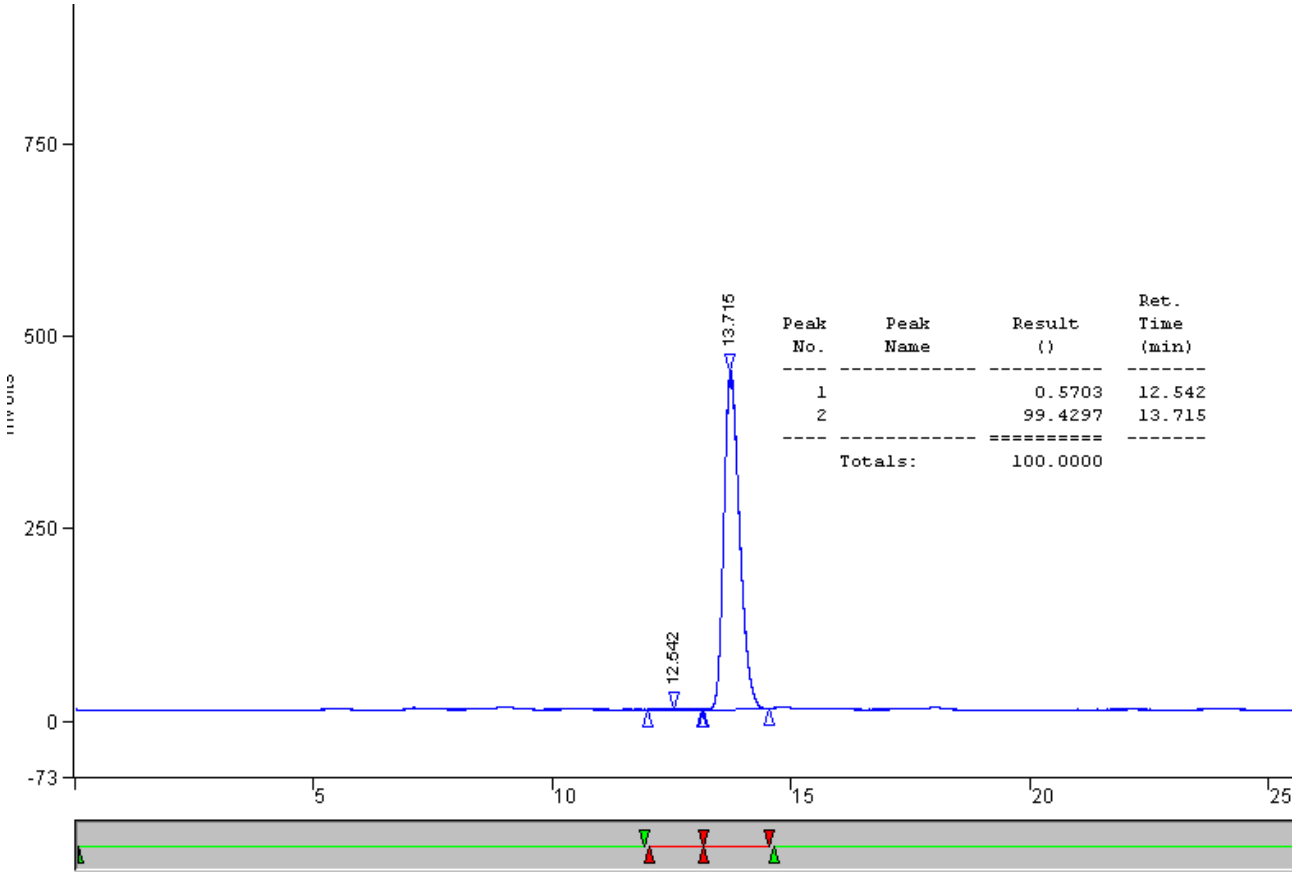

Peak No.	Peak Name	Result ()	Ret. Time (min)
1		0.5703	12.542
2		99.4297	13.715
	Totals:	100.0000